Physicochemical Studies of Molecular Recognition Using Functionalized Porphyrins

Tadashi Ema

1994

Physicochemical Studies of Molecular Recognition Using Functionalized Porphyrins

Tadashi Ema

1994

Preface

The study presented in this thesis has been carried out under the direction of Professor Hisanobu Ogoshi during April, 1989-January, 1994, at the Department of Synthetic Chemistry at Kyoto University.

In the present thesis, the physicochemical studies of molecular recognition process, together with the design and syntheses of functionalized porphyrin hosts, are summarized. The author is very lucky that he has encountered with many interesting organic compounds, a few exciting phenomena, and many respectable persons during his doctor-course, and he is also very happy that the present studies have made some contribution to the development of bioorganic and biomimetic chemistry.

The author would like to express his sincerest gratitude to Professor Hisanobu Ogoshi for his nice guidance, exciting and valuable discussions, and warm encouragement throughout this work. The author has learned from Professor Ogoshi a lot of things not only about chemistry but also about life. The author would also like to express his sincere gratitude to Dr. Tadashi Mizutani for his helpful advise, constant discussions, and warm encouragement during the course of this work. The author would like to thank Associate Professor Yasuhisa Kuroda and Dr. Takashi Hayashi for their nice discussions.

The author would like to express his gratitude to Professor Zen-ichi Yoshida, Associate Professor Sadao Miki at Kyoto Institute of Technology, Professor Yoshiaki Kobuke at Shizuoka University, and Dr. Akihiro Suzuki at Nagaoka Technology High School for their kind suggestions.

The author would like to express his deep appreciation to Professor Kevin M. Smith at University of California, Davis in U. S. A. for his giving the author a wonderful and exciting opportunity to work in his group during summer vacation in

1993.

The author would like to thank Dr. Masahiko Hada for his kind suggestion about the computer calculations.

The author would also like to thank Messrs. Hitoshi Hamashima, Hideki Takagi, Akio Naka, Takashi Tomita, Takashi Yoshida, Thomas Renné, and Miss Akiko Nomura for their very active collaborations, and all the other members of Ogoshi's group for their friendship and kind considerations.

The author is thankful to Mr. Haruo Fujita and Mr. Tadao Kobatake for the measurement of 400 MHz NMR and Mass spectra, respectively.

Finally, the author wishes to express his deep appreciation to his parents, Mr. Takeshi Ema and Mrs. Taeko Ema for their affectionate encouragement throughout this work. My late father used to tell me to do what I like as I believe. It seems to be easy, but actually is very difficult. I hope that this thesis will be a prelude as a chemist and that I will be able to continue to do my best in future.

Tadashi Ema

Department of Synthetic Chemistry
Faculty of Engineering
Kyoto University

January, 1994.

Contents

General Introduction

Molecular Recognition Chemistry. Molecular recognition plays a central role in the biological system. Specific molecular recognitions are essential for biological molecules to create well-ordered molecular networks. Actually, it is quite difficult to find out the naturally-occurring functional molecule which has no molecular recognition ability. Strict molecular recognition process is the initial step in biological reactions and functions.[1] Enzymes first recognize substrates, and then catalyze chemical reactions via the successive intermolecular interaction processes.[2] A lot of efforts from several scientific fields have been devoted to the studies of naturally-occurring macromolecules such as enzyme, antibody, receptor, DNA, and so on. From bioorganic chemistry, model approaches have been effectively adopted to study the molecular recognition.[3] D. J. Cram suggested the concept of *preorganization*, defined *host, guest, complex*, and extensively studied *host-guest chemistry*.[4c] For the formation of well-*structured* host-guest complex, the recognition sites of host molecules should be fixed and arranged by covalent bonds in a complementary manner to the structure of guest molecules (preorganization). The concept of preorganization originates from *the lock and key theory* for enzymes proposed by E. Fischer.[5] Flexible host must pay the large entropy cost associated with the conformational change of host, and will show weak recognition ability. Therefore, the rigid host molecule preorganized for the guest molecule is necesssary for the effective recognition. The preorganization of the host molecule can be achieved by elaborate organic syntheses in advance of the noncovalent intermolecular interaction (host-guest complexation). As an example, Cram designed and synthesized the host molecule preorganized for amino acids as shown in Figure 1.[4c] He succeeded in the enantioselective extraction and transport of amino acids.

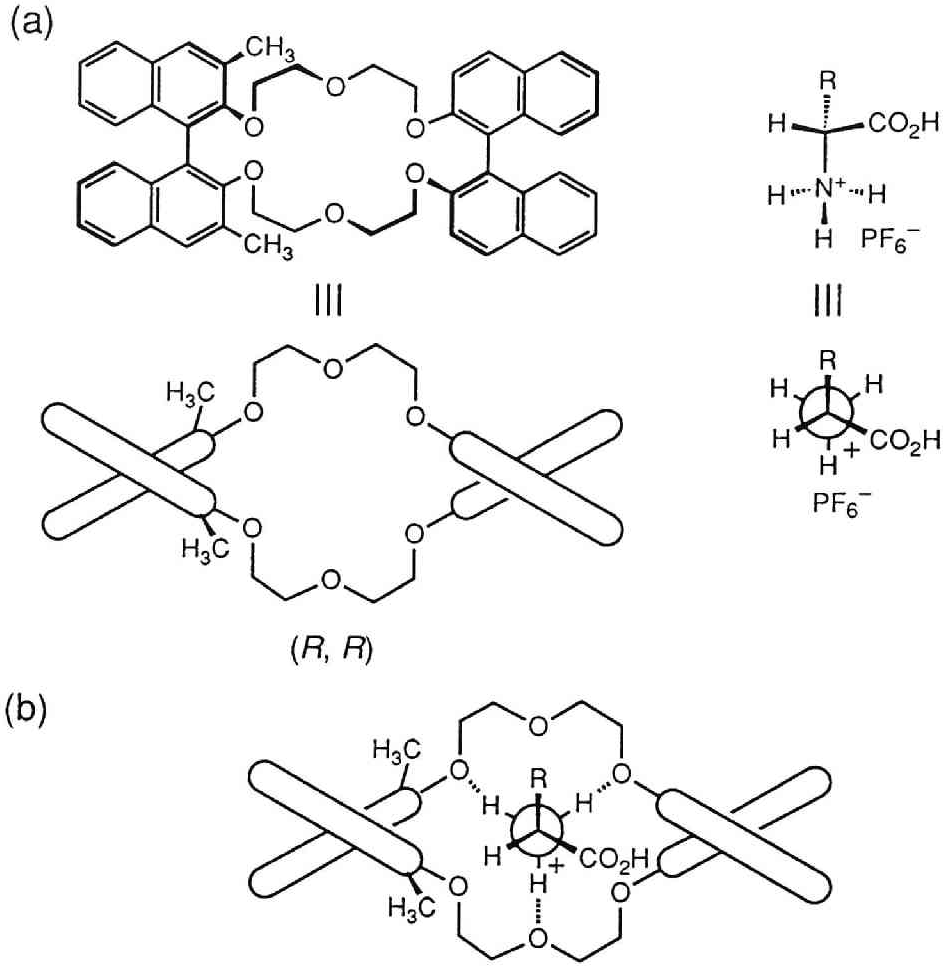

Figure 1. (a) Cram's host molecule preorganized for amino acids. (b) The proposed structure of the host-guest complex.

J. Rebek, Jr. designed and synthesized sophisticated host molecules, *molecular cleft* with *convergent* interaction sites.[4a] The functional groups of the molecular cleft shown in Figure 2 are directed inside convergently in a complementary manner to the *divergent* functional groups of the adenine guest. The complex is stabilized by simultaneous Watson-Click and Hoogsteen hydrogen bonding interactions, and by the π-stacking interaction between the naphthyl moiety of the bottom of the shallow cleft and the adenine. Many other elegant studies of molecular recognition have also

been reported so far.[4]

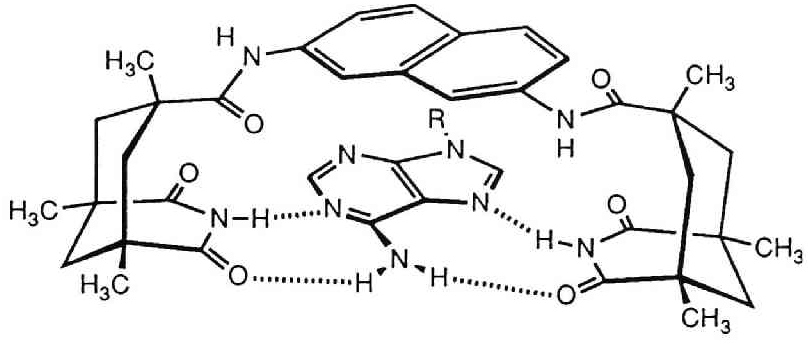

Figure 2. Rebek's molecular cleft complexed with adenine.

Those model studies so far have been very successful and fruitful indeed.[4] However, those are not yet satisfactory in the following three points.

(1) In most cases, only the phenomenological aspect of association behaviors has been stressed, and little attention has been paid to the physicochemical aspect of molecular recognition which will enable us to understand the general principle of highly specific molecular recognition of biological molecules and in turn to create further intriguing artificial molecules.

(2) Molecular recognition between rigid molecules has been extensively studied, but some of the biologically important molecules do have flexible structures. It is recognized, moreover, that in some biological systems, *complexation-induced conformational changes* and/or reorganization processes of interaction sites are important trigger for the following biological function.[6] Well-known examples are *allosterism* and *induced fit* phenomena of naturally-occurring macromolecules. Nevertheless, the detection and investigation of such conformational change processes are difficult because of complexity of macromolecules, and an answer based on well-designed model experiments is desired both about the advantage and about the physicochemical property of the

induced-fit phenomena of natural macromolecules.

(3) Molecular recognition should be followed by the successive chemical reaction or function. Precious examples along this line are the attempt to create artificial enzymes.[7] However, one more breakthrough seems to be necessary.

Research Strategy. The design and construction of the model system suitable for the purpose are necessary in order to carry out the research projects. Some of the most important criteria for the selection of the physicochemical studies of the molecular recognition are the followings.

(1) Intermolecular interaction is easily and sensitively detected by several spectroscopic methods.

(2) Functional groups can be spatially fixed and arranged on the host molecule to form the well-defined recognition environment.

(3) The organic synthetic methods are available for elaborate functionalizations and modifications of the host molecule.

Porphyrin derivatives meet the above conditions for the physicochemical studies of the molecular recognition. The porphyrin, the macrocyclic aromatic chromophore, provides several characteristic spectroscopic detection methods such as NMR, UV-vis, CD, resonance Raman spectroscopy, and so on. The porphyrin's rigid structure is also suitable for the spatial arrangement of the recognition groups.

Besides, porphyrin derivatives are cyclic tetrapyrrole widely distributed in nature, and in many cases, exist as prosthetic groups in enzyme active sites.[8] Therefore, the construction of functional porphyrin derivatives corresponds to the spatial fixation of essential functional groups of active sites onto the rigid porphyrin skeleton. This means that a part of the results of these studies can be used to understand the molecular mechanism of the biological system,[9] and will also lead to novel functional molecules superior to the naturally-occurring molecules according to the idea of *biomimetic chemistry*. For example, it has been suggested from X-ray

analysis that cytochrome P-450 binds camphor primarily by hydrophobic interaction and orients it by the hydrogen bonding between the camphor carbonyl group and the hydroxyl group of Tyr in proximity,[10] and that this orientational fixation of camphor by hydrogen bonding in the active pocket is necessary to achieve highly selective enzymatic oxidation reaction.

Both the construction of model systems by means of the organic synthetic method and the physicochemical studies will enable us to solve and understand complicate molecular recognition behaviors of biological macromolecules and molecular mechanisms of biological functions. In this thesis, the model systems of the multi-point interactions essential for the specific molecular recognition were constructed by functionalizing porphyrin, and their molecular mechanisms were analyzed from the physicochemical viewpoints. In particular, the thermodynamic evaluation and spectroscopic detection of the molecular recognition processes accompanied by conformational change were studied.

Survey of the Thesis. In chapter 1, the two-point recognition process of chiral amino acid esters by bifunctional porphyrin host via simultaneous coordination and hydrogen bonding was detected by means of three kinds of spectroscopic methods, and studied from the thermodynamic point of view. The thermodynamic contributions from the coordination and the hydrogen bonding interaction were separately evaluated by comparison of the association constants determined by the UV-vis titration using a reference porphyrin host lacking the hydrogen bonding site. In the two-point recognition system, the selectivity for several amino acid esters was observed in contrast to the low selectivity in the one-point interaction system, which reflected the fixation of the degree of internal rotational freedom of flexible amino acids. Furthermore, split-type of circular dichroism (CD) was induced in the Soret region when the mobility of amino acid esters was freezed by the hydrogen bonding, but not in the one-point interacting

complex. (Figure 3)

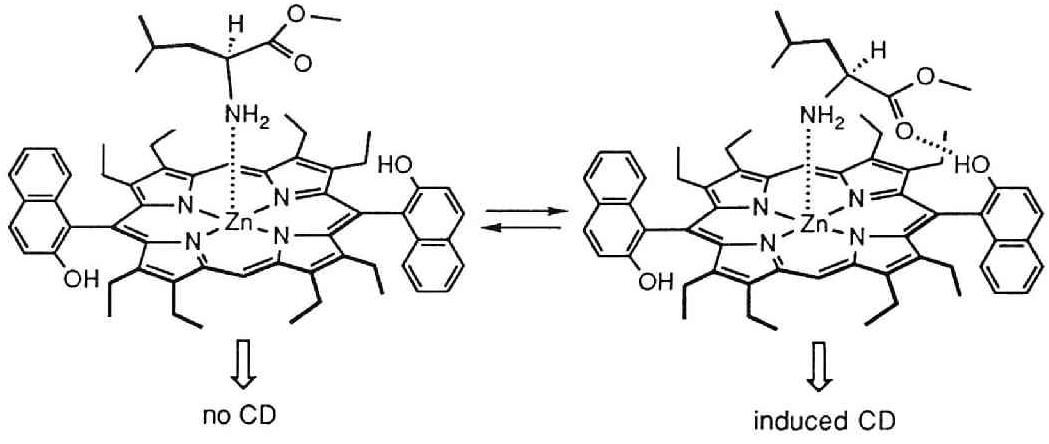

Figure 3. Detection of molecular recognition mode by CD spectroscopy.

Theoretically, the rotational strength of induced CD is determined by the dot product of the transition moments in the chromophores spatially fixed in a chiral manner,[11] and actually it was successfully demonstrated that CD spectroscopy can be a useful probe for the detection of orientation of molecules and/or functional groups in host-guest complexes.

In chapter 2, the inducement mechanism of the split-type Cotton effect was investigated both theoretically and experimentally. The computer assisted-calculations based on the perturbation theory indicated that the following mechanism is valid: Hydrogen bonding fixed the orientation of the carbonyl group of amino acid ester ligated, and consequently, the coupling of the electric dipole transition moments of the Soret transition of porphyrin with the magnetic and/or electric dipole transition moments of amino acid ester resulted in the Cotton effect. It is well-known that native hemoproteins also exhibit induced CD in the porphyrin Soret region.[12] However, the inducement mechanism is not clearly understood, so it is difficult to correspond the induced CD to the structural change of the active site or

surrounding conformational change definitely. Therefore, it is expected that a part of the results of the present study will give some useful piece of information for the elucidation of the induced CD mechanism of hemoproteins.

In chapter 3, a selective synthetic method useful for the introduction of functional groups in a regio-specific manner to give unsymmetrical porphyrin was developed, and this synthetic method was successfully applied to the synthesis of new trifunctional chiral porphyrin with C_2 symmetry shown in Figure 4.

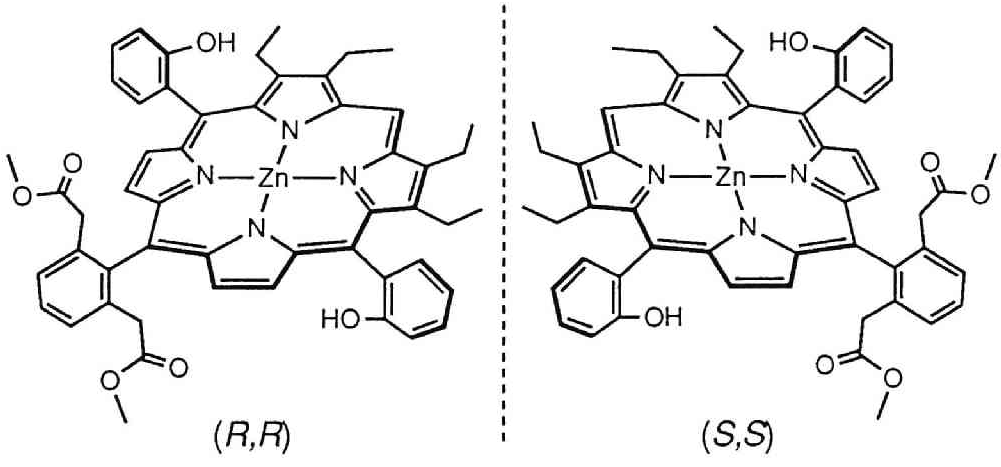

Figure 4. Structure of trifunctional chiral porphyrin host.

In chapter 4, the chiral recognition ability and mechanism by trifunctional chiral porphyrin for optically active amino acid esters were investigated. It was suggested from UV-vis and ^{1}H NMR titration that the chiral recognition occurred by means of the three-point diastereomeric interactions, based on the simultaneous coordination, hydrogen bonding, and steric repulsion (or hydrogen bonding). The thermodynamic contributions from each interaction point were estimated by comparison of association constants between the chiral or reference porphyrins and various amino acid esters. Among the three interactions, the hydrogen bonding to

fix the internal rotational freedom of the amino acids was suggested to be the driving force for chiral recognition.

The molecular recognition studies in chapter 1 and chapter 4 were carried out in nonpolar organic solvent such as chloroform, corresponding to the model system for molecular recognition at nonpolar environment such as hydrophobic binding pocket of macromolecules and inside the membrane. On the other hand, it is well-known that some of the biologically important macromolecules have a highly polar recognition site exposed to water phase.[1] In chapter 5, a model system for molecular recognition in water was studied.[13] Water-soluble porphyrin shown in Figure 5, which does not self-aggregate, was designed and synthesized, and molecular recognition behavior of the porphyrin host for several guest molecules was elucidated.

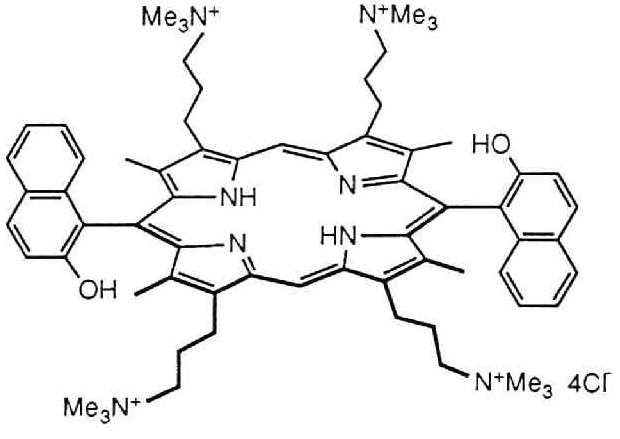

Figure 5. Structure of water-soluble porphyrin.

Interestingly, some anionic guests bound to the porphyrin accelerated the metal insertion reaction into the porphyrin cavity. This reaction is interesting in connection with *ferrochelatase*. In the last step of the biosynthesis of heme, ferrochelatase catalyzes the insertion of ferrous ion into the protoporphyrin.[14] It has

been suggested that ferrochelatase has the hydrophobic pocket to accommodate the porphyrin macrocycle as well as the metal binding site which consists of serine or cystein residues although detailed structure of ferrochelatase is still unknown.

References

(1) (a) Stryer, L. *Biochemistry*; Freeman: New York, 1988. (b) Alberts, B.; Bray, D.; Lewis, J.; Raff, M.; Roberts, K.; Watson, J. D. *Molecular Biology of the Cell*;Garland Publishing, Inc.: New York, 1989. (c) Branden, C.; Tooze, J. *Introduction to Protein Structure*; Garland Publishing, Inc.: New York, 1991.

(2) (a) Jencks, W. P. *Catalysis in Chemistry and Enzymology*; McGraw-Hill: New York, 1969. (b) Zeffren, E.; Hall, P. L. *The Study of Enzyme Mechanisms*; John Wiley & Sons, Inc.: New York, 1973.

(3) (a) Dugas, H. *Bioorganic Chemistry*; Springer-Verlag: New York, 1988. (b) *Bioorganic Chemistry Frontiers*; Dugas, H. Ed.; Springer Verlag: Berlin, Vol 1, 1990; Vol 2, 1991.

(4) (a) Rebek, J., Jr. *Science (Washington, DC)* **1987**, *235*, 1478. (b) Lehn, J.-M. *Angew. Chem.* **1988**, *100*, 91; *Angew. Chem. Int. Ed. Engl.* **1988**, *27*, 89. (c) Cram, D. J. *Angew. Chem.* **1988**, *100*, 1041; *Angew. Chem. Int. Ed. Engl.* **1988**, *27*, 1009. (d) Petti, M. A.; Shepodd, T. J.; Barrans, R. E., Jr.; Dougherty, D. A. *J. Am. Chem. Soc.* **1988**, *110*, 6825. (e) Zimmerman, S. C.; VanZyl, C. M.; Hamilton, G. S. *J. Am. Chem. Soc.* **1989**, *111*, 1373. (f) Furuta, H.; Magda, D.; Sessler, J., L. *J. Am. Chem. Soc.* **1991**, *113*, 978.(g) Ferguson, S. B.; Sanford, E. M.; Seward, E. M.; Diederich, F. *J. Am. Chem. Soc.* **1991**, *113*, 5410. (h) Chang, S. -K.; Engen, D.V.; Fan, E.; Hamilton, A. D. *J. Am. Chem. Soc.* **1991**, *113*, 7640. (i) Adrian, J. C.; Wilcox, C. S. *J. Am. Chem. Soc.* **1992**, *114*, 1398. (j) Wang, X.; Erickson, S. D.; Iimori, T.; Still, W. C. *J. Am. Chem. Soc.* **1992**, *114*, 4128. (k) Schneider, H.-J.; Shiestel, T.; Zimmermann, P. *J. Am. Chem. Soc.* **1992**, *114*, 7698. (l) Kobayashi, K.; Asakawa, Y.; Kikuchi, Y.; Toi, H.; Aoyama, Y. *J. Am. Chem. Soc.* **1993**, *115*, 2648.

(5) Fischer, E. *Ber. Dtsch. Chem. Ges.* **1894**, *27*, 2985.

(6) Hervé, G. *Allosteric Enzymes*; CRC Press, Inc.: 1989.

(7) (a) Bender, M. L.; Komiyama, M. *Cyclodextrin Chemistry*; Springer-Verlag: 1978.(b) Breslow, R. *Acc. Chem. Res.* **1980**, *13*, 170. (c) Tabushi, I. *Acc. Chem. Res.* **1982**, *15*, 66. (c) Rebek, J., Jr. *J. Inclusion Phenom. Mol. Recognit. Chem.* **1989**, *7*, 7. (d) Kelly, T. R.; Zhao, C.; Bridger, G. J. , F. *J. Am. Chem. Soc.* **1989**, *111*, 3744. (e) Hosseini, M. W.; Blacker, A. J.; Lehn, J.-M. *J. Am. Chem. Soc.* **1990**, *112*, 3896.(f) Tecilla, P.; Chang, S. K.; Hamilton, A. D. *J. Am. Chem. Soc.* **1990**, *112*, 9586. (g) Tam, S.-W.; Jimenez, L.; Diederich, F. *J. Am. Chem. Soc.* **1992**, *114*, 1503. (h) Smith, J.; Ariga, K.; Anslyn, E. V. *J. Am. Chem. Soc.* **1993**, *115*, 362.

(8) (a) *Porphyrins and Metalloporphyrins*; Smith, K. M. Ed.; Elsevier: Amsterdam, 1975. (b) *The Porphyrins*; Dolphin, D., Ed.; Academic Press: New York, 1978; Vol. 1-7.

(9) Morgan, B. Dolphin, D. In *Structure and Bonding*, Buchler, J. W. Ed.; Springer-Verlag, Berlin, 1987, Vol 64, pp115-203.

(10) Poulos, T. L. In *Cytochrome P-450*; Montellano, P. R. O. Ed.; Plenum Press: New York, 1986; pp 505.

(11) Snatzke, G. *Optical Rotatory Dispersion and Circular Dichroism in Organic Chemistry*; Heyden and Son Ltd.: London, 1967; .

(12) Myer Y. P.; Pande, A. In *The Porphyrins*; Dolphin, D., Ed.; Academic Press: New York, 1978; Vol. 3, pp.271-322.

(13) (a) Bender, M. L.; Komiyama, M. *Cyclodextrin Chemistry*; Springer-Verlag: 1978.(b) Breslow, R. *Acc. Chem. Res.* **1980**, *13*, 170. (c) Tabushi, I. *Acc. Chem. Res.* **1982**, *15*, 66. (d) Hosseini, M. W.; Blacker, A. J.; Lehn, J.-M. *J. Am. Chem. Soc.* **1990**, *112*, 3896.(e) Ferguson, S. B.; Sanford, E. M.; Seward, E. M.; Diederich, F. *J. Am. Chem. Soc.* **1991**, *113*, 5410. (f)

Schneider, H.-J.; Shiestel, T.; Zimmermann, P. *J. Am. Chem. Soc.* **1992**, *114*, 7698.(g) Rotello, V. M.; Viani, E. A.; Deslongchamps, G.; Murray, B. A.; Rebek, J., Jr. *J. Am. Chem. Soc.* **1993**, *115*, 797.

(14) (a) Mazanowska, A. M.; Neuberger, A.; Tait, G. H. *Biochem. J.* **1966**, *98*, 117. (b) Daily, H. A. *Biochemistry*, **1985**, *24*, 1287. (c) Daily, H. A.; Jones, C. S.; Karr, S. W. *Biochim. Biophys. Acta*, **1989**, *999*, 7. (d) Abbas, A.; Labbe-Bois, R. *J. Biological Chem.* **1993**, *268*, 8541.

Chapter 1

Thermodynamic and Spectroscopic Studies of Two-Point Recognition of Amino Acid Esters by Bifunctional Porphyrin Host.

Abstract

Association constants between [*trans*-5, 15–bis(2–hydroxy-1-naphthyl)-2, 3, 7, 8, 12, 13, 17, 18-octaethylporphyrinato]zinc(II) (**1**) and a series of α–amino acid esters ($RCHNH_2CO_2CH_3$) were determined in chloroform by use of a UV-vis titration method. Association constants increased in the order Ala-OMe < Glu-OMe < Val-OMe < Leu-OMe, showing a preference for bulky amino acid esters. Contributions from the metal coordination and hydrogen bonding interactions to the total free energy change were estimated by use of reference compounds having no hydrogen bonding site. Free energy change for the binding of Leu-OMe to **1** in chloroform at 15 ℃ was –5.3 kcal/mol, which was separated into two contributions, (1) the metal coordination interaction $\Delta G^\circ_{MC} = -3.8$ kcal/mol and (2) the hydrogen bonding interaction $\Delta G^\circ_{HB} = -1.5$ kcal/mol. Circular dichroism (CD) induced in the porphyrin Soret band of **1** by complexation with optically active amino acid esters was of split type for all the amino acid esters examined, whereas induced CD of a reference host, [*trans*-5, 15–bis(2–methoxy–1–naphthyl)-2, 3, 7, 8, 12, 13, 17, 18-octaethylporphyrinato]zinc(II) (**2**), was negligibly small. A good correlation existed between the free energy of the hydrogen bonding and the CD intensity for a number of aliphatic amino acid esters-**1** complexes. Both the presence and the fixation of the carbonyl group of the amino acid ester were essential to the split Cotton effect, which is named "anchor effect".

Introduction

Molecular recognition of amino acids or their derivatives is a key step in protein synthesis and how aminoacyl-transfer RNA synthases can recognize a specific amino acid is an interesting problem. Consequently, recognition of amino acids or their derivatives has been challenging subjects in biomimetic chemistry.[1] Besides, molecular recognition of amino acids is an interesting problem because they are flexible molecules and the internal rotational freedom of amino acid derivatives should be effectively frozen by multi-point interactions. The physicochemical aspect such as thermodynamic properties of multi-point recognition process of flexible molecules must be fascinating.

In the present chapter, two-point recognition of amino acid derivatives by a host molecule bearing both coordination and hydrogen bonding recognition sites, *trans*-[5, 15–bis(2–hydroxy-1-naphthyl)-2, 3, 7, 8, 12, 13, 17, 18-octaethylporphyrinato]zinc(II) (**1**) are studied both from thermodynamic and from spectroscopic (CD and ^{1}H NMR) viewpoints.

Circular dichroism (CD) spectroscopy has been widely used in order to elucidate the conformation and relative orientation of the host–guest complex including hemoproteins.[2, 3] Because the rotational strength of CD is determined by the dot product between the transition moments of the chromophores fixed in a chiral environment,[4] CD spectroscopy can be a useful molecular recognition probe to detect the disposition and orientation of the two chromophores in host-guest complexes.

Results and Discussion

Host **1** has two recognition sites, a metal coordination site (Zn) and a hydrogen bond donor site (OH), while host **2** lacks the hydrogen bond donor site and host **3** lacks the hydrogen bonding site. Hosts **2** and **3** were used as reference hosts in order to evaluate additional stabilizing energies associated with hydrogen bonding interaction.

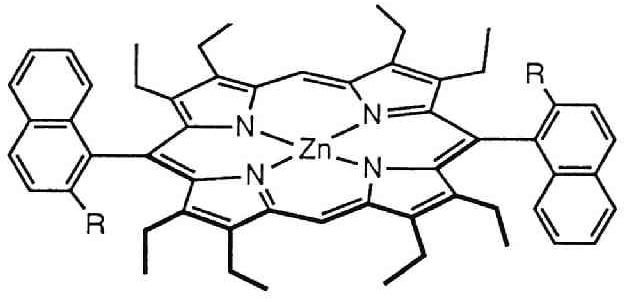

1 : R = OH
2 : R = OMe
3 : R = H

Thermodynamic Studies. The complex formation of the porphyrin hosts with the amino acid esters was monitored by UV-vis spectrophotometric titration. A representative example of the spectral change of host **1** upon addition of amino acid ester is shown in Figure 1. Several isosbestic points are observed in the spectra, indicating 1:1 complexation between **1** and the guest molecule. The binding constants (K_a) between the hosts and the guests were determined by nonlinear least-square curve fitting method as summarized in Table I. Association constants K_a (**1**) between **1** and amino acid esters were in the range $2.0 \times 10^3 \sim 1.1 \times 10^4$ M^{-1}, while those K_a (**2**) between **2** and amino acid esters were in the range $2.0 \times 10^2 \sim 1.6 \times 10^3$ M^{-1}. The higher recognition capacity of host **1** compared with that of host **2** can be ascribed to the hydrogen bonding interaction between the carbonyl oxygen of amino acid esters and the hydroxyl group on the naphthyl moiety of **1**, which is supported by other spectroscopic techniques (*vide infra*).

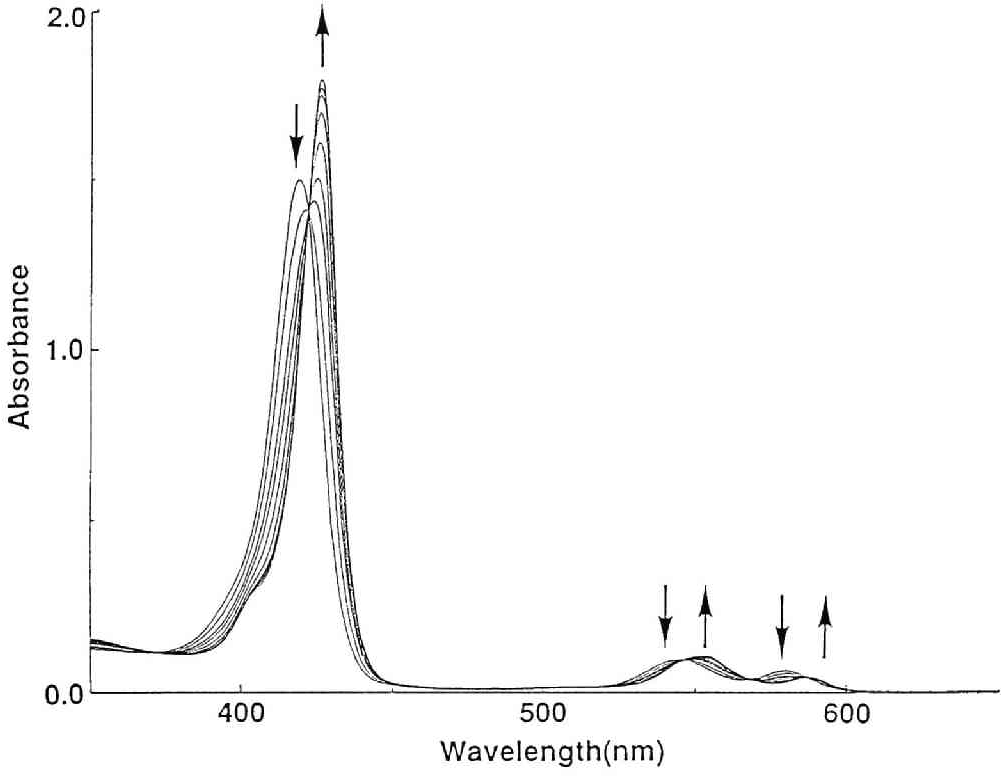

Figure 1. Electronic absorption spectra of a solution of host **1** (5.3×10^{-6} M) in the presence of varying concentrations of L-leucine methyl ester (0, 3.03×10^{-5}, 9.01×10^{-5}, 1.49×10^{-4}, 2.90×10^{-4}, 6.02×10^{-4}, 1.22×10^{-3}, 1.82×10^{-3}, 3.28×10^{-3} M) in $CHCl_3$ at 15°C. Arrows indicate the absorbance changes with increasing guest concentrations.

Table I. Association Constants between Porphyrin Hosts **1** (or **2**) and Amino Acid Esters (or Related Compounds) in $CHCl_3$ at 15°C.

	K_a, M^{-1}		
	1	**2**	K_a(**1**) /K_a(**2**)
Gly-OMe	3460 ± 30	920 ± 20	3.8
L-Ala-OMe	2230 ± 20	330 ± 10	6.8
L-Asp-OMe	2280 ± 50	300 ± 10	7.6
L-Glu-OMe	1710 ± 20	220 ± 10	7.8
L-Met-OMe	2460 ± 50	310 ± 10	7.9
L-Val-OMe	8070 ± 110	350 ± 10	23.1
L-Leu-OMe	10900 ± 150	270 ± 10	40.4
L-Leu-OBu^t	1780 ± 30	——[b]	——[c]
L-Phe-OMe	3660 ± 50	990 ± 20	3.7
L-Trp-OMe	10230 ± 80	1630 ± 10	6.3
L-Phg-OMe	10990 ± 110	520 ± 10	21.1
(*S*)-leucinol[a]	9870 ± 120	5290 ± 90	——[d]
4-heptylamine	4250 ± 50	1500 ± 40	2.8
n-butylamine	4450 ± 40	1570 ± 30	2.8

[a] K_a(**3**) = 2480 ± 50 M^{-1}. [b] K_a(**3**) = 390 ± 10 M^{-1}.
[c] K_a(**1**) / K_a(**3**) = 4.6 [d] K_a(**1**) / K_a(**3**) = 4.0

For aliphatic amino acid esters, **2** showed a slight preference for less bulky amino acid esters, and the selectivity of **2** for the amino acid esters is low. On the other hand, **1** showed a significant preference for bulky amino acid esters in the order Ala-OMe < Glu-OMe < Val-OMe < Leu-OMe. Thus, the selectivity of **1** for the amino acid esters is much higher than that of **2**, regardless of the same structure of the recognition sites of the amino acid esters (NH_2 and CO_2Me). This selectivity for amino acid esters is interesting because host **1** has no recognition site to distinguish the side chain of the amino acid esters. This enhanced selectivity of **1** seems to reflect the conformational flexibility of the amino acid esters (*vide infra*).

Aromatic amino acid esters exhibited somewhat different association behavior. Because of the low solubility of aromatic amino acid esters in chloroform, UV-vis spectrophotometric titration studies were carried out for only Phe-OMe , Trp-OMe, and Phg-OMe (phenylglycine methyl ester). These aromatic amino acid esters were bound to host **2** more strongly than aliphatic amino acid esters. Since host **2** has no hydrogen bond donor site, the association enhancements of aromatic amino acid esters should be ascribed to other interactions. CPK model suggested that π-stacking interactions between the porphyrin plane and the aromatic side chain stabilize the association complex, which was also suggested by CD spectroscopic studies (*vide infra*).

The magnitude of association constants of Asp-OMe and Glu-OMe to host **1** was similar to that of Ala-OMe to host **1**. This indicates that the presence of an additional ester group in the amino acid side chain does not lead to an increase in the magnitude of association constants.

The ratio of K_a (**1**) to K_a (**2**) is a qualitative measure of the association enhancement due to the hydrogen bonding interaction, but K_a (**2**) involves contributions both from steric repulsions between the OMe group of **2** with the amino acid esters and from some inductive effect. Free energy changes due to

hydrogen bonding can be more precisely estimated by correcting the ratio of K_a (**1**) to K_a (**2**) for the above interactions using reference guest molecules,[1m] which are primary amines with similar bulkiness and have no hydrogen bonding sites. 4-Heptylamine or *n*-butylamine were used as reference guests. Association enhancements due to hydrogen bonding (K_{HB}) were thus estimated from the following equation:

$$K_{HB} = \frac{K_a(\textbf{1}\text{-Guest}) / K_a(\textbf{2}\text{-Guest})}{K_a(\textbf{1}\text{-Reference Guest}) / K_a(\textbf{2}\text{-Reference Guest})}$$

The values of hydrogen bonding free energy are summarized in Table II, together with the values of ΔG°_{MC} and ΔG°_{Total}, which are calculated as follows.

$$\Delta\Delta G^\circ_{HB} = -RT\ln K_{HB}$$

$$\Delta G^\circ_{Total} = -RT\ln K_a(\textbf{1})$$

$$\Delta G^\circ_{MC} = \Delta G^\circ_{Total} - \Delta\Delta G^\circ_{HB}$$

The ΔG°_{MC} term may involve contributions from entropy changes upon complexation and steric repulsion energies such as those between the naphthyl groups of host and the amino acid side chain of guests in addition to the metal coordination energy. In the case of leucinol and Leu-OBu^t, the association enhancements due to hydrogen bonding were estimated by use of a reference host **3**, which lacks the hydrogen bonding site. In this case the difference in the steric repulsion energies between the hydrogen bonding complex and the reference non-hydrogen bonding complex was assumed to be negligible.

In aliphatic series of amino acid esters, the hydrogen bonding increases as the side chain is bulkier, with Leu-OMe being largest. This trend may be ascribed to

the conformational change of amino acid esters upon complexation to the porphyrin host as follows. (1) Upon two-point recognition, flexible amino acid esters with a less bulky side chain lose larger entropy of internal rotation than rigid amino acid esters with a bulky side chain. Because of the differences in the bulkiness of the side chain of the guests, the energy barrier for rotation around the α-carbon - the carbonyl carbon would change, resulting in the difference in distribution of the distances between amino nitrogen and carbonyl oxygen atoms. In order to be bound through two point fixation, the distance should be fixed. In the case of Leu-OMe, the bulky *sec*-butyl group may fix the N•••O(=C) distance to some extent even in uncomplexed state, and consequently, entropy loss upon two-point fixation will be smaller. On the other hand, in the case of Gly-OMe, the distance fluctuates in uncomplexed state, resulting in a large entropy loss upon two-point fixation. This explanation was supported by ab initio calculations at 3-21G level and molecular statistical machanics calculations.[5] (2) The coordination interaction between the amino group in the guest and the zinc in the host makes the side chain tilts away from the porphyrin plane, due to steric repulsions between the bulky side chain (R) of the guest and the porphyrin plane, and these steric repulsions would direct the ester group to the hydroxyl group of the naphthyl moiety, leading to a favorable conformation for hydrogen bonding to take place (induced fit). A space filling model suggested that the hydrogen bonding interaction between the carbonyl oxygen atom and the naphthyl hydroxyl group is favorable in the Leu-OMe–**1** complex. Otherwise, that trend might be ascribed to the stronger London's dispersion forces between host and guest for bulkier amino acid esters.[6] However, host **2** showed opposite preference for aliphatic amino acid esters series, least bulky guest (Gly-OMe) being bound most strongly, which indicates that attractive intermolecular force does not operate between the porphyrin and the side chain of the amino acid esters.

Table II. Hydrogen Bonding, Metal Coordination, and Total Free Energy Changes (kcal / mol) Evaluated by Use of Reference Hosts and Guests in $CHCl_3$ at 15°C.[a]

Host	Guest	$\Delta\Delta G°_{HB}$	$\Delta G°_{MC}$	$\Delta G°_{Total}$
1	Gly-OMe	-0.2	-4.5	-4.7
1	L-Ala-OMe	-0.5	-3.9	-4.4
1	L-Asp-OMe	-0.6	-3.8	-4.4
1	L-Glu-OMe	-0.6	-3.7	-4.3
1	L-Met-OMe	-0.6	-3.9	-4.5
1	L-Val-OMe	-1.2	-3.9	-5.1
1	L-Leu-OMe	-1.5	-3.8	-5.3
1	L-Leu-OBu^t [c]	-0.9	-3.4	-4.3
1	L-Phe-OMe	-0.2	-4.5[b]	-4.7
1	L-Trp-OMe	-0.5	-4.8[b]	-5.3
1	L-Phg-OMe	-1.2	-4.1[b]	-5.3
1	(*S*)-leucinol[c]	-0.8	-4.5	-5.3
2	(*S*)-leucinol[c]	-0.4	-4.5	-4.9

[a] 4-Heptylamine or *n*-butylamine were used as reference guests except for **1**-, and **2**-leucinol complexes and **1**-L-Leu-OBu^t complex.

[b] Contribution from π-stacking interaction are involved.

[c] **3** was used for a reference host.

^{1}H NMR Studies. The hydrogen bonding interaction was also studied by ^{1}H NMR spectroscopy. Spectral change of host **1** in $CDCl_3$ at 24℃ induced by the addition of L-Leu-OMe is shown in Figure 2. The signal of the naphthyl hydroxyl protons shifted to lower magnetic field and was broadened as the concentration of L-Leu-OMe increased. This clearly indicates that the hydrogen bonding between the carbonyl oxygen of the guest and the naphthyl hydroxyl group occurs.[7]

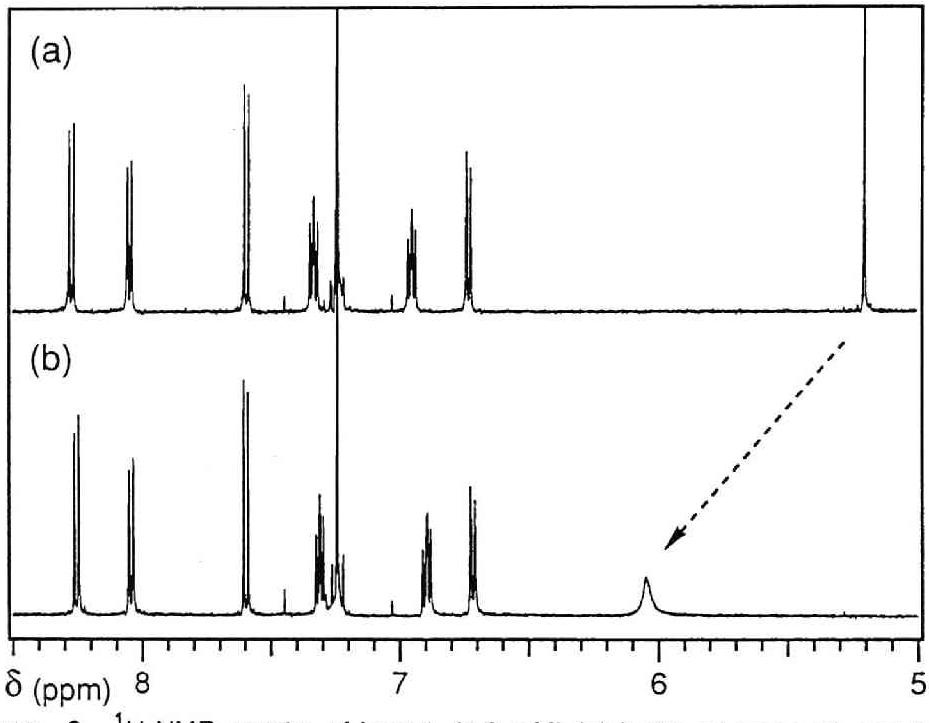

Figure 2. ^{1}H NMR spectra of host **1** (1.9 mM) (a) in the absence of, and (b) in the presence of L-Leu-OMe (3.4 mM, 2 equiv.) in $CDCl_3$ at 24℃. The signal shift of the OH group of **1** is shown by the arrow.

Circular Dichroism Studies. CD spectroscopy can be used as a molecular recognition probe to detect the disposition and orientation of the chromophores in host-guest complexes, because the rotational strength of CD is determined by the dot product between the transition moments of the chromophores fixed in a chiral environment.[4] The CD spectra induced in the absorption region of the achiral porphyrin **1**-**3** are exclusively due to the complexation with optically active guest, because **1**-**3** are optically inactive. Typical induced CD spectra are shown in Figure 3, and the molecular ellipticities in the Soret region are summarized in Table III. The complex of **1** with L- (and D-) Leu-OMe, where hydrogen bonding is operating, showed split Cotton effects in the Soret region (Figure 3(a)). On the other hand, **2** – L- (and D-) Leu-OMe complex exhibited no appreciable Cotton effect.[8] It is noteworthy that these two types of induced CD were observed for all the aliphatic and aromatic amino acid esters examined; the induced CD in **1** is of split type and that in **2** is not (Table III).[9] Thus, the hydrogen bonding interaction can be easily detected and studied by measuring induced CD for the present system.[10] Furthermore, in all complexes of **1** with L-amino acid esters, the longer-wavelength peak of the Soret band was negative and the shorter-wavelength peak was positive (Table III). These results suggest that the induced CD reflects the spatial orientation around the chiral carbon directly. For aliphatic amino acid esters – **1** complexes, positive and negative peaks of the CD induced in the Soret region exhibited almost the same intensity, while for aromatic amino acid esters – **1** complexes, the induced CD was not symmetric and the longer-wavelength peak of the induced CD (the negative peak in the case of L-amino acid esters) was stronger than the shorter-wavelength peak (Figure 3 (b)). Single peak CD was observed for the complexes between **2** and the aromatic amino acid esters. Additional electronic perturbation by the aromatic side chain may operate because aryl -aryl interactions between hosts and guests were suggested from the comparison of the association

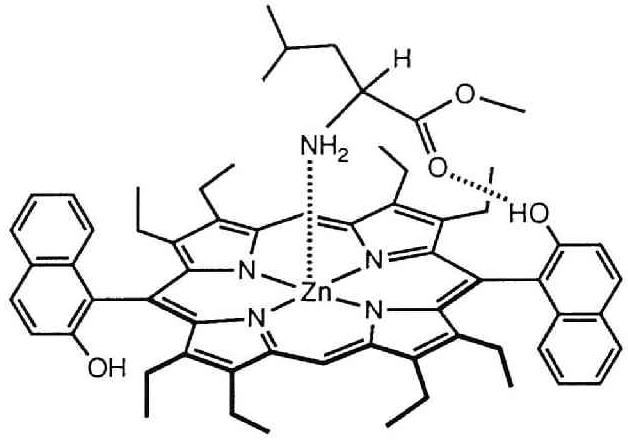

1-L-(or D-)Leu-OMe complex

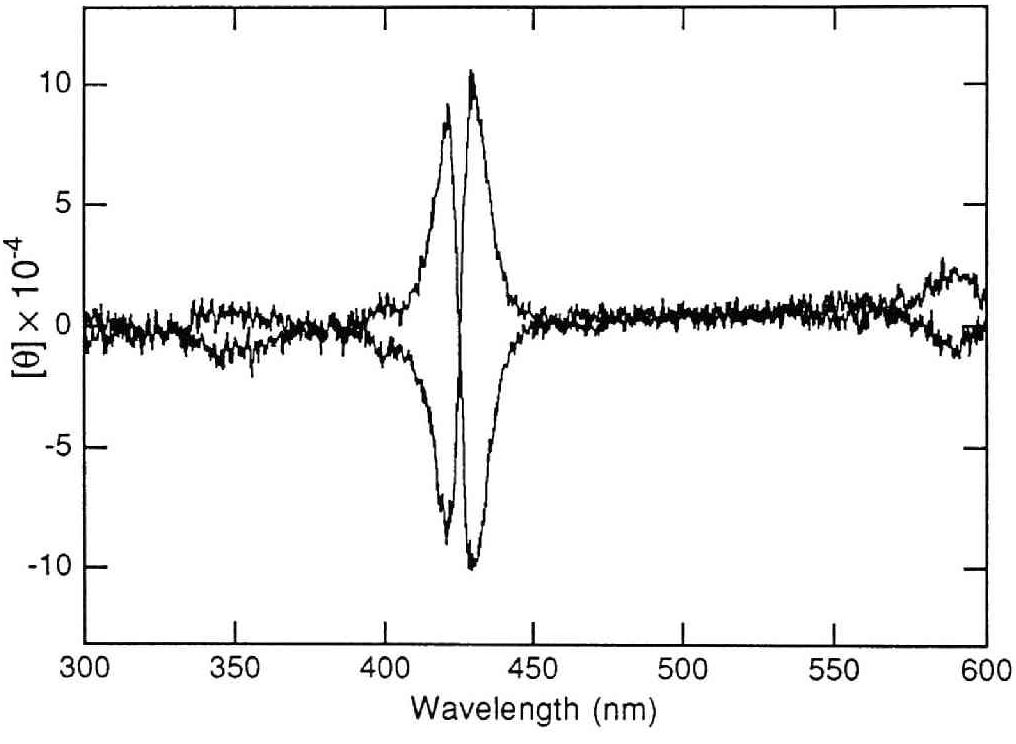

Figure 3(a). CD spectra of a solution of host **1** (4.8×10^{-6} M) and L- and D-leucine methyl ester (3.3×10^{-3} M) in $CHCl_3$ at 15°C.

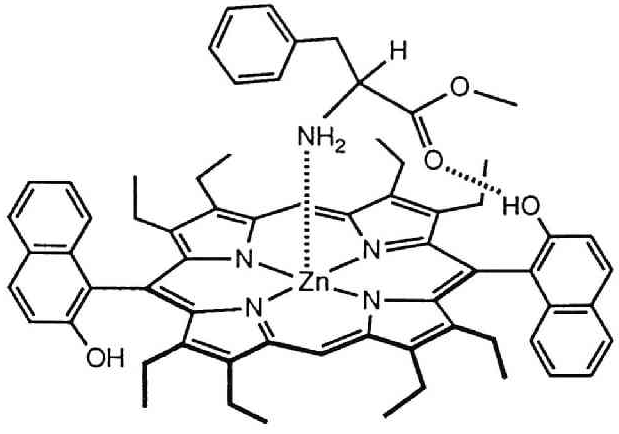

1-L-(or D-)Phe-OMe complex

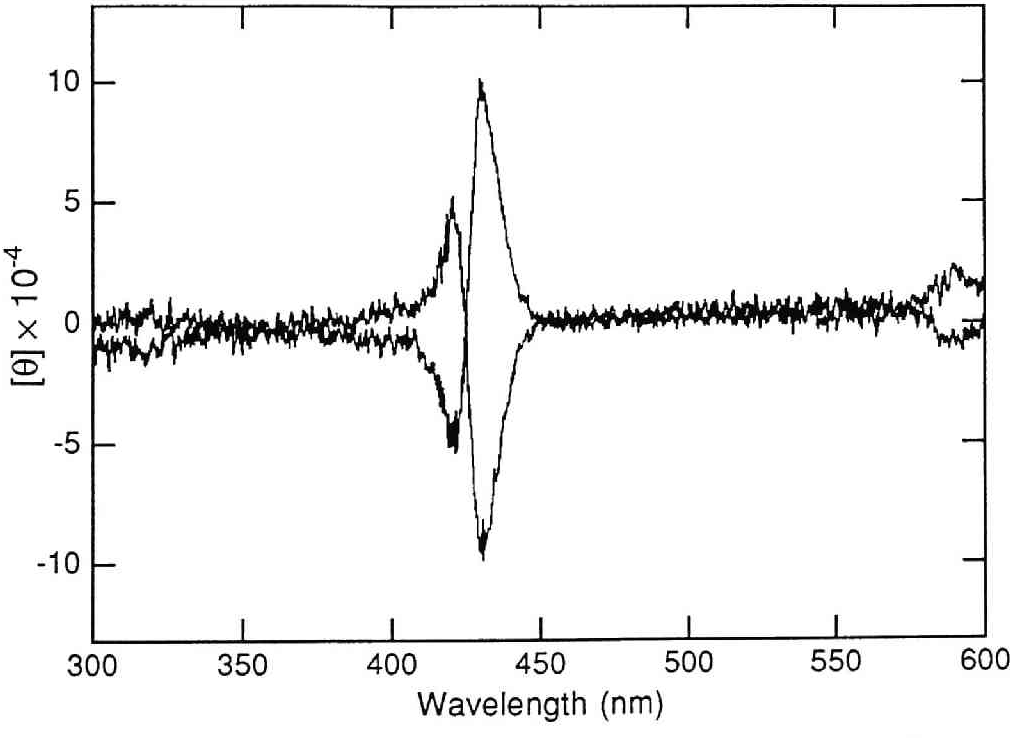

Figure 3(b). CD spectra of a solution of host **1** (4.8×10^{-6} M) and L- and D-phenylalanine methyl ester (3.3×10^{-3} M) in $CHCl_3$ at 15°C.

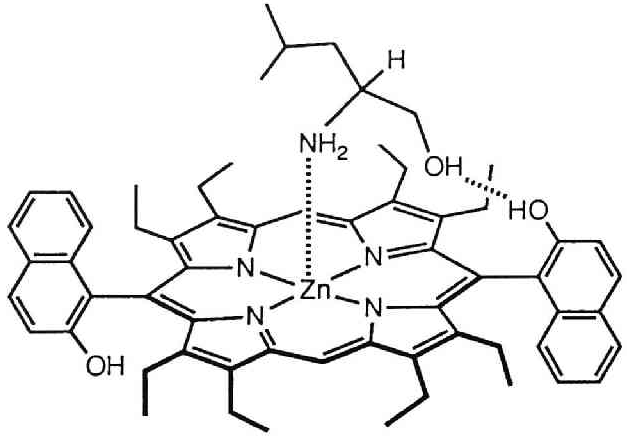

1-(*S*)-(or (*R*)-)leucinol complex

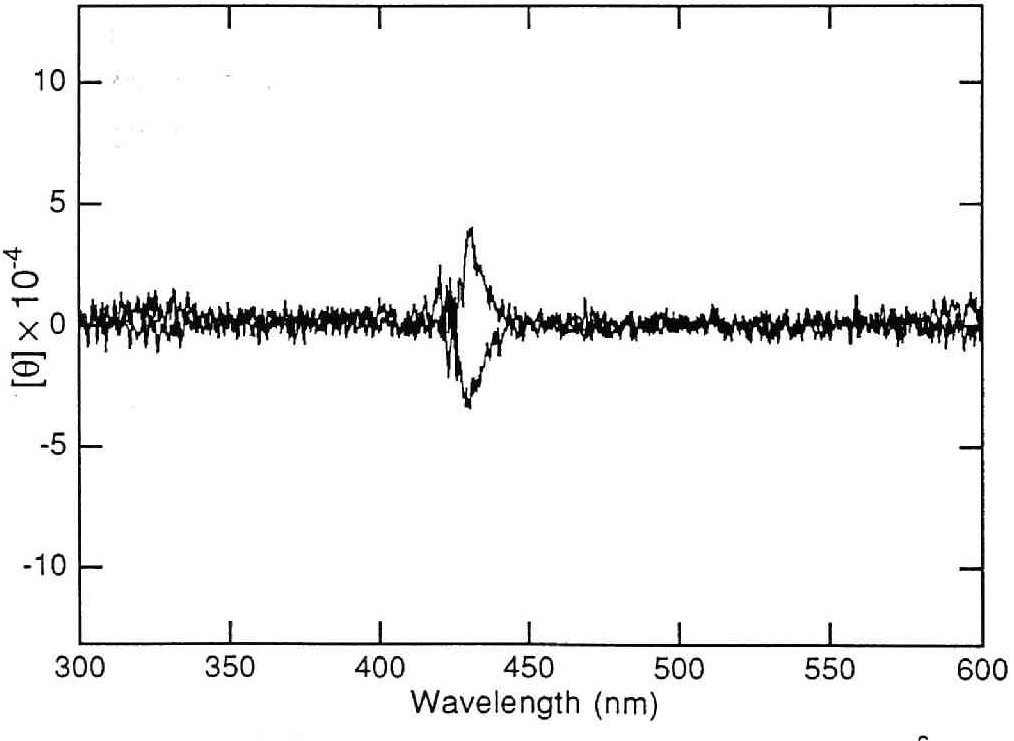

Figure 3(c). CD spectra of a solution of host **1** (4.8×10^{-6} M) and (*S*)- and (*R*)-leucinol (5.7×10^{-3} M) in $CHCl_3$ at 15°C.

constants (*vide supra*). Therefore, in the case of the complexes between host **1** and aromatic amino acid esters, two interactions (hydrogen bonding and aryl aryl interaction) give rise to contribute additively to the observed Cotton effects (*vide infra*).

The rotational strength induced in the Soret region of porphyrins complexed with amino acid esters are summarized in Table IV. The rotational strengths R_a were determined by means of the curve fitting method. Interestingly, in the case of the aliphatic amino acid esters, there is a good correlation between the magnitude of hydrogen bonding energies and the induced CD intensities. For example, Ala-OMe is bound to host **1** weakly, and the induced CD is also weak in intensity, whereas Leu-OMe is bound to host **1** strongly and the induced CD is also intense. The relationship between the rotational strength (Table IV) and the free energy of the hydrogen bonding (Table II) is plotted in Figure 4. These observations may reflect the tightness of the host – guest complex, where a less fluctuating carbonyl group will cause stronger induced CD. For aromatic amino acid esters (Phe-OMe, Trp-OMe, Phg-OMe), an obvious deviation from the correlation line is observed. Because the aromatic amino acid esters exhibited small single-sign Cotton effects upon complexation with the reference host **2**, the induced CD of **1** caused by Phe-OMe, Trp-OMe, and Phg-OMe can be understood as superposition of effects of two perturbers, the carbonyl group and the aromatic group. Other chromophores in the side chains (-COOMe, -SMe) did not show any drastic effects on the induced CD. These chromophores are extended far from the porphyrin plane and may be fluctuating when the amino group of the guest is coordinated to zinc. Among the chromophores in the side chain, only aromatic chromophores were found to make important contributions to the induced CD.

In order to investigate the contribution of the carbonyl group to the observed split Cotton effect, the CD spectra of **1**-or **2**– (*S*)-or (*R*)-leucinol complexes were

Table III. CD Induced in the Soret Region of Porphyrin Hosts **1** (or **2**) Complexed with Chiral Amino Acid Esters in $CHCl_3$ at 15°C. [a]

	1	$[\theta](\times 10^{-4})$[b]	**2**	$[\theta](\times 10^{-4})$[b]
	3.0	(421 nm)		
L – Ala - OMe	0.0	(426 nm)	___[c]	
	−2.6	(431 nm)		
	3.8	(422 nm)		
L – Asp- OMe	0.0	(425 nm)	___[c]	
	−4.2	(430 nm)		
	3.9	(422 nm)		
L – Glu- OMe	0.0	(425 nm)	___[c]	
	−3.1	(430 nm)		
	3.4	(421 nm)		
L – Met- OMe	0.0	(425 nm)	___[c]	
	−4.1	(430 nm)		
	8.5	(422 nm)		
L – Val - OMe	0.0	(426 nm)	___[c]	
	−7.8	(431 nm)		
	8.3	(422 nm)		
L – Leu - OMe	0.0	(425 nm)	___[c]	
	−9.9	(430 nm)		
	5.6	(421 nm)		
L – Leu - OBu^t	0.0	(426 nm)	___[d]	
	−8.7	(432 nm)		
	4.5	(422 nm)		
L – Phe - OMe	0.0	(425 nm)	−4.5	(426 nm)
	−9.3	(430 nm)		
	9.7	(422 nm)		
L – Trp - OMe	0.0	(426 nm)	−6.9	(427 nm)
	−15.1	(431 nm)		
	4.5	(420 nm)		
L – Phg - OMe	0.0	(424 nm)	−3.7	(424 nm)
	-11.1	(429 nm)		
(*S*) – leucinol	−2.7	(430 nm)	−3.2	(430 nm)[e]

[a] Induced CD spectra were also measured for D-amino acid esters. It was confirmed that the spectra were mirror images of the L-isomers. [b] Errors were within ± 10%. [c] Negligibly small. [d] Not measured for host **2** but negligibly small for host **3**. [e] Negligibly small for host **3**.

Table IV. The Rotational Strength of **1**-(or **2**-) Amino Acid Ester Complexes.[a]

Guest[b]	Host	λmax (nm)	R_a / 10^{-40}, cgs	λmax (nm)	R_a / 10^{-40}, cgs
Ala-OMe	**1**	424.5	19.2	429.3	-18.0
Asp-OMe	**1**	424.0	20.6	429.6	-20.3
Glu-OMe	**1**	422.9	16.1	429.9	-12.5
Met-OMe	**1**	422.1	10.9	428.1	-13.4
Val-OMe	**1**	424.5	31.5	430.2	-30.2
Leu-OMe	**1**	422.2	32.3	427.2	-36.5
Leu-OBu^t	**1**	425.0	30.7	430.3	-36.3
Phe-OMe	**1**	422.6	19.0	429.3	-29.9
Trp-OMe	**1**	423.0	38.3	429.1	-51.4
Phg-OMe	**1**	422.3	17.0	427.6	-26.3
leucinol	**1**	---[c]	---[c]	431.0	-3.6
leucinol	**2**	---[c]	---[c]	431.4	-3.1
Phe-OMe	**2**	425.0	-3.8	---[c]	---[c]
Trp-OMe	**2**	426.0	-1.7	---[c]	---[c]
PhgOMe	**2**	422.1	-5.7	---[c]	---[c]

[a] In $CHCl_3$ at 15°C. R_a values were calculated by the curve fitting analyses of CD spectra (see text.). [b]All guests were L-or (*S*)- configuration.
[c] Not observed.

measured. The Cotton effect induced in the Soret band was very weak and was not of split type (Figure 3 (c) and Table III). Based on the UV-vis spectral titration studies, it was confirmed that (*S*)-leucinol was hydrogen bonded to host **1** (Table II). The deviation from the correlation line is observed in Figure 4. Only structural difference between (*S*)-leucinol and L-Leu-OMe is the presence or absence of the carbonyl group. Therefore these observations indicate that the presence and the fixation of the carbonyl group are important for the split Cotton effects. Furthermore, the induced CD of the complex of **1** and L-Leu-OBu^t supported the above conclusion. The carbonyl group may be tilted in the hydrogen bonded complex due to the steric repulsions between the *tert*-butyl group and the porphyrin plane, leading to unsymmetrically induced CD (Table III).

All these data indicate that both the presence and the fixation of the carbonyl group is essential to the observed split Cotton effect and that orientational fixation of chromophores enhances the intensity of induced CD. This interesting phenomenon was named "anchor effect". Induced CD spectroscopy clearly reflected the molecular recognition mode. In the next chapter, the mechanisms of the induced CD of this supramolecular system are studied.

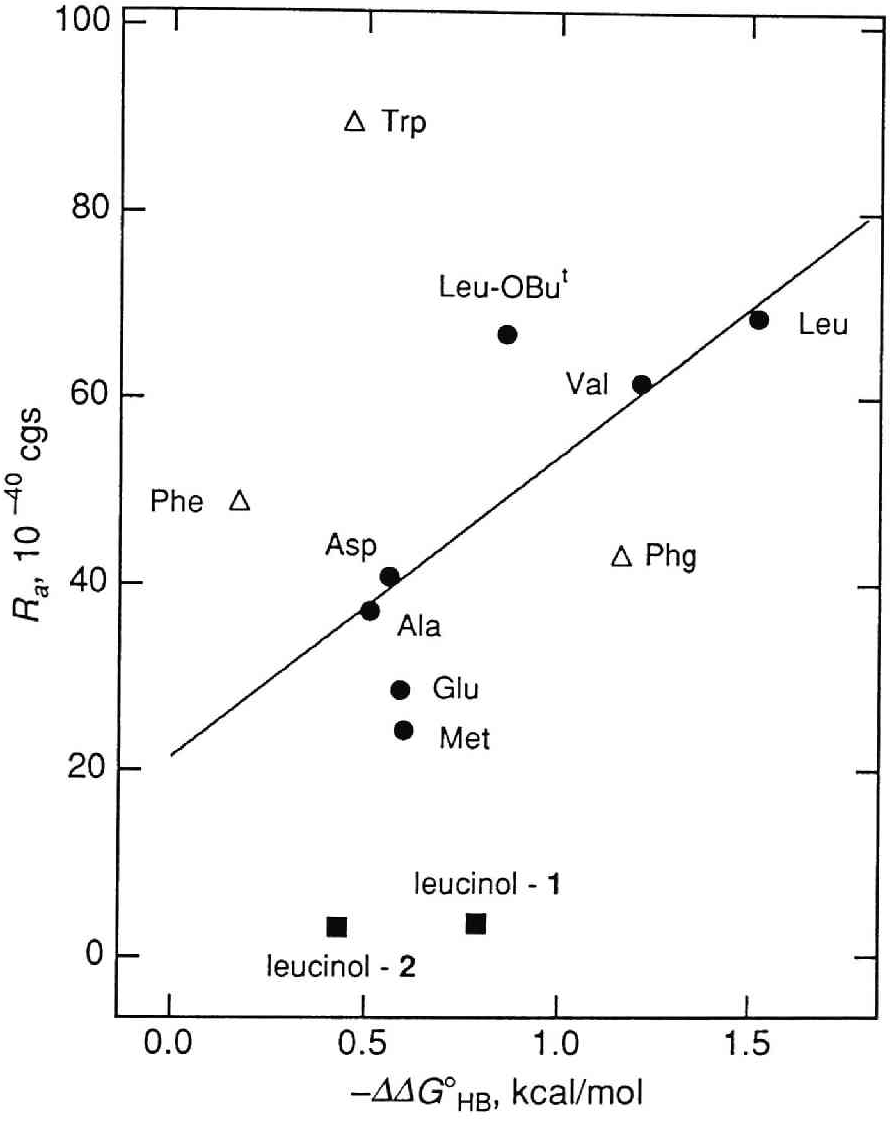

Figure 4. Plot of the rotational strengths(R_a) against the hydrogen bonding energy($-\Delta\Delta G^\circ_{HB}$).

Experimental Section

General Remarks. ^{1}H NMR spectra were recorded on either a JEOL A-500, or a JEOL GX-400, or a JEOL JNM FX 90Q FT NMR spectrometer, and chemical shifts are reported relative to internal Me_4Si. UV-vis spectra were recorded on either a Hitachi U-3410 spectrometer or a Hewlett-Packard 8452 diode array spectro photometer with a thermostatted cell compartment, and the $CHCl_3$ used in the UV-vis titration and in the CD measurement as solvent was Spectrosol purchased from Dojindo Laboratories, which contains *ca.* 1% ethanol as a stabilizer. Circular dichroism spectra were recorded on a JASCO J-600 spectropolarimeter with a thermostatted cell compartment, which is calibrated with an aqueous solution containing 0.06 wt% ammonium d-camphor-10-sulfonate. IR spectra were recorded on a Bio-rad FTS-7 FT-IR spectrometer. Mass Spectra were obtained with a JEOL JMS DX-300 mass spectrometer. Elemental analyses were performed at the Microanalysis Center of Department of Pharmacy of Kyoto University. Thin layer chromatography (TLC) was performed on Merck Kieselgel 60 F_{254}.

UV – vis Spectrophotometric Titration. To a solution of 3.4×10^{-6} ~ 5.3×10^{-6} M of **1** (or **2**, **3**) in chloroform was added a stock solution of α-amino acid ester in chloroform at 15℃ and changes in absorbance at 414~416 nm and at 428~430 nm of the Soret band were monitored at eight different concentrations of the guest molecules. The association constants were calculated assuming 1:1 complexation[11] by use of a computer-assisted non-linear least-square method within 4% error. The concentration range of α-amino acid esters was 3×10^{-5} ~ 1×10^{-2} M for host **1** and 3×10^{-4} ~ 7×10^{-2} M for hosts **2** and **3**.

Determination of the Rotational Strengths by Curve Fitting Analyses of CD Spectra. CD spectra of the solutions used in the UV-vis titrations were measured at 15℃. The molecular ellipticities were calculated

according to the formula with the following modification. Complexation-ratios calculated from the association constants were corrected into 100% by computer-assisted extrapolation, and the concentration diluted during the titrations were also corrected. For the split type Cotton effects, the rotational strength R_a was determined on the assumption that the induced CD is composed of two Gaussian curves with opposite signs. The following Gaussian functions were used: $a_1 \exp(-((\lambda-a_2) / a_3)^2) - a_4 \exp(-((\lambda-a_5) / a_6)^2)$ where a_1, a_2,a_3, a_4, a_5 and a_6 are parameters to be determined. In the case of the single-peaked Cotton effect, $a_1 \exp(-((\lambda-a_2) / a_3)^2)$ was used instead. The curve fitting was carried out by use of Igor, WaveMetrics, Inc.

Materials. Amino acid methyl ester hydrochlorides used were commercially available, or prepared from the corresponding amino acids by the thionyl chloride method.[12] (*S*)-(+)-or (*R*)-(-)-Leucinol were purchased from Aldrich Chemical Company, Inc. L-Leucine *t*-butyl ester (Leu-OBu^t) was purchased from Sigma Chemical Company. (*S*)-(+)-2-Phenylglycine methyl ester (abbreviated as L-Phg-OMe) was purchased from Kokusan Chemical Works. After neutralization and extraction with dichloromethane, all amino acid esters except tryptophan methyl ester were freshly distilled just before use for UV-vis titration, CD measurements or ^{1}H NMR titration experiments. 4-Heptylamine and *n*-butylamine were also commercially available and distilled.

trans–5, 15-Bis(2–hydroxy–1–naphthyl)-2, 3, 7, 8, 12, 13, 17, 18-octaethylporphyrin was prepared according to the reported method.[13] Zinc was incorporated by the method reported in the literature,[14] and the zinc complex **1** obtained was recrystallized from dichloromethane–hexane. mp >250℃ decomposition. TLC R_f 0.39 ($CHCl_3$); UV-vis ($CHCl_3$) λ_{max}: nm (log ε), 419 (5.45), 544 (4.26), 580 (4.09). FAB MS (3-nitrobenzyl alcohol matrix, chloroform solvent) shows a cluster of peaks at 881-888 amu (calcd for

$C_{56}H_{56}N_4O_2Zn{\bullet}H^+$ 881 and 883). Anal. Calcd for $C_{56}H_{56}N_4O_2Zn$: C, 76.22; H, 6.40; N, 6.35. Found: C, 75.45; H, 6.32; N, 6.15.

[*trans*–5, 15–Bis(2–methoxy–1–naphthyl)-2, 3, 7, 8, 12, 13, 17, 18-octaethylporphyrinato]zinc(II) (**2**) was prepared by methylation of the two hydroxyl groups of **1** with methyl iodide using potassium carbonate as a base in acetone, and purified by column chromatography on silica gel, followed by recrystallization from dichloromethane–hexane. mp > 300℃. TLC R_f 0.67 ($CHCl_3$). ^1H NMR($CDCl_3$, ppm) ; δ 0.85(t , 12H, CH_3) , 1.85(t, 12H, CH_3), 2.4(m, 4H, CH_2), 2.7(m, 4H, CH_2), 3.8(s, 6H, OCH_3), 4.0(m, 8H, CH_2), 6.5-8.5(m, 12H, naphthalene ring protons), 10.25(s, 2H, meso). IR(KBr) no OH. FAB MS (3-nitrobenzyl alcohol matrix, chloroform solvent) shows a cluster of peaks at 909-940 amu (calcd for $C_{58}H_{60}N_4O_2Zn{\bullet}H^+$ 909 and 911). UV–vis($CHCl_3$) λ_{max}: nm (log ε), 418(5.53), 544(4.27), 580(4.00). Anal. Calcd for $C_{58}H_{60}N_4O_2Zn$ $\bullet 2CH_2Cl_2$: C, 66.70; H, 5.97; N, 5.19. Found: C, 66.73; H, 5.98; N, 5.17.

trans–5, 15-Bis-(1-naphthyl)-2, 3, 7, 8, 12, 13, 17, 18-octaethylporphyrin was prepared according to the literature[13] and the zinc complex **3** was obtained in a usual manner.[14] Complex **3** was used as a trans and cis isomer mixture. mp > 300℃. TLC R_f 0.52 ($CHCl_3$:hexane = 1:1). UV-vis ($CHCl_3$) λ_{max}: nm (log ε), 416(5.55), 542(4.25), 578(4.00). FAB MS (3-nitrobenzyl alcohol matrix, chloroform solvent) shows a cluster of peaks at 849-854 amu (calcd for $C_{56}H_{56}N_4Zn{\bullet}H^+$ 849 and 851). Anal. Calcd for $C_{56}H_{56}N_4Zn{\bullet}CH_2Cl_2{\bullet}0.5C_6H_{14}$: C, 73.65; H, 6.70; N, 5.73. Found: C, 74.42; H, 6.45; N, 6.00.

References

(1) (a) Kyba, E. B.; Koga, K.; Sousa, L. R.; Siegel, M. G.; Cram, D. J. *J. Am. Chem. Soc.* **1973**, *95*, 2692. (b) Behr, K. -P. ; Lehn, J. M. *J. Am. Chem. Soc.* **1973**, *95*, 6108. (c) Peacock, S. C.; Cram, D. J. *J. Chem. Soc., Chem. Commun.* **1976**, 282. (d) Peacock, S. C.; Domeier, L. A.; Gaeta, F. C. A.; Helgeson, R. C.; Timko, J. M.; Cram, D. J. *J. Am. Chem. Soc.* **1978**, *100*, 8190. (e) Newcomb, M. ; Toner, J. L. ; Helgeson, R. C. ; Cram, D. J. *J. Am. Chem. Soc.* **1979**, *101*, 4941. (f) Rebek, J., Jr. ; Nemeth, D. *J. Am. Chem. Soc.* **1985**, *107*, 6738. (g) Tabushi, I. ; Kuroda, Y. ; Mizutani, T. *J. Am. Chem. Soc.* **1986**, *108*, 4514. (h) Rebek, J., Jr. ; Askew, B. ; Nemeth, D. ; Parris, K. *J. Am. Chem. Soc.* **1987**, *109*, 2432. (i) Aoyama, Y. ; Yamagishi, A. ; Asakawa, M. ; Toi, H. ; Ogoshi, H. *J. Am. Chem. Soc.* **1988**, *110*, 4076. (j) Mikros, E.; Gaudemer, A.; Pasternack, R. *Inorg. Chim. Acta* **1988**, *153*, 199. (k) Echavarren, A.; Galán, A.; Lehn, J.-M.; de Mendoza, J. *J. Am. Chem. Soc.* **1989**, *111*, 4994. (l) Sanderson, P. E.J.; Kilburn, J. D.; Still, W. C. *J. Am. Chem. Soc.* **1989**, *111*, 8314. (m) Aoyama, Y. ; Asakawa, M. ; Yamagishi, A. ; Toi, H. ; Ogoshi, H., *J. Am. Chem. Soc.* **1990**, *112*, 3145. (n) Verchere-Beaur, C.; Mikros, E.; Perree-Fauvet, M.; Gaudemer, A. *J. Inorg. Biochem.* **1990**, *40*, 127. (o) Famulok, M.; Jeong, K.-S.; Deslongchamps, G.; Rebek, J., Jr. *Angew. Chem. Int. Ed. Engl.* **1991**, *30*, 858. (p) Hong, J.-I.; Namgoong, S. K.; Bernardi, A.; Still, W. C. *J. Am. Chem. Soc.* **1991**, *113*, 5111. (q) Impellizzeri, G.; Maccarrone, G.; Rizzarelli, E.; Vecchio, G.; Corradini, R.; Marchelli, R. *Angew. Chem. Int. Ed. Engl.* **1991**, *30*, 1348. (r) Mikros, E.; Gaudemer, F.; Gaudemer, A. *Inorg. Chem.* **1991**, *30*, 1806. (s) Galán, A.; Andreu, D.; Echavarren, A. M.; Prados, P.; de Mendoza, J. *J. Am. Chem. Soc.* **1992**,

114, 1511. (t) Lipkowitz, K. B.; Raghothama, S.; Yang, J. *J. Am. Chem. Soc.* **1992**, *114*, 1554.

(2) (a) Houssier, C. ; Sauer, K. *J. Am. Chem Soc.*, **1970**, *92*, 779. (b) Philipson, K. D. ; Tsai, S. C. ; Sauer, K. *J. Phys. Chem.*, **1971**, *75*, 1440. (c) Hsu, M. C. ; Woody, R. W. *J. Am. Chem. Soc.*, **1971**, *93*, 3515.

(3) (a) Fiel, R. J.; Howard, J. C.; Mark, E. H.; Gupta, N. D. *Nucleic Acids Res.* **1979**, *6*, 3093. (b) Pasternack, R. F.; Giannetto, A.; Pagano, P.; Gibbs, E. J. *J. Am. Chem. Soc.* **1991**, *113*, 7799. (c) Rodley, G. A. ; Choon, O. C. *Inorg. Chim. Acta*, **1983**, *78*, 171.

(4) (a) Tinoco, I. *Adv. Chem. Phys.*, **1962**, *4*, 113.(b) Mizutani, T. ; Nakashima, R. *Chem. Lett.*, **1991**, 1491.

(5) To be submitted.

(6) (a) Tabushi, I.; Kuroda, Y.; Mizutani, T. *Tetrahedron* **1984**, *40*, 545.

(7) (a) Askew, B. ; Ballester, P. ; Buhr, C. ; Jeong, K. S. ; Jones, S. ; Parris, K. ; Williams, K. ; Rebek, J., Jr. *J. Am. Chem. Soc.* **1989**, *111*, 1082. (b) Tadayoni, B. M. ; Huff, J. ; Rebek, J., Jr. *J. Am. Chem. Soc.* **1991**, *113*, 2247. (c) Vincent, C. ; Hirst, S. C. ; Garcia Tellado, F. ; Hamilton, A. D. *J. Am. Chem. Soc.* **1991**, *113*, 5466.

(8) Host **2** did not show any Cotton effects in the presence of much more concentrated chiral amino acid ester. For example, no Cotton effects were observed for a solution of **2** in L-Val-OMe:$CHCl_3$ = 1:1 (v/v).

(9) Most of natural hemoproteins exhibit single peak CD in the Soret region, and some exhibit split Cotton effects: see Myer Y. P.; Pande, A. In *The Porphyrins*; Dolphin, D., Ed.; Academic Press: New York, 1978; Vol. 3, pp.271-322.

(10) Theoretical derivation indicates that, by use of CD titration, the only hydrogen-bonded complex can be detected and that the association constant for the

hydrogen-bonded complex and that for the non-hydrogen-bonded complex can be evaluated separately. However, the low S/N ratio made it impractical. The association constant for the **1**–L-Val-OMe complex determined by CD titration was 7.8×10^3 M^{-1}, in a good agreement to that determined by UV-vis titration.

(11) (a) Miller, J. R.; Dorough, G. D. *J. Am. Chem. Soc.* **1952**, *74*, 3977. (b) Kirksey, C. H.; Hambright, P.; Storm, C. B. *Inorg. Chem.* **1969**, *8*, 2141.

(12) Brenner, M. ; Huber, W. *Helv. Chim. Acta.* **1953**, *36*, 1109.

(13) Ogoshi, H. ; Sugimoto, H. ; Nishiguchi, T. ; Watanabe, T. ; Matsuda, Y. ; Yoshida, Z. *Chem. Lett.* **1978**, 29.

(14) Smith, K. M. In *Porphyrins and Metalloporphyrins*, Smith, K. M. Ed., Elsevier: Amsterdam. 1975; pp 884-885.

Chapter 2

Mechanism of Induced Circular Dichroism of Supramolecular Complexes.

Abstract

The mechanisms of induced CD of the porphyrin-amino acid ester supramolecular complexes were studied. Computational calculations for the Cotton effect induced in the Soret region were carried out according to the following mechanism: the two-point fixation of the amino acid esters results in effective coupling of the two nearly degenerate electric transition moments of the Soret band with the magnetic and electric transition moments of the carbonyl group of the amino acid esters. The geometries of porphyrin and glycine methyl ester were optimized by the MOPAC/MNDO method, and the Soret transitions were obtained by the CI calculation according to the Gouterman's four-orbital model. The orientation of the carbonyl chromophore was taken from the single crystal structure of a similar two-point adduct determined by X-ray analysis. Tinoco's perturbation theory was applied to the computational calculation of the rotational strength. The calculated rotational strengths were $R_a(B_x) = +5.7 \times 10^{-40}$ and $R_a(B_y) = -3.4 \times 10^{-40}$(esu•cm•erg•gauss^{-1}), which predicted split Cotton effect in accord with the observed spectral feature. Other mechanisms were also studied briefly, one of which was ruled out by the algebraic treatment. Implication to the hemoprotein CD are also described.

Introduction

Circular dichroism (CD) spectroscopy has been utilized to investigate chiral properties of organic compounds, because it reflects the absolute geometry of chromophores quite sensitively. It has also been widely used in protein chemistry to retrieve information on the secondary structure of the peptide backbone and on the structure around particular prosthetic groups.[1] The induced CD of porphyrin chromophore in hemoproteins has attracted the interest of numerous chemists, and has frequently been used as an important probe for the local structure around heme. Naturally occuring hemoproteins exhibit mostly single Cotton effects and some exhibit split type Cotton effects in the Soret region.[1, 2] Investigation of the origin of the induced CD is an important subject. Woody et al[3] reported that the aromatic moieties of the amino acid residues make important contributions to the induced CD of porphyrin of myoglobin and hemoglobin based on the molecular orbital calculations. These hemoproteins are structurally complex and many interactions will contribute to the induced CD. Therefore simplified model studies will be helpful in elucidating the mechanism of induced CD in hemoproteins.

It is demonstrated in chapter 1 that the complexes of [*trans*-5, 15–bis(2–hydroxy-1-naphthyl)-2, 3, 7, 8, 12, 13, 17, 18-octaethylporphyrinato] zinc (**1**) and optically active amino acid esters exhibited split Cotton effects in the Soret region, and both the presence and the fixation of the carbonyl group was essential to the split Cotton effect. In the present chapter, the mechanism of the induced CD are studied.

Results and Discussion

Mechanisms of Induced CD. Because the Soret band consists of two nearly degenerate transitions (B_x and B_y) in a porphyrin plane,[4] the two being perpendicular to each other, it is reasonable to assume that the positive and negative CD peaks observed for the amino acid ester porphyrin **1** complex are assignable to these two nearly degenerate transitions as shown in Figure 1. Then, splitting of the energy levels of the two Soret transitions should be very important. The energy levels of the two Soret transitions depend on the symmetry of the porphyrin chromophore. For example, the two transitions (B_x and B_y) of the highly symmetric porphyrins such as [octaethylporphyrinato]zinc(II), OEP(Zn), and [tetraphenylporphyrinato]zinc(II), TPP-(Zn), must be equivalent and completely degenerate because they belong to the D_{4h} symmetry. Therefore, they have tendency to show single-peaked Cotton effect in the Soret region. On the other hand, it is considered that the two Soret transitions of **1**, which belongs to the C_{2h} symmetry, are

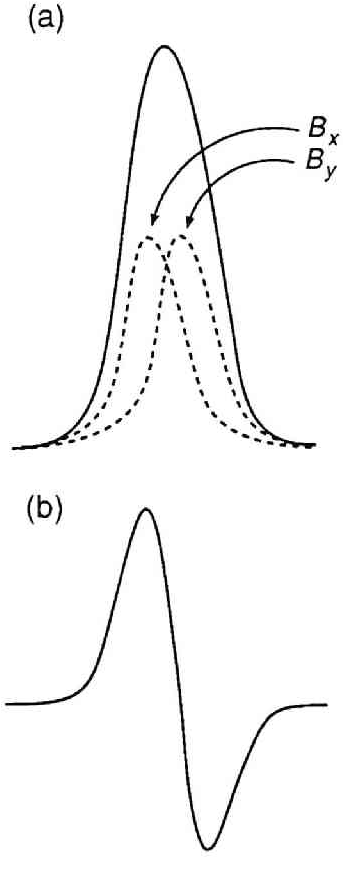

Figure 1. The assignment of the Cotton effects induced in the Soret region. (a) UV-vis spectrum. The Soret band consists of two nearly degenerate transitions (*Bx*, *By*). (b) CD spectrum in the Soret region. The split Cotton effects can be induced if the transition energy of the *Bx* are different from that of *By* .

Chart I.

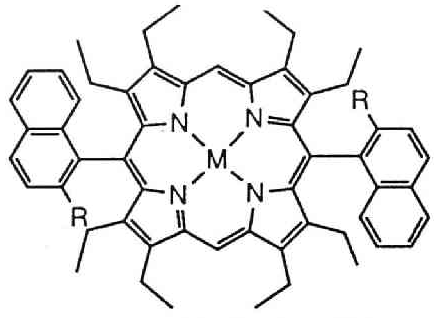

1 ; M = Zn, R = OH
6 ; M = Zn, R = OMe
2 ; M = Rh (Cl), R = OH

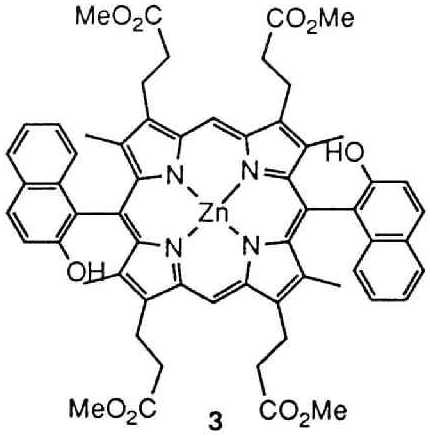

3

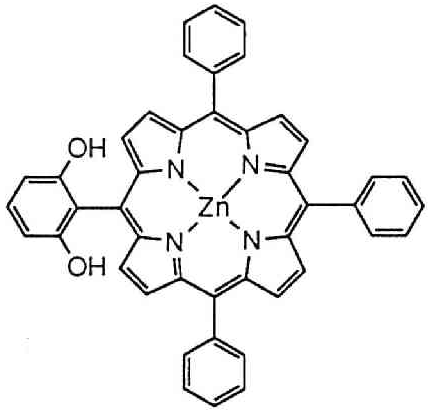

4

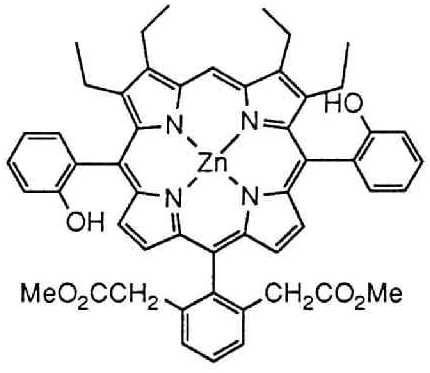

5

Table I. The Half-widths and the Rotational Strengths of the Soret Band of Porphyrin **1-5** - L-Leu-OMe Complexes. [a]

	Half-width,[b] nm	R_a / 10^{-40}, cgs[c]	
1	14	32.3 (422nm)	-36.5 (427nm)
2	26	29.8 (411nm)	-24.1 (427nm)
3	13	11.0 (420nm)	-19.0 (426nm)
4	10	——— [d]	
5	11	0.7 (425nm)	-1.4 (429nm)

[a] ^{1}H NMR and the association constants indicated that the carbonyl group of L-Leu-OMe is hydrogen bonded to the OH group of hosts (**1-5**). [b] Obtained directly from the UV-vis spectra. [c] Calculated from CD spectra as described in chapter 1. [d] Negligibly small.

nonequivalent, and that the two energy levels are different, which will allow the split Cotton effect to be observed as shown in Figure 1. Hosts **1**, **2**, and **3** have two naphthyl groups at meso positions along y axis and two hydrogens along x axis.(Figure 2) Therefore it is reasonable to assume that the transition energy of x polarization and that of y polarization will be different due to the substituent effects. In Table I are listed both the half-widths of the Soret band (B_x and B_y), which may reflect the degree of the energy splitting of the Soret band, and the rotational strengths induced in the Soret region. There is a qualitative relationship between the symmetry of the porphyrins, the half-widths, and the rotational strengths. The two-point complexes of **4** and **5** with L-Leu-OMe exhibited negligibly small or very weak induced CD in the Soret region. This observation can be ascribed to the near degeneracy of the B_x and B_y transition owing to the high symmetry. Therefore it should be stressed here that the two-point fixation of optically active amino acid esters above the porphyrin chromophore does not necessarily induce the split Cotton effect. The spectral feature of the induced CD partly depends on the symmetry and the electronic structure of the porphyrin derivatives.

The next question, which is the focus of this chapter, is what is the origin of the induced CD. Three possible mechanisms for the induced CD were proposed as follows:[5]

(1) Binding of the guest molecule to the host through coordination and hydrogen bonding interactions fixed the relative orientation of the two chromophores (the carbonyl group and the porphyrin group), and the coupling between the magnetic (the $n\pi^*$ transition) and/or electric (the $\pi\pi^*$ transition) transition moment of the carbonyl group and the electric transition moment of the porphyrin Soret band caused the induced CD (Figure 2(a)). (porphyrin-carbonyl coupling mechanism).

(2) The complexation with amino acid esters caused the tilting of the naphthyl group and the coupling between the electric transition moment of the naphthyl group and that of the porphyrin Soret region induced the observed CD. (porphyrin-naphthalene coupling mechanism).

(3) Chiral ruffling of the porphyrin plane caused by the complexation with chiral amino acid esters results in the induced CD. (porphyrin puckering mechanism).

These mechanisms can be classified into the two categories: (a) conformational change of the guest, to which the mechanism (1) belongs, and (b) conformational change of the host, to which the mechanism (2) and (3) belong.

Porphyrin-Carbonyl Coupling Mechanism. The coupling between the magnetic transition moment of a carbonyl group and the electric transition moment of ethylene or phenyl groups is considered to be an important origin of optical activity of many ketones.[6] For example, β, γ-unsaturated ketones show much larger CD than the corresponding saturated ketones. This enhancement in CD is attributed to the coupling between the magnetic transition moment of the carbonyl group and the electric transition moment of the ethylene group.[7] In the present supramolecular system, the similar coupling between the electric transition moment of porphyrin Soret band and the magnetic transition moment of the carbonyl $n\pi^*$ transition of the guest can cause the induced CD, although there is no covalent bond between the carbonyl group and the porphyrin moiety.

Several experimental results support this mechanism. As studied in chapter 1, all the complexes between amino acid esters (Ala-OMe, Asp-OMe, Glu-OMe, Met-OMe, Val-OMe, Leu-OMe, Leu-OBu^t, Phe-OMe, Trp-OMe, Phg-OMe) and host **1**, where hydrogen bonding between the carbonyl group of the guest and the hydroxyl group of the host is operating, exhibited split type Cotton effects. In contrast, the complexes between aliphatic amino acid esters and host **6**, where no

hydrogen bonding is operating, did not show any appreciable Cotton effects in the Soret region. Furthermore, a good correlation existed between the free energy of the hydrogen bonding and the CD intensity for a number of aliphatic amino acid ester-**1** complexes, as described in chapter 1. Therefore the hydrogen bonding is the driving force of the induced CD. Furthermore, the leucinol - host **1** complex exhibited very small induced CD, although the OH group of leucinol is hydrogen bonded to the OH group of **1**. All these results suggests that both the presence and the fixation of the carbonyl group are essential to the split type of the indued CD (in detail see chapter 1). Therefore we can assume that the hydrogen bonding to the carbonyl chromophore of the guest fixes the relative geometry of the carbonyl group, resulting in the split Cotton effects. The correlation observed between the free energy of the hydrogen bonding and the CD intensity implies that strong hydrogen bond will fix the carbonyl orientation in the host - guest complex, resulting in the strong induced CD. Weak hydrogen bond will allow the carbonyl group to fluctuate to some extent and it will bring about the averaging of the rotational strength for a range of conformers, and thus reduce the observed induced CD. The fact that the amino acid ester - host **6** complexes did not exhibited any induced CD in the Soret region except for Phe-OMe, Trp-OMe, and Phg-OMe is also consistent with the above mechanism, since no fixation of the carbonyl group can be expected in the amino acid ester - **6** complexes. The fact that the variation in the side chains (bulkiness, polarity etc.) did not affect the split pattern of induced CD indicates that the induced CD is caused by the interaction between the -$CH(NH_2)CO$- part of the amino acid ester and the porphyrin. The intensity of the induced CD varied with varying the side chains, suggesting that the magnitude of interaction changes with the side chains. Based on this mechanism the mobility of the guest in the complex can be sensitively detected by the induced CD measurements.

Computational Calculations. Tinoco's formalism was used to calculate the rotational strength induced in the Soret band by the interaction with the carbonyl group.[8] The basic assumption in that theory that the electrons in the molecule can be assigned to particular groups are valid in the present system, because the two chromophores (the carbonyl group and the porphyrin group) are well isolated. Delocalization or mixing of the wave functions of the carbonyl group to the wave functions associated with the porphyrin Soret transition was assumed to cause the induced CD. Expressions for the rotational strength by this mechanism were obtained by a perturbation approximation.[8] The coupling between the magnetic (the n-π^* transition, eq. (4)) and/or the electric (the π-π^* transition, eq. (3)) dipole transition moment of the carbonyl group and the electric transition moment (the π-π^* transition, eq. (2)) of the porphyrin chromophore were explicitly considered. The perturbation matrix and the rotational strength were calculated by using the equation (5) and (1), respectively.

$$R_a = \frac{2\nu_a \ \mathrm{Im}\ (V_{i0a\,;\,jb0}\ \overrightarrow{\mu_{i0a}} \cdot \overrightarrow{m_{jb0}})}{h\,(\,\nu_a^2 - \nu_b^2\,)} - \frac{2\pi}{c}\frac{\nu_a\,\nu_c\,V_{i0a\,;\,jc0}\ \overrightarrow{R_{ij}} \bullet \overrightarrow{\mu_{i0a}} \times \overrightarrow{\mu_{j0c}}}{h\,(\,\nu_a^2 - \nu_c^2\,)} \qquad (1)$$

$$\overrightarrow{\mu_{i0a}} = < \phi_{i0} \mid e\vec{r}_i \mid \phi_{ia} > \qquad (2)$$

$$\overrightarrow{\mu_{j0c}} = < \phi_{j0} \mid e\vec{r}_j \mid \phi_{jc} > \qquad (3)$$

$$\overrightarrow{m_{jb0}} = \frac{eh}{4\pi mci} < \phi_{jb} \mid \vec{r}_j \times \overrightarrow{\nabla}_j \mid \phi_{j0} > \qquad (4)$$

$$V_{ioa\,;\,jb0} = < \phi_{i0}\phi_{ia} \mid \frac{e^2}{r_{ij}} \mid \phi_{jb}\phi_{j0} > \qquad (5)$$

where i denotes group i (porphyrin), j denotes group j (carbonyl group), ϕ_{i0} and ϕ_{j0} represent the ground state of the chromophore i and j, respectively, ϕ_{ia} represents the singlet excited state of the porphyrin Soret transition, ϕ_{jb} represents the singlet

excited state of the carbonyl $n\pi^*$ transition, ϕ_{jc} represents the singlet excited state of the carbonyl $\pi\pi^*$ transition, R_{ij} is the distance between the center of the group i and that of the group j, and r_{ij} is the distance between the electron belonging to group i and the electron belonging to group j. ν_a, ν_b and ν_c are the transition wavenumbers for the Soret transition, $n\pi^*$ transition, and $\pi\pi^*$ transition of the carbonyl group, respectively, h is the Planck's constant, $-e$ is the electron charge, m is the electron mass, c is the velocity of light, and ∇ is the gradient operator. Molecular orbital calculations were carried out by use of the MOPAC/MNDO method to optimize the geometry of porphyrin **1** and glycine methyl ester.[9] For the calculation of the molecular orbitals of **1**, configuration interaction (CI) calculations were carried out according to the Gouterman's four orbital model.[4] The electric transition moment, the magnetic transition moment, and the perturbation matrix element were calculated by expressing the Slater's atomic orbital with Gaussian functions as follows.[10]

$$\phi_{i0} = \sum_m c_m \, exp\,(-\alpha_m \,|\, \vec{r} - \overrightarrow{R_m} \,|^2) \tag{6}$$

$$\phi_{ia} = \sum_n c_n \, exp\,(-\alpha_n \,|\, \vec{r} - \overrightarrow{R_n} \,|^2) \tag{7}$$

$$\phi_{j0} = \sum_p c_p \, exp\,(-\alpha_p \,|\, \vec{r} - \overrightarrow{R_p} \,|^2) \tag{8}$$

$$\phi_{jb} = \sum_q c_q \, exp\,(-\alpha_q \,|\, \vec{r} - \overrightarrow{R_q} \,|^2) \tag{9}$$

$$\phi_{jc} = \sum_r c_r \, exp\,(-\alpha_r \,|\, \vec{r} - \overrightarrow{R_r} \,|^2) \tag{10}$$

Whitten's lobe orbitals were employed to express the Gaussian functions.[11] The electric transition moment, the magnetic transition moment, and the matrix element were calculated by the following equations.

$$\overrightarrow{\mu_{i0a}} = \sum_m \sum_n e\, c_m\, c_n \left(\frac{\pi}{\alpha_m + \alpha_n}\right)^{3/2} \times exp\left(-\frac{\alpha_m\, \alpha_n}{\alpha_m + \alpha_n} \left|\overrightarrow{R_m} - \overrightarrow{R_n}\right|^2\right) \times \frac{\alpha_m \overrightarrow{R_m} + \alpha_n \overrightarrow{R_n}}{\alpha_m + \alpha_n} \tag{11}$$

$$\overrightarrow{m_{jb0}} = \frac{eh}{8\pi mci} \sum_p \sum_q c_p\, c_q \left(\frac{\pi}{\alpha_p + \alpha_q}\right)^{3/2} \times exp\left(-\frac{\alpha_p\, \alpha_q}{\alpha_p + \alpha_q} \left|\overrightarrow{R_p} - \overrightarrow{R_q}\right|^2\right) \times \frac{\alpha_p\, \alpha_q}{\alpha_p + \alpha_q} \overrightarrow{R_p} \times \overrightarrow{R_q} \tag{12}$$

$$V_{ioa\,;\,jbo} = \sum_m \sum_n \sum_p \sum_q \frac{2\pi^{5/2} e^2 c_m c_n\, c_p\, c_q}{(\alpha_m + \alpha_n)(\alpha_p + \alpha_q)(\alpha_m + \alpha_n + \alpha_p + \alpha_q)^{1/2}} \times exp\left(-\frac{\alpha_m\, \alpha_n}{\alpha_m + \alpha_n} \left|\overrightarrow{R_m} - \overrightarrow{R_n}\right|^2 - \frac{\alpha_p\, \alpha_q}{\alpha_p + \alpha_q} \left|\overrightarrow{R_p} - \overrightarrow{R_q}\right|^2\right) \times F_0\left(\frac{(\alpha_m + \alpha_n)(\alpha_p + \alpha_q)}{\alpha_m + \alpha_n + \alpha_p + \alpha_q} \times \left|\frac{\alpha_m \overrightarrow{R_m} + \alpha_n \overrightarrow{R_n}}{\alpha_m + \alpha_n} - \frac{\alpha_p \overrightarrow{R_p} + \alpha_q \overrightarrow{R_q}}{\alpha_p + \alpha_q}\right|^2\right)$$

$$F_0(x) = \frac{1}{2}\left(\frac{\pi}{x}\right)^{1/2} erf\left(\sqrt{x}\right) \tag{13}$$

The matrix element and the electric transition moment involving ϕ_{jc} can be similarly obtained.[10a)] For the Soret transition, CI calculations were carried out and the CI coefficients for the excited state α_1 and α_2 were used to calculate the electric transition moment and the matrix element as shown below.

$$\overrightarrow{\mu_{i0a}} = \alpha_1 \left\langle \phi_{i0} \left| \vec{er} \right| \phi_{ia1} \right\rangle + \alpha_2 \left\langle \phi_{i0} \left| \vec{er} \right| \phi_{ia2} \right\rangle \tag{14}$$

$$V_{i0a\,;\,jb0} = \alpha_1 \left\langle \phi_{i0}\, \phi_{ia1} \left| \frac{e^2}{r_{ij}} \right| \phi_{j0}\, \phi_{jb} \right\rangle + \alpha_2 \left\langle \phi_{i0}\, \phi_{ia2} \left| \frac{e^2}{r_{ij}} \right| \phi_{j0}\, \phi_{jb} \right\rangle \tag{15}$$

The calculated electric transition moments (B_x and B_y) for **1** were parallel to the C5 - C15, and C10 - C20 (meso carbons) axises (Figure 2(a)). This direction

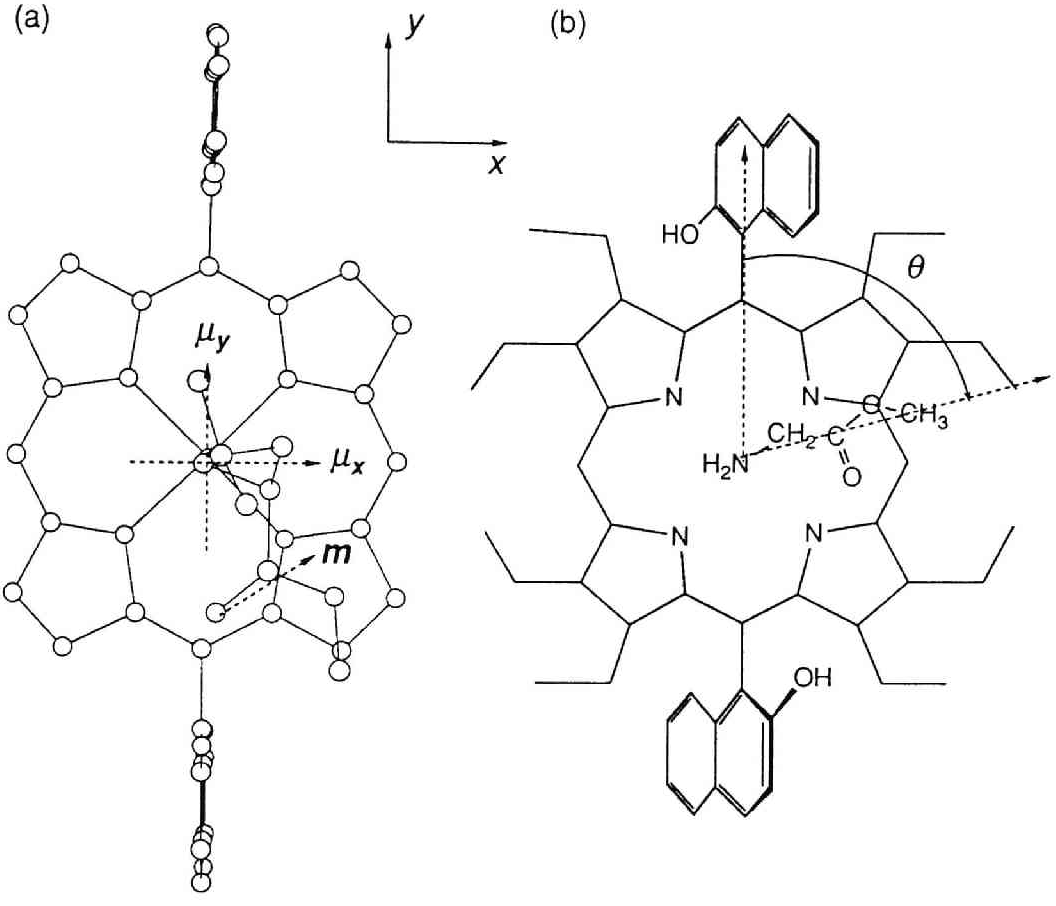

Figure 2. (a) The directions of the electric transition moments of the Soret band and that of the magnetic transition moment of the carbonyl group are shown by arrows. The direction of the electric transition moment of the carbonyl group is omitted for clarity. The orientation of Leu-OMe is taken from the X-ray single crystal structure of a similar complex. The eight ethyl groups at the β-positions are omitted for clarity. (b) Coordinate and angle θ for the complex between host **1** and glycine methyl ester. The glycine methyl ester was rotated at 15° increment, and the rotational strengths were calculated at each configuration.

of the transition moments is in agreement with those reported for iron porphyrin.[3,12] The magnetic transition moment of the carbonyl $n\pi^*$ transition and the electric transition moment of the carbonyl $\pi\pi^*$ transition calculated based on the optimized geometry of glycine methyl ester were found to be tilted toward the methoxy group approximately by 5° and 13° relative to the C=O axis, respectively. The glycine methyl ester was placed above the porphyrin plane with the carbonyl plane parallel to the porphyrin plane and the distance between the two planes was kept at 2.4Å according to the geometry observed in a crystal of a similar host guest complex.[13] (Glycine methyl ester is optically inactive, but each conformation, such as the absolute configuration shown in Figure 2(b), makes the complex to be chiral.) The angle θ was defined as shown in Figure 2(b). At θ = 45° and 135°, the carbonyl carbon was above the pyrrole nitrogen. The carbonyl group was rotated by 15° increment and the rotational strengths were calculated by the above equations for each configuration. The absorption maxima for the porphyrin Soret band and the carbonyl $n\pi^*$ and $\pi\pi^*$ bands were taken to be 420, 210, and 170 nm, respectively. The former value is the experimentally observed value for host **1** and the latters are that for ethyl acetate.[14] The results of the calculations are shown in Figure 3. For a particular region of θ, the coupling between the magnetic (or the electric) transition moment of the carbonyl group and the electric transition moment of the porphyrin caused the rotational strength in an opposite sign in B_x and B_y. This is reasonable because the two electric transition moments B_x and B_y are perpendicular to each other and if the orientation of the magnetic (or electric) transition moment is appropriate, then the relationship in space between B_x and B_y is pseudo-enantiomeric. The X-ray diffraction analysis of the crystals of a complex of a similar porphyrin with L-Leu-OMe indicated that the line connecting between the N atom of the amino group and the C atom of the carbonyl group of Leu-OMe bisects the two meso-meso

lines (θ = 135° in Figure 2(b)).[13] The calculated rotational strengths at θ = 135° were $R_a(B_x)$ = + 5.7 × 10^{-40} and $R_a(B_y)$ = -3.4 × 10^{-40}(esu•cm•erg•gauss^{-1}), which is consistent with the observed split feature. The experimental values of the rotational strengths obtained from the CD spectra was +32.3 × 10^{-40}, and –36.5 × 10^{-40} cgs for the L-Leu-OMe - host **1** complex, and +19.2 × 10^{-40}, and –18.0 × 10^{-40} cgs for the L-Ala-OMe - host **1** complex (Table IV in chapter 1).[15]

Figure 3 also indicates that the rotational strength is sensitive to changes in the relative geometry of the two chromophores (the carbonyl group and the porphyrin group). Most of the amino acid ester host **1** complexes exhibited symmetrically split induced CD. However the following three complexes showed unsymmetrically split Cotton effect: (1) aromatic amino acid ester host **1** complexes, (2) Leu-OBu^t host **1** complex, and (3) the Leu-OMe **3** complex. The unsymmetrically induced Cotton effects for aromatic amino acid ester-**1** complexes can be explained by the additional contribution from the electric transition moment of the aromatic side chain. The rotational strength arising from the coupling between the porphyrin Soret transition and benzene π-π^* transition was calculated by use of the same program in order to compare the relative importance of the carbonyl and aromatic chromophores. The benzene ring was placed similarly with its plane parallel to the porphyrin plane and the distance between the two planes were 2.4Å, and the angle between the benzene transition moment and the y axis in Figure 2(b) was θ=135°. The rotational strength was +11.7 × 10^{-40} esu•cm•erg•gauss^{-1} for B_x and –13.8 × 10^{-40} esu•cm•erg•gauss^{-1} for B_y transitions, respectively. These values were two to four times larger than those arising from the coupling with the carbonyl π-π^* transition. This result implies that the aromatic chromophore makes more important contribution to the induced CD than the carbonyl chromophore when fixed. The unsymmetrical induced CD observed for Leu-OBu^t-**1** complex suggests that the carbonyl group is tilting in the

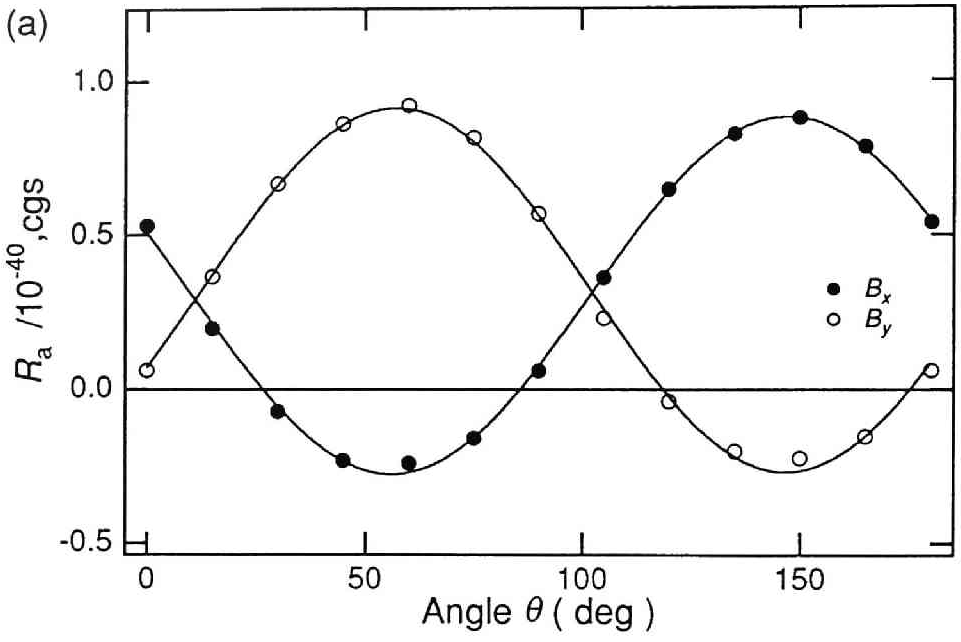
(a)
1.0
0.5
0.0
-0.5
R_a /10^{-40},cgs
0
50
100
150
Angle θ (deg)
B_x
B_y

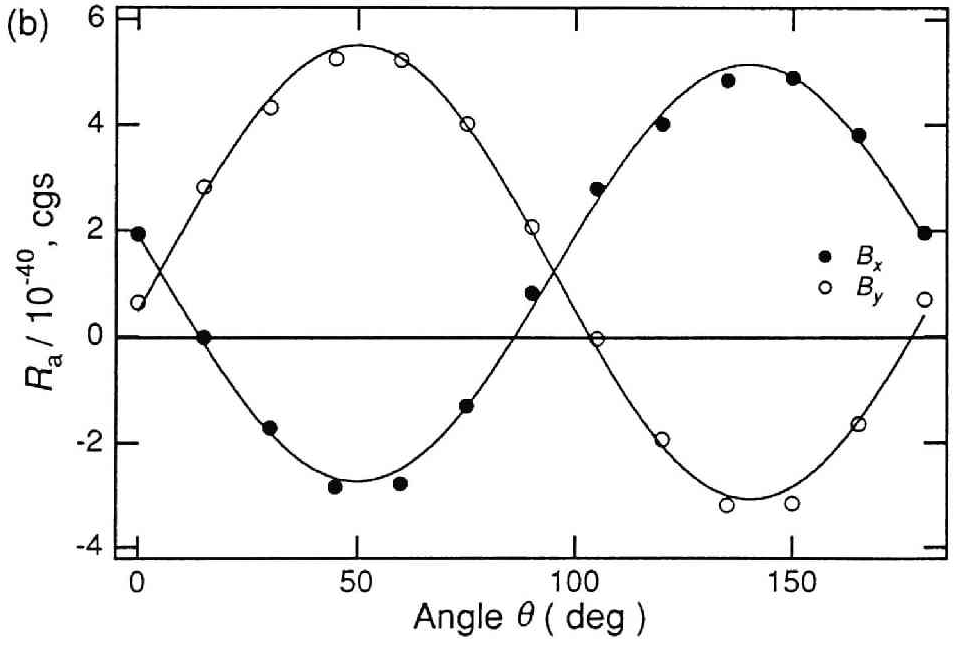
(b)
6
4
2
0
-2
-4
R_a / 10^{-40}, cgs
0
50
100
150
Angle θ (deg)
B_x
B_y

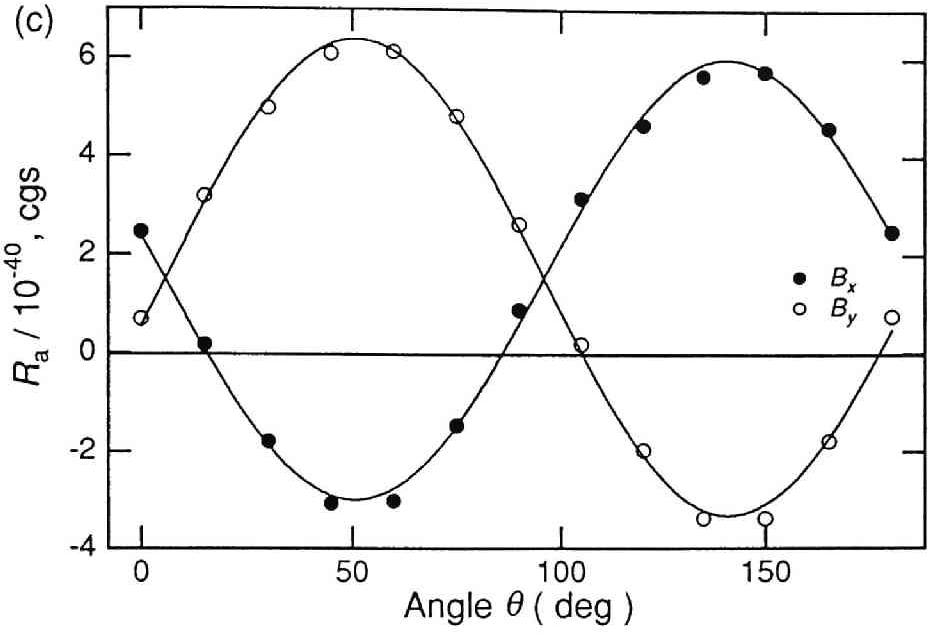

Figure 5. Rotational strength calculated by the perturbation approximation. (a) The rotational strength arising from the coupling between the magnetic transition moment of the carbonyl group ($n\pi^*$ transition) and the electric transition moment of the porphyrin Soret transition (B_x and B_y). (b) The rotational strength arising from the coupling between the electric transition moment of the carbonyl group ($\pi\pi^*$ transition) and the electric transition moment of the porphyrin Soret transition (B_x and B_y). (c) Sum of the above two contributions.

hydrogen bonding complex owing to the steric repulsion, and that observed for the Leu-OMe-**3** complex may reflect the slightly different configuration in the hydrogen bonding complex from that of Leu-OMe-host **1** complex due to steric repulsion between the methyl propionate substitutes of **3** and the amino acid esters ligated.

Porphyrin-Naphthalene Coupling Mechanism. This mechanism was easily ruled out by the algebraic treatment, with the result that the coupling between the naphthyl electric transition moment and the two Soret electric transition moments should induce the Cotton effects with the same sign in both B_x and B_y bands as shown in Figure 4.

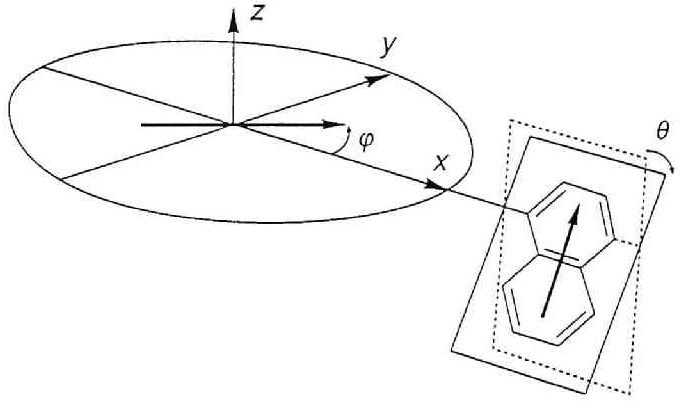

Figure 4. Orientation of electric transition dipole moments of porphyrin and naphthyl chromophores.

Based on Tinoco's theory,[8] the coupling between two electric transition dipole moments will give the rotational strength R_a:

$$R_a = -\frac{2\pi}{c}\frac{\nu_a \nu_b V_{i0a;jb0}\ \overrightarrow{R_{ij}} \cdot \overrightarrow{\mu_{i0a}} \times \overrightarrow{\mu_{j0b}}}{h\,(\nu_a^2 - \nu_b^2)} \qquad (16)$$

where ν_a and ν_b are the transition frequencies for the porphyrin Soret band and the $\pi - \pi^*$ transition of the naphthyl group, respectively, μ_{i0a} and μ_{jb0} are the electric transition dipole moments of the porphyrin Soret band and the $\pi - \pi^*$ transition of

the naphthyl group, respectively. The perturbation term $V_{ioa;jb0}$, the potential energy, can be calculated by use of the dipole-dipole approximation:

$$V_{i0a;jbo} = \frac{|\mu_i||\mu_j|}{|r_{ij}|^3}\left\{\mathbf{e}_i \cdot \mathbf{e}_j - 3(\mathbf{e}_i \cdot \mathbf{e}_{ij}) \cdot (\mathbf{e}_j \cdot \mathbf{e}_{ij})\right\} \tag{17}$$

where $\mathbf{e}_i$ and $\mathbf{e}_j$ are unit vectors parallel to the electric transition moment μ_{i0a} and μ_{jb0}, respectively, $\mathbf{e}_{ij}$ is a unit vector parallel to a line connecting centers of the chromophores of porphyrin and the naphthyl group. When we substitute $\mathbf{e}_i$ = (cos φ, sin φ, 0), $\mathbf{e}_j$ = (0, sin θ, cos θ), and $\mathbf{e}_{ij}$ = (1, 0, 0) in the above equations, where θ is a tilt angle of the naphthyl group and φ is an angle of electric transition dipole moments in the porphyrin plane (Figure 4), then we obtain

$$R_a \propto -\sin^2\varphi \sin\theta \cos\theta. \tag{18}$$

Therefore, the sign of the rotational strength does not vary even if the angle φ varies. This relation suggests that the induced CD caused by mechanism 2 cannot be of split type.

Porphyrin Puckering Mechanism. Some porphyrins such as peripherally crowded ones[17] and nickel complexes of porphyrins[18] have been reported to be nonplanar. Steric hindrance and coordination to a small metal ion are suggested to be the driving forces of nonplanarity, respectively. Therefore it is possible that the induced CD observed in the present system is also caused by the puckering of the porphyrin plane by complexation. For a puckered porphyrin, zinc tetraphenyl-octaethylporphyrin, nearly 30 nm red shifts and broadening of the Soret band have been observed, and this red shift is considered as a good evidence for the puckering along with the other experimental and theoretical results.[17] However,

in the present system, absorption maxima of host **1** are normal, indicating that no puckering occurred in an uncomplexed state. The maximum of the Soret peak of the complex between L-Leu-OMe and the methoxy derivative **6**, where no hydrogen bonding was observed and almost no induced CD was observed, was the same as that of L-Leu-OMe • **1** complex (428 nm). The Soret band was also very sharp. In the case of amino acid ester - host **1** complexes, the peak separation between B_x peak and B_y peak ranged from 5 nm to 7 nm, and can be considered as constant as the structure of amino acid ester changed (Table III and IV in chapter 1). ^{1}H NMR titration indicated that the signals of **1** did not shifted so much except the OH protons upon addition of amino acid esters. These results rather support the carbonyl coupling mechanism because the carbonyl coupling mechanism implies that the difference in the transition energies for the perpendicularly polarized transition is determined by the naphthyl substituent and should not vary with varying the guest structure. In contrast to that, according to the puckering mechanism the difference in the transition energies for the perpendicularly polarized transition can be varied depending on the extent of puckering caused by the intermolecular interactions. Driving forces for the puckering in the present system can be hydrogen bonding interaction or steric repulsion interaction. Almost all amino acid esters with varying side chains of bulkiness exhibited a similar induced CD pattern. It is difficult to explain this fact by puckering mechanism due to the steric repulsion. Molecular orbital calculations by the PM3 method also showed that the porphyrin plane in the Leu-OMe-**1** complex is almost planar, while the calculation by the same method can predict the nonplanarity of zinc tetraphenyloctaethylporphyrin.[19] However we have little information on the relationship between the degree of puckering and the intensity of the induced CD. Other good models will be required to investigate this interesting problem.

Implications to the Origin of Hemoprotein Induced CD. Induced CD of hemoprotein has been utilized as a useful probe of conformational change of proteins.[1] For example, it has been reported that binding of cytochrome c to cytochrome c oxidase, which induces a conformational change in both proteins as well as a change of the electronic structure of the heme of cytochrome c, can be monitored by the CD spectral change.[20] CD induced in the Soret region of myoglobin is primarily ascribed to the coupling with aromatic side chains of His, Phe, and Tyr.[3] Contribution from the peptide backbone is considered to be minor. In Figure 5, CD spectrum of horse heart myoglobin is shown. Single positive Cotton effect is induced in the heme Soret region.

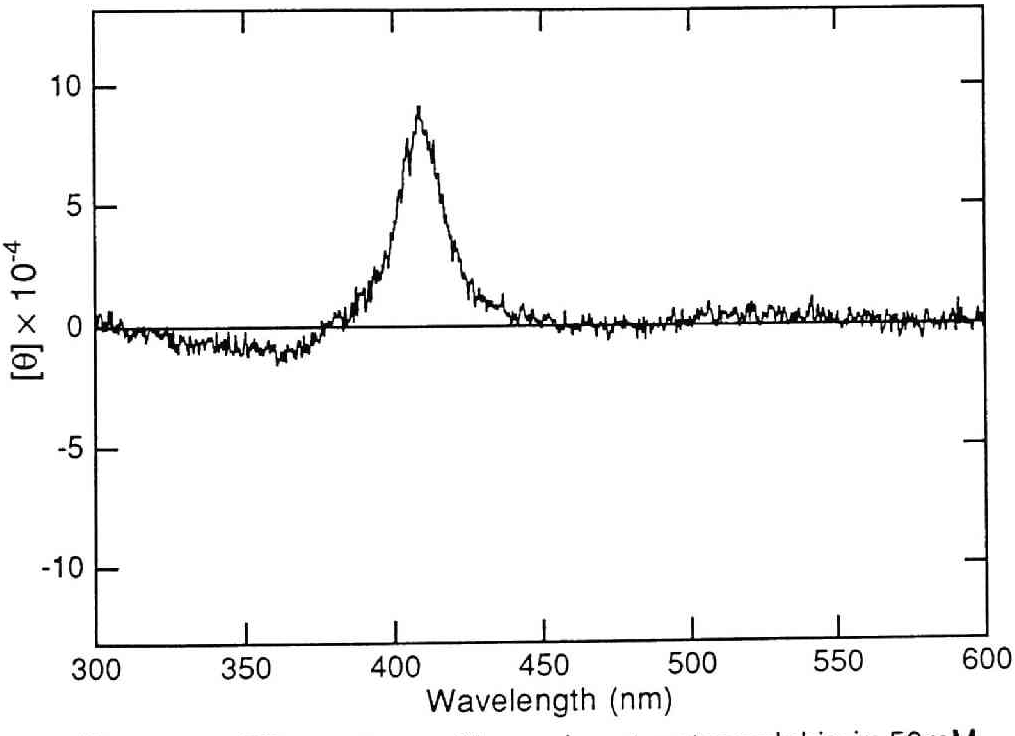

Figure 5. CD spectrum of horse heart metmyoglobin in 50mM phosphate buffer (pH7.0).

The rotational strengths in human oxy-, deoxy-, and methemoglobin are estimated to be +21, +35, and +28 $\times 10^{-40}$ cgs, respectively.[3] These values are comparable to those observed in our system (Table IV in chapter 1). The fact that only one chiral center can induce the comparable magnitude of CD as those of hemoprotein indicates that the induced CD of hemoprotein is caused by cancellation of many elemental interactions.[3] In the present two-point fixation system, comparison of the rotational strength between aromatic amino acid ester (R_a of 19 - 51 $\times 10^{-40}$ cgs) and aliphatic ones (R_a of 18 37 $\times 10^{-40}$ cgs) indicates that the additional contribution from the coupling to aromatic side chain is appreciable but not dominant (Table IV in chapter 1). In the one-point fixation system, the induced CD was also observed for the complex between aromatic amino acid esters and host **6**, where the guest molecule can freely rotate around the Zn and the guest N bond. This demonstrates that the aromatic side chain makes a contribution to the induced CD even if it is rotating. This is in sharp contrast with the carbonyl chromophore, which makes almost no contribution to the induced CD where free rotation is allowed in the **6** - aliphatic amino acid esters. The results shown in Table III and IV in the previous chapter indicate that coupling with aliphatic side chain (Me, Pr^i, Bu^i, $CH_2CH_2COOCH_3$, CH_2COOCH_3) is also negligibly small. These observations indicate that the coupling with the carbonyl group is more important than the coupling with aromatic side chains for the present system. However, the present results do not necessarily mean that the peptide carbonyl group should be more important for the induced CD in the case of hemoproteins than the aromatic residues because the mobility of the side chains in the present host - guest complexes is not particularly controlled. In hemoprotein, on the other hand, the aromatic side chains may be relatively fixed owing to the three dimensional structure of the proteins. Addtional recognition sites should be introduced to investigate the contribution of the side chain chromophores to the

induced CD.

The induced CD discussed above is considered to be caused by the spatial fixation of chromophore of the optically active guests by the noncovalent intermolecular interactions. Chiral disposition of chromophores around porphyrin by covalent bond will also cause induced CD. Consequently, the C_2 symmetric chiral porphyrin **10** intramolecularly bridged by the benzene rings was designed and synthesized as shown in Scheme I. The CD spectra of both enantiomers of **10** resolved by HPLC on an optically active column are shown in Figure 6. Intense Cotton effect is observed in the Soret region comparable with that of the hemoprotein such as myoglobin (cf Figure 5). The rotational strength of the Cotton effect induced in the Soret region of the first eluted enantiomer of **10** was -47.9×10^{-40} cgs. This value gives a good estimate of the rotational strength caused by fixed benzene chromophores, because the enantiomer of **7**, which has no bridging aromatic chromophore, showed very weak induced CD (less than one-tenth-fold of that of **10**) in the Soret region.

Scheme I.[a]

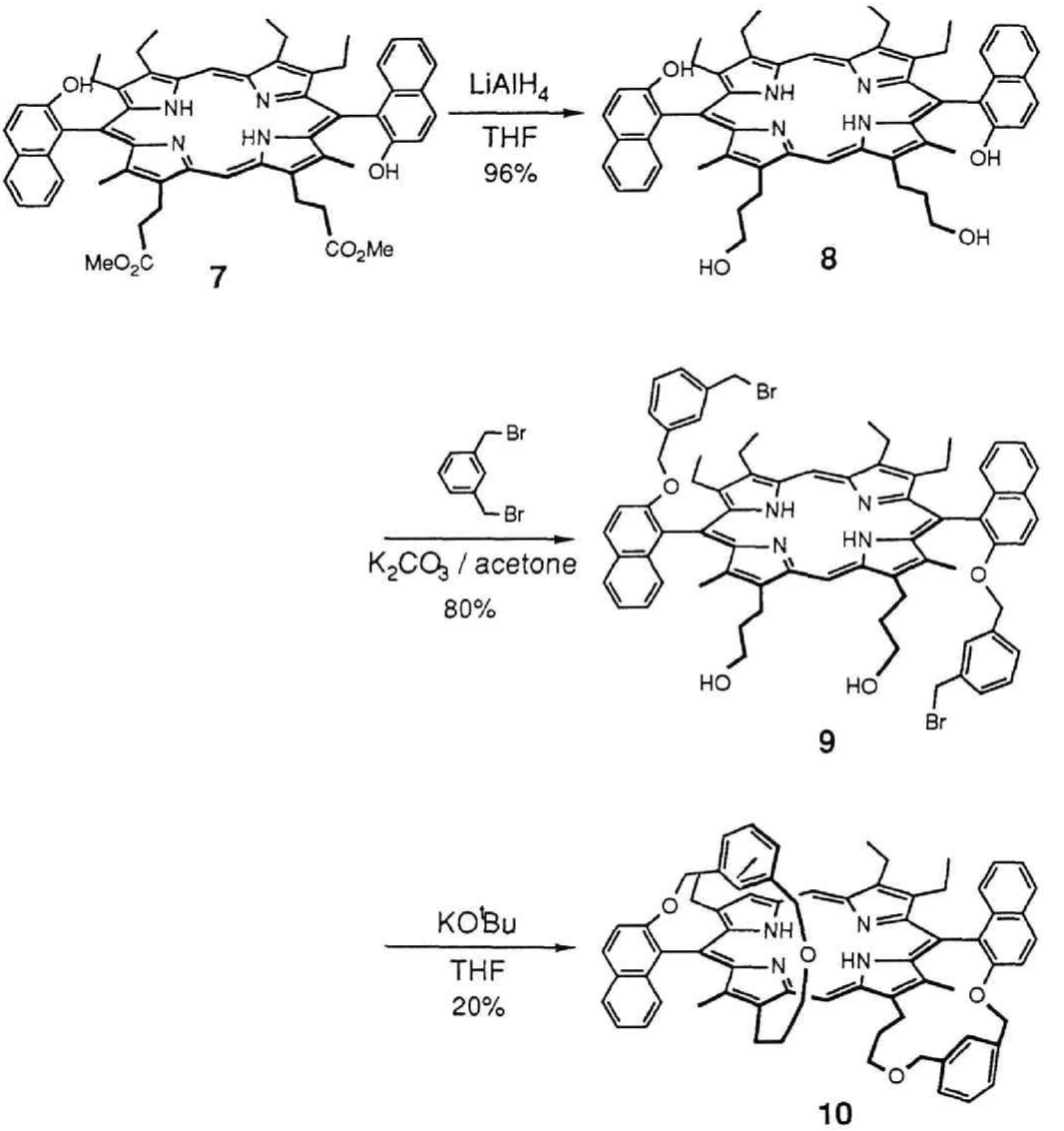

[a] The other enantiomers of **7-10** are omitted for clarity.

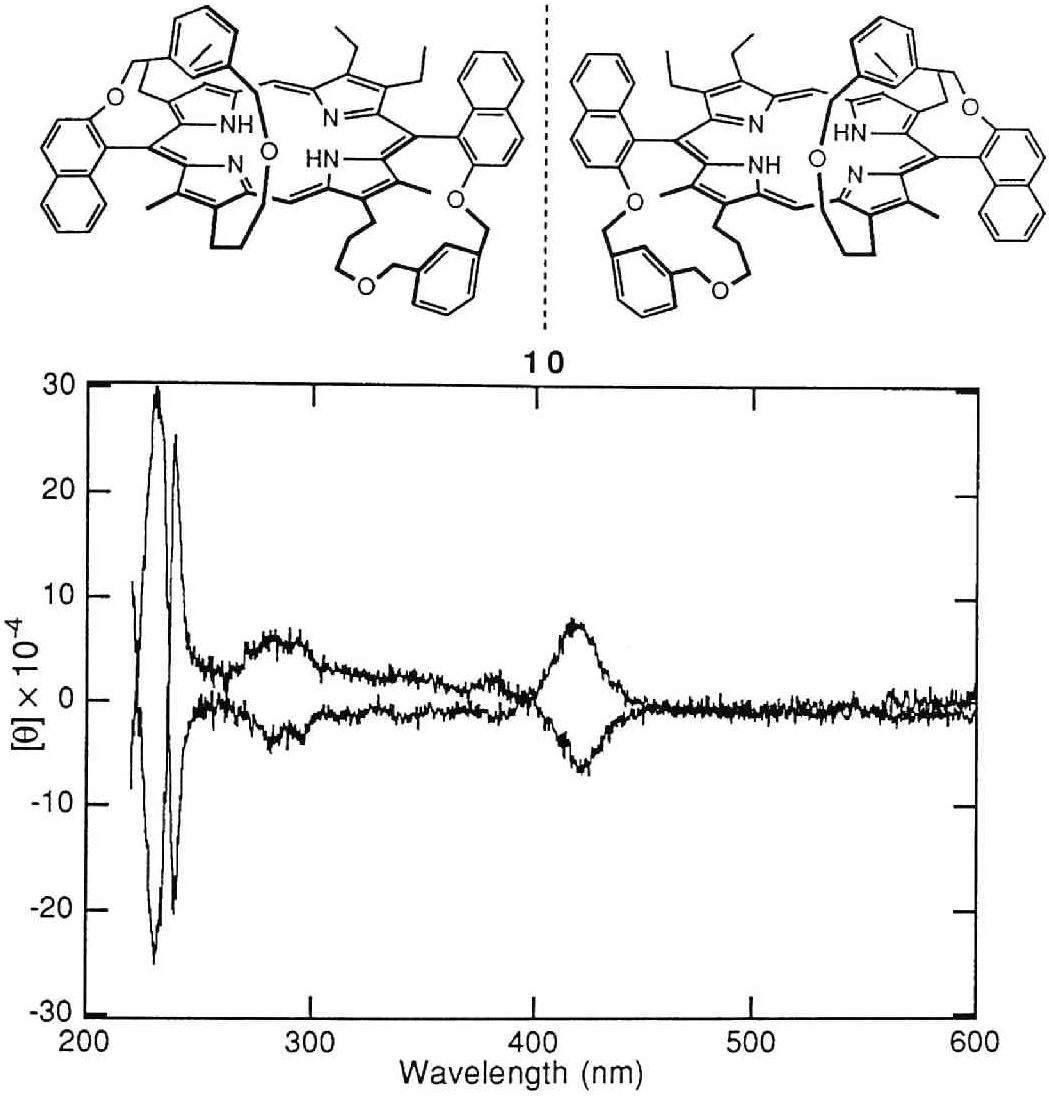

Figure 6. CD spectra of the chiral porphyrin **10** in hexane/EtOH (10/1). Optical resolution of **10** was performed by HPLC using CHIRALCEL OD column eluted with hexane/2-propanol (8/2). The first and second eluted enantiomer exhibit the negative and positive Cotton effect in the Soret region around 420nm, respectively.

Experimental Section

General Remarks. ^{1}H NMR spectra were recorded on either a JEOL JNM FX 90Q, a JEOL GX-400, or JEOL A-500 FT NMR spectrometer. IR spectra were recorded on a Bio-rad FTS-7 FT-IR spectrometer. UV-vis spectra were recorded on either a Hitachi U-3410 spectrometer or a Hewlett-Packard 8452 diode array spectrophotometer with a thermostatted cell compartment. Circular dichroism spectra were recorded on a JASCO J-600 spectropolarimeter with a thermostatted cell compartment, which is calibrated with an aqueous solution containing 0.06 wt% ammonium d-camphor-10-sulfonate. Mass Spectra were obtained with a JEOL JMS DX-300 mass spectrometer. High performance liquid chromatography (HPLC) was performed on a Waters Model 6000 instrument with a Waters 600E system controller and a Tosoh UV-8010 detector. Thin layer chromatography (TLC) was performed on Merck Kieselgel 60 F_{254}.

Computational Calculations. Molecular orbital calculations were performed by use of MOPAC/MNDO method.[9] The computer programs for the calculations of the rotational strength were written in FORTRAN 77 language. Numerical calculations were carried out either on a Hewlett Packered Apollo 9000 workstation, a Silicon Graphics IRIS Indigo XS 24 workstation, or a FACOM VP-2600 at the Data Processing Center of Kyoto University.

Materials. A chlororhodium (III) complex of *trans*-5,15-bis(2-hydroxy-1-naphthyl)-2,3,7,8,12,13,17, 18-octaethylporphyrin (**2**) was prepared similarly.[21] [*trans*-5,15-Bis(2-hydroxy-1-naphthyl)-3,7,13,17-tetramethyl-2,8,12,18-{tetra(2-methoxycarbonylethyl)}porphyrinato]zinc(II) (**3**) was prepared according to the literature.[21] {5-(2, 6-Dihydroxylphenyl)-10, 15, 20-triphenylporphyrinato}-zinc(II) (**4**) was prepared by the mixed aldehyde method.[22] [*trans*-5, 15-Bis(2-hydroxyphenyl)-10-{2, 6-bis(methoxycarbonylmethyl)phenyl}-2, 3, 17, 18-

tetraethylporphyrinato]zinc(II) (**5**) was prepared as shown in chapter 3.

***trans*-5, 15-Bis(2-hydroxynaphthyl)-8, 12-bis(3-hydroxypropyl)-7, 13-dimethyl-2, 3, 17, 18-tetraethylporphyrin (8).** A solution of *trans*-5, 15-bis(2-hydroxynaphthyl)-8, 12-bis(2-methoxycarbonylethyl)-7, 13-dimethyl-2, 3, 17, 18-tetraethylporphyrin (**7**)[21] (40 mg, 44 mmol) in dry THF (8 mL) was added dropwise to a suspension of $LiAlH_4$ (30 mg, 790 mmol) in dry THF (2 mL) under N_2. After the suspension was vigorously stirred for 30 min at room temperature under dark, the reaction mixture was poured into water carefully, extracted with ethyl acetate, dried over Na_2SO_4, evaporated to dryness. The product thus obtained was used in the following reaction without further purification: R_f 0.30 ($CHCl_3$:EtOAc = 1:3) ; ^1H NMR (200 MHz, d_5-pyridine) δ 1.34 (t, 6H, -CH_2CH_3), 1.83 (t, 6H, -CH_2CH_3), 2.53-2.66 (m, 4H, -$CH_2CH_2CH_2OH$), 2.70 (s, 6H, -CH_3), 2.98-3.15, 3.20-3.35 (dq, 4H, -CH_2CH_3), 3.88-4.09 (m, 4H, -CH_2CH_3), 4.18 (t, 4H, -$CH_2CH_2CH_2OH$), 4.27-4.50 (m, 4H, -$CH_2CH_2CH_2OH$), 7.06-8.50 (m, 12H, naphthyl), 10.41, 10.85 (s, 2H, meso), –1.62 (br s, 2H, NH); FABMS 851 (M+1); UV-vis ($CHCl_3$) λ_{max} (nm) 412.5, 510, 544, 574.5, 628.

***trans*-5, 15-Bis[2-(3-bromomethylbenzyloxy)naphthyl]-8, 12-bis(3-hydroxypropyl)-7, 13-dimethyl-2, 3, 17, 18-tetraethylporphyrin (9).** A mixture of the tetraol porphyrin derivative (**8**) (13 mg, 15.3 mmol), *m*-xylylene dibromide (116 mg, 440 mmol), and K_2CO_3 (20 mg, 145 mmol) in dry acetone (1 mL) was heated to reflux for 3 h under N_2 with vigorous stirring. After filtration to remove K_2CO_3, the solution was evaporated. The residue was purified by column chromatography (silica, $CHCl_3$) to obtain **9** (14.9 mg, 12.3 mmol, 80%). R_f 0.50 (SiO_2, $CHCl_3$:EtOAc = 1:1)); ^1H NMR (200MHz, $CDCl_3$) δ 0.80 (t, 6H, -CH_2CH_3), 1.8 (t, 6H, -CH_2CH_3), 2.1 (s, 6H, -CH_3), 2.2-2.4 (m, 4H, -$CH_2CH_2CH_2OH$), 2.5-2.8 (m, 4H, -CH_2CH_3), 3.2 (s, 4H, PhCH_2Br), 3.8-4.2 (m, 12H, -CH_2CH_3, -$CH_2CH_2CH_2OH$), 5.2 (d-d, 4H, OCH_2Ph), 10.3, 10.4 (s, 2H,

meso), –2.0 (br s, 2H, NH); IR (KBr) 3350 (OH), no C=O peak; FABMS 1215 ($M(2^{79}Br)^+$+1), 1216, 1217($M(^{79}Br^{81}Br)^+$+1), 1218, 1219($M(2^{81}Br)$)$^+$+1) ; UV-vis($CHCl_3$) λ_{max} 416.5, 511, 544, 578, 629.

Preparation of C_2-symmetric chiral porphyrin (10). The diol porphyrin derivative (**9**) (7.5 mg, 6.2 mmol) dissolved in a small amount of dry THF was quickly added to a solution of KO^tBu (100 mg, 893 mmol) in a dry THF(700 mL). The highly diluted solution (9 mM) was refluxed under Ar for 3 h. After the reaction was quenched with small amount of water, the solvent was removed by evaporator. The resultant reaction mixture was dissolved in $CHCl_3$ and passed through a short pad of Cerite to remove polymeric by-products. The crude product was purified by preparative TLC using $CHCl_3$/EtOAc (20:1) as an eluent (average yield was 20%). Recrystallization from CH_2Cl_2-MeOH gave purple needles : R_f 0.4 (SiO_2, $CHCl_3$:EtOAc = 20:1)) ; ^{1}H NMR (400 MHz, $CDCl_3$) δ 0.97 (t, 6H, -CH_2CH_3, *J* = 7.4Hz), 1.82 (t, 6H, -CH_2CH_3, *J* = 7.6Hz), 2.11 (s, 6H, -CH_3), 2.42 (dq, 2H, -CH_2CH_3), 2.7-2.9 (m, 4H, -$CH_2CH_2CH_2$-), 2.89 (dq, 2H, -CH_2CH_3), 3.5-3.65 (dq, 4H, -$CH_2CH_2CH_2O$-), 3.6-3.75 (m, 2H, -$CH_2CH_2CH_2O$-), 3.8-4.1 (m, 4H, -CH_2CH_3), 4.08 (d, 2H, -OCH_2Ph, *J* = 13.7Hz), 4.35-4.43 (m, 2H, -$CH_2CH_2CH_2O$-), 4.56 (d, 2H, OCH_2Ph, *J* = 13.8Hz), 4.79 (d, 2H, naphthyl-OCH_2Ph, *J* = 12.4Hz), 5.28 (d, 2H, naphthyl-OCH_2Ph, *J* = 12.5Hz), 6.81 (d, 4H, *J*=7.6Hz), 6.93 (t, 2H, *J* = 8.4Hz), 7.01 (d, 4H, *J* = 4.8Hz), 7.07 (s, 2H, phenyl), 7.31 (t, 2H, naphthyl, *J* = 8.0Hz), 7.66 (d, 2H, *J* = 9.2Hz), 8.11 (d, 2H, *J*=8.4Hz), 8.25 (d, 2H, *J* = 8.8Hz), 10.10 (s, 1H, meso), 10.23 (s, 1H, meso), –1.91 (br s, 2H, NH); high resolution FABMS Found, 1055.5470, Calcd., 1055.5480; UV-vis ($CHCl_3$) λ_{max} (log ε) 416.5(5.40), 510.5(4.28), 545(3.78), 577(3.90), 629(3.30). The racemic mixture of **10** was resolved by means of HPLC on an optically active column (CHIRALCEL OD, hexane : 2-propanol = 8:2).

References

(1) (a) Myer Y. P.; Pande, A. In *The Porphyrins*; Dolphin, D., Ed.; Academic Press: New York, 1978; Vol. 3, pp.271-322. (b) Woody, R. W.; Tinoco, I. *J. Chem. Phys.* **1967**, *46*, 4927.

(2) (a) Philipson, K. D.; Tsai, S. C.; Sauer, K. *J. Phys. Chem.* **1971**, *75*, 1440. (b) Houssier, C.; Sauer, K. *J. Am. Chem. Soc.* **1970**, *92*, 779-791. (c) Gonzalez, M. C.; Weedon, A. C. *Can. J. Chem.* **1985**, *63*, 602.

(3) Hsu, M.-C.; Woody, R. W. *J. Am. Chem. Soc.* **1971**, *93*, 3515.

(4) (a) Gouterman, M. *J. Mol. Spectroscopy* **1961**, *6*, 138-163. (b) Gouterman, M.; Wagniere, G. H. *J. Mol. Spectroscopy* **1963**, *11*, 108-127.

(5) Possibilities that the split Cotton effects were caused by porphyrin–porphyrin aggregation are excluded because the concentration of the porphyrin is as low as 5×10^{-6} M and the naphthyl groups should prevent π–π stacking of the porphyrin planes. ^{1}H NMR spectroscopy also indicated that no self-aggregation occurs at a higher concentration of the host **1**.

(6) (a) Moscowitz, A.; Mislow, K.; Glass, M. A. W.; Djerassi, C. *J. Am. Chem. Soc.* **1962**, *84*, 1945-1955. (b) Moscowitz, A.; Hansen, A. E.; Forster, L. S.; Rosenheck, K. *Biopolym. Symp.* **1964**, *1*, 75-89. (c) Snatzke, G. *Optical Rotatory Dispersion and Circular Dichroism in Organic Chemistry*; Heyden and Son Ltd.: London, 1967; .

(7) (a) Labhart, H.; Wagniere, G. *Helv. Chim. Acta* **1959**, *42*, 2219-2227. (b) Schippers, P. H.; Dekkers, H. P. J. M. *J. Am. Chem. Soc.* **1983**, *105*, 79-84.

(8) (a) Tinoco, I. *Adv. Chem. Phys.* **1962**, *4*, 113-160. (b) Mizutani, T.; Nakashima, R. *Chem. Lett.* **1991**, 1491-1494. (c) Mizutani, T.; Nakashima, R. *Chem. Lett.* **1991**, 2131-2134.

(9) MOPAC Ver. 5 and Ver. 6, Stewart, J. J. P. *QCPE Bull.* **1989**, *9*, 10.

(10) (a) Donkersloot, M. C. A.; Buck, H. M. *J. Mol. Structure (Theochem)* **1986**, *137*, 347-364. (b) Mizutani, T.; Nakashima, R. *Chem. Lett.* **1991**, 1491-1494. (c) Mizutani, T.; Nakashima, R. *Chem. Lett.* **1991**, 2131-2134.

(11) Whitten, J. L. *J. Chem. Phys.* **1963**, *39*, 349.

(12) (a) Du, P.; Loew, G. H. *J. Phys. Chem.* **1991**, *95*, 6379-6383. (b) Eaton, W. A.; Hofrichter, J. In *Methods in Enzymology*; Antonin, E.; Rossi-Barnardi, L. Chiancone, E.; Academic Press: New York, 1981; Vol. 76, pp 175 .

(13) Ogoshi, H., ; Masuda, H., ; Uzawa, T. ; Aoyama, Y. Unpublished results.

(14) (a) Schreibe, G.; Povenz, F.; Linström, C. F. *Z. Phys. Chem.* **1933**, *20*, 283. (b) Silverstein, R. M.; Bassler, G. C.; Morrill, T. C. *Spectroscopic Identification of Organic Compounds*; John Wiley & Sons, Inc.: New York, 1981.

(15) The small calculated values are consistent with the results for unsaturated ketones, where the similar calculation gave the rotational strength one order of magnitude smaller than experiment.[16] cgs = esu•cm•erg•gauss^{-1}

(16) Mizutani, T.; Ema, T.; Ogoshi, H. To be published.

(17) (a) Barkigia, K. M.; Chantranupong, L.; Smith, K. M.; Fajer, J. *J. Am. Chem. Soc.* **1988**, *110*, 7566-7567. (b) Barkigia, K. M.; Berber, M. D.; Fajer, J.; Medforth, C. J.; Renner, M. W.; Smith, K. M. *J. Am. Chem. Soc.* **1990**, *112*, 8851.

(18) Shelnutt, J. A.; Medforth, C. J.; Berber, M. D.; Barkigia, K. M.; Smith, K. M. *J. Am. Chem. Soc.* **1991**, *113*, 4077-4087.

(19) X-ray crystallographic analysis of zinc tetraphenyloctaethylporphyrin showed that β protons of pyrrole rings displaced by ~1Å relative to the plane of the four nitrogens.[21b] The calculation by the MOPAC/PM3 method (MOPAC Ver. 5 and Ver. 6, Stewart, J. J. P. *QCPE Bull.* **1989**, *9*, 10.) showed that the displacement was about 0.45Å.

(20) Weber, C.; Michel, B.; Bosshard, H. R. *Proc. Natl. Acad. Sci. USA* . **1987**, *84*, 6687.

(21) (a) Aoyama, Y.; Yamagishi, A.; Tanaka, Y.; Toi, H.; Ogoshi, H. *J. Am. Chem. Soc.* **1987**, *109*, 4735. (b) Aoyama, Y.; Uzawa, T.; Saita, K.; Tanaka, Y.; Toi, H.; Ogoshi, H. *Tetrahedron Lett.* **1988**, *29*, 5271. (c) Ogoshi, H.; Sugimoto, H.; Nishiguchi, T.; Watanabe, T.; Matsuda, Y.; Yoshida, Z. *Chem. Lett.* **1978**, 29.

(22) (a) Little, R. G.; Anton, J. A.; Loach, P. A.; Ibers, J. A. *J. Heterocyclic Chem.* **1975**, *12*, 343. (b) Walker, F. A.; Balke, V. L.; McDermott, G. A. *Inorg. Chem.* **1982**, *21*, 3342. (c) Milgrom, L. R. *J. Chem. Soc., Perkin Trans.* 1, **1984**, 1483.

Chapter 3

Design and Synthesis of Trifunctional Chiral Porphyrin according to New Synthetic Method.

Abstract

Trifunctional chiral porphyrin host, [*trans*-5, 15-bis(2-hydroxyphenyl)-10-{2, 6-bis(methoxycarbonylmethyl)phenyl}-2, 3, 17, 18-tetraethylporphyrinato] zinc(II) (**1**), was designed to have three recognition elements; metal coordination, hydrogen bond donor, and steric repulsion (and/or hydrogen bond acceptor) groups. These groups are arranged in a convergent fashion, forming a chiral recognition environment. **1** was synthesized in a stepwise manner and fully characterized. The key reaction step is the selective condensation between two differently functionalized dipyrrylmethanes (**8** and **16**). **8** has hydroxyl groups at the α-methines of the dipyrrylmathane to accomplish the selective attack at the α-positions of the other α, α-free dipyrrylmethane **16** in acidic condition. The reference porphyrin hosts **2**-**4** which lack one or two of the three recognition groups were also prepared according to the newly developed synthetic method.

Introduction

Many elegant synthetic methods for unsymmetrical porphyrin derivatives, including naturally occurring cyclic tetrapyrroles such as chlorophyll, have been extensively developed,[1] but most of the selective synthetic methods for unsymmetrical porphyrins can not necessarily be applicable to the *meso*-aryl substituted porphyrins such as 5, 10, 15, 20-tetraphenylporphyrin (TPP) derivatives. Conventional mixed-aldehyde method gives a mixture of many kinds of *meso*-aryl porphyrins, which should be followed by laborious and difficult chromatographic separation.[2] Recently, stepwise synthetic strategies for *meso*-aryl substituted unsymmetrical porphyrin have been developed by Smith's group[3] and by Ogoshi's group[4] independently.

In this chapter, trifunctional chiral porphyrin **1** with C_2 symmetry shown in Chart I is designed and synthesized according to the newly developed synthetic strategy.

Chart I.

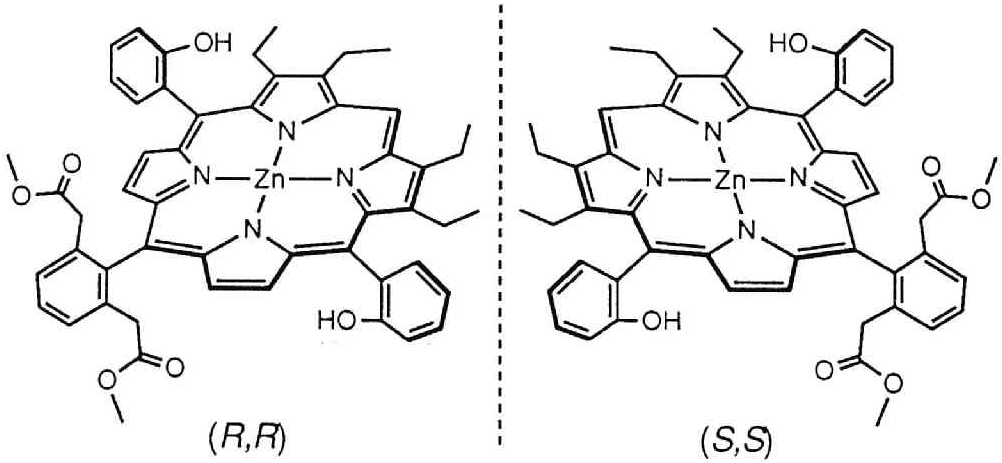

1

Results and Discussion

Molecular Design. In order to achieve chiral recognition, at least three recognition groups should be spatially arranged in a convergent manner to constitute a chiral binding pocket. Starting from the structure of the bifunctional porphyrin studied in chapter 1, new trifunctional chiral porphyrin host **1** was designed as shown in Chart I. Host **1** has a metal coordination site (the zinc ion), a hydrogen bonding site (the phenolic hydroxyl group), and a steric repulsion and/or hydrogen bonding acceptor site (the methoxycarbonyl group). These three groups with varying recognition abilities form a chiral recognition environment. The chiral binding sites above and below the porphyrin plane are equivalent each other, and the whole molecule belongs to the C_2 symmetry. Both of the OH and CH_2CO_2Me groups are introduced into the ortho positions of the *meso*-phenyl moieties to maximize intermolecular contact with guest molecules. Zinc ion was used because the zinc complex of porphyrin is known to form only a 1:1 complex.[5] In the design of host **1**, four ethyl groups on the β-position of pyrrole were introduced (1) to prevent the free rotation of the *o*-hydroxyphenyl groups (atropisomerism[6]), (2) to improve solubility of hosts in organic solvents, and (3) to facilitate synthesis of dipyrromethane (*vide infra*). It is quite important to give rigidity to the host structure and to fix the distance between recognition groups, because flexibility of the recognition site will reduce the selectivity of molecular recognition considerably. Reference hosts **2**-**4**, where two recognition groups (OH or CH_2CO_2Me groups) or both of them are replaced with hydrogen, were also designed to investigate the roles of each recognition group in thermodynamics of the binding process.

Synthetic Strategy. Retrosynthetic analysis of **1** is shown in Scheme I. The target unsymmetrical porphyrin skeleton should be constructed from two kinds of differently functionalized dipyrrylmethane; a dipyrrylmethane unit having *o*-methoxyphenyl groups, and a dipyrrylmethane unit having 2, 6-bis(methoxycarbonylmethyl)phenyl moiety. The former has hydroxylmethine groups at α-position of the dipyrrylmethane, which would be very acid-labile, and would attack the latter α,α'-free dipyrrylmethane to give the target unsymmetrical porphyrin skeleton selectively. Each symmetrical dipyrrylmethane unit would be prepared by condensation of the pyrrole derivatives as shown in Scheme I. Such a stepwise synthetic strategy will lead to a well-defined molecular architecture and meet well the concept of molecular preorganization.[7] On the other hand, conventional cyclization of pyrroles and aldehydes (the mixed-aldehyde method[2] or the mixed-dipyrromethane method[8]) would give a mixture of many regioisomers when applied to the preparation of this unsymmetrically substituted porphyrin, and the separation would be very difficult and laborious, and moreover, the absolute geometry of the functional groups would be ambiguous .

Scheme I. Retrosynthetic Analysis

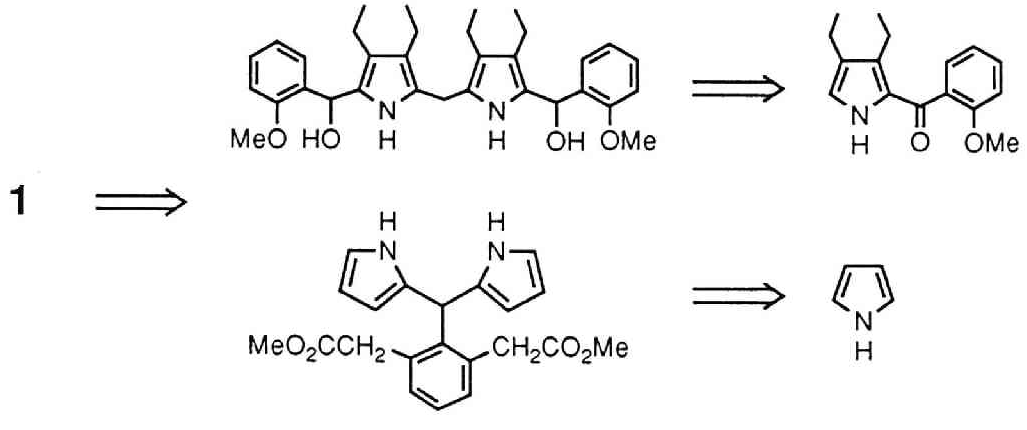

Synthesis. Total syntheses of the target chiral porphyrin **1**, together with other reference porphyrins **2**-**4**, are shown in Scheme II. **1** was constructed from two kinds of dipyrrylmethanes (**8** and **16**). Compound **8** was synthesized from diethylpyrrole **5**, which was prepared according to the literature method.[8] Treatment of **5** with ethyl magnesium bromide, followed by addition of *o*-anisoyl chloride, afforded the anisoylpyrrole **6**. Condensation of **6** with dimethoxymethane in the acidic condition gave the dipyrrylmethane **7**. **7** was converted into the corresponding diol derivative **8** by reduction with $NaBH_4$ This compound **8** was acid sensitive and gradually decomposed in air, on silica gel TLC, and on alumina TLC, so was used for the following condensation reaction without any purification. Attempts to prepare a pyrrylmethanol having no diethyl groups on the β-positions via a similar route were unsuccessful because the condensation of 2-benzoylpyrrole with dimethoxymethane (Scheme II, step c) did not proceed when 2-benzoylpyrrole was used instead of **6** or **21**. Therefore β-ethyl groups on pyrrole were found to be necessary for the condensation reaction with dimethoxymethane to proceed. In view of the host design, the rotational freedom of *o*-hydroxyphenyl groups should be restricted, because the rotation of the *o*-hydroxyphenyl groups will cause fluctuation in the distance between recognition sites (OH---Zn distance), which in turn may reduce the selectivity of the binding. The β-ethyl groups provide the rigidity to the host structure and also improve solubility of host in organic solvents. To prevent fluctuation of the OH recognition groups, we also tried to prepare hosts with similar structure in which the *o*-hydroxyphenyl group was replaced by either the 2-hydroxy-6-methylphenyl or the 2-hydroxy-1-naphthyl group. However, attempts to reduce the carbonyl group to a hydroxymethine group (Scheme II, step d) were unsuccessful when the *o*-methoxyphenyl group in **7** was replaced with either the 2-methoxy-6-methylphenyl or the 2-methoxy-1-naphthyl group. Steric hindrance by the naphthyl or methyl group may make the reducing agents

Scheme II. Total Synthetic Routes for Porphyrin Hosts **1-4**.[a]

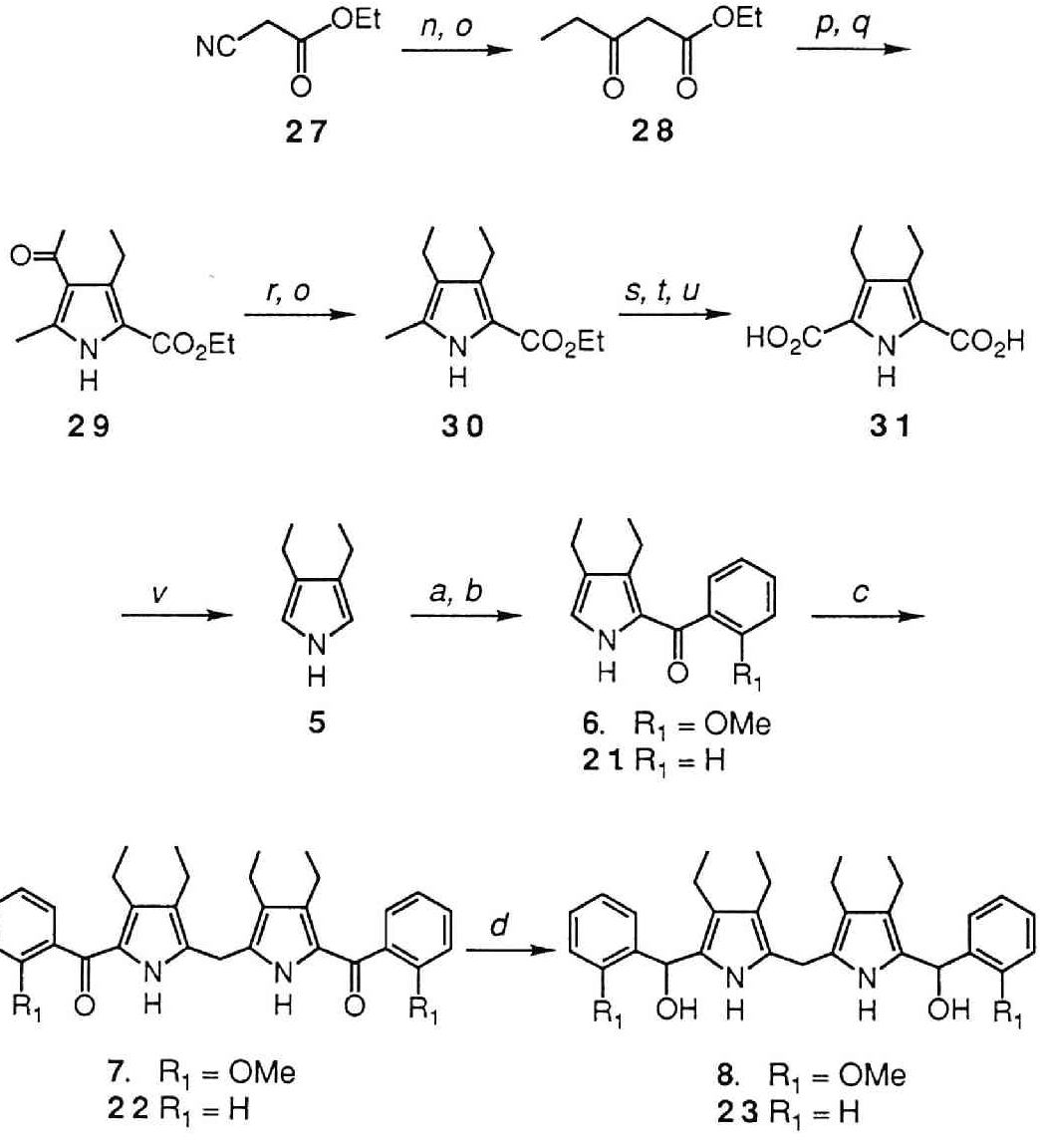

(Scheme II. continued.)

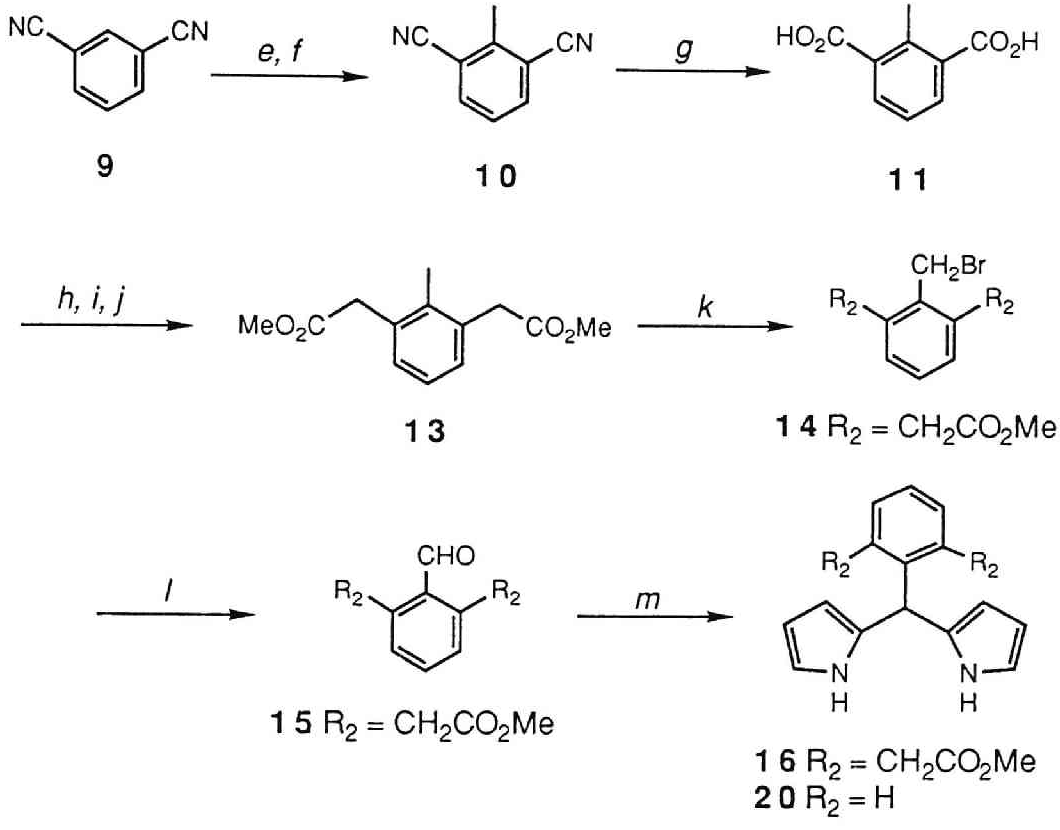

[a] Reagents: (a) EtMgBr/Et_2O. (b) *o*-$R_1C_6H_4COCl$/toluene. (c) $CH_2(OCH_3)_2$/conc. HCl /EtOH.(d) $NaBH_4$/EtOH. (e) LDA/THF (f) CH_3I. (g) KOH/H_2O. (h) $SOCl_2$. (i) CH_2N_2/Et_2O. (j) Ag_2O/MeOH. (k) $Br_2/CCl_4/h\nu$. (l) $Me_2SO/NaHCO_3$. (m) pyrrole(excess)/*p*-TsOH/MeOH. (n) EtMgI/Et_2O. (o) HCl/H_2O. (p) $NaNO_2/H_2O$/AcOH. (q) acetylacetone/Zn/AcOH/NaOAc. (r) $NaBH_4/BF_3OEt_2$/THF. (s) SO_2Cl_2/Et_2O. (t) NaOAc/H_2O. (u) NaOH/H_2O. (v) ethanolamine/Δ.

(Scheme II. continued.)

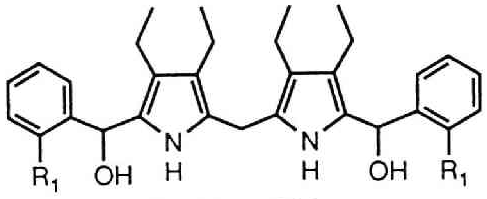

8. R_1 = OMe
23 R_1 = H

+

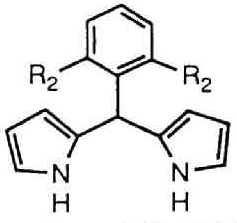

16 $R_2 = CH_2CO_2Me$
20 R_2 = H

w

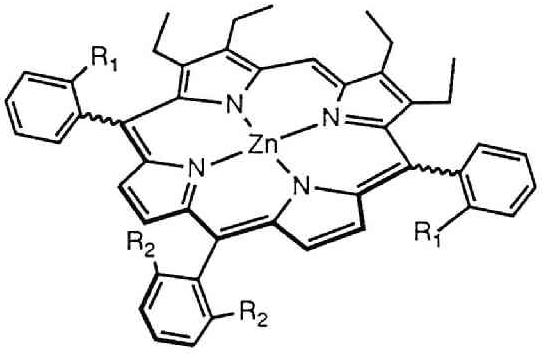

trans-atropisomer

x, y → **17.** R_1 = OMe, $R_2 = CH_2CO_2Me$
→ **1.** R_1 = OH, $R_2 = CH_2CO_2Me$

x, y → **24** R_1 = OMe, R_2 = H
→ **2.** R_1 = OH, R_2 = H

3. R_1 = H, $R_2 = CH_2CO_2Me$
4. R_1 = H, R_2 = H

cis-atropisomer

x, y → **18** R_1 = OMe, $R_2 = CH_2CO_2Me$
→ **19** R_1 = OH, $R_2 = CH_2CO_2Me$

x, y → **25** R_1 = OMe, R_2 = H
→ **26** R_1 = OH, R_2 = H

[a] Reagents: (w) $Zn(OAc)_2/CH_3CH_2CO_2H$. (x) BBr_3/CH_2Cl_2. (y) $Zn(OAc)_2$/MeOH

($NaBH_4$ and $LiAlH_4$) inaccessible to the carbonyl group.[9] We also observed that **7** was less reactive toward $NaBH_4$ than **22** which has no methoxy group on the phenyl rings. The reduction of **22** was completed within 6 h whereas stirring for 48 h was necessary for the reduction of **7**. These results indicate that the reduction of the carbonyl groups is affected by the *ortho*-substituents on the benzene rings.

Another dipyrrylmethane unit **16** was prepared via eight steps from 1, 3-dicyanobenzene (**9**). Methylation of **9** with LDA/MeI[10] followed by saponification[11] afforded dicarboxylic acid **11**. Insertion of methylene groups between the carboxylic group and the benzene ring according to the Arndt-Eistert reaction gave dimethyl ester **13**. Photobromination of **13** yielded the benzylbromide derivative **14**, which was oxidized with DMSO in the presence of $NaHCO_3$ to afford aldehyde **15**. The bromination reaction was carried out by carefully controlling the amount of added bromine, the rate of the bromine addition, and the reaction temperature, because the methylene groups of **13** were also brominated under uncontrolled conditions. Acid-catalyzed condensation of **15** with excess pyrrole afforded the desired dipyrrylmethane unit **16**.

We first attempted to carry out the condensation of dimethyl 2-formyl-1, 3-benzenedicarboxylate (**27**) with pyrrole (Scheme III).

Scheme III.

27

Reagents: (a) H_2SO_4/MeOH. (b) $Br_2/CCl_4/h\nu$. (c) $Me_2SO/NaHCO_3$. (d) pyrrole(excess)/TsOH/benzene.

Compound **27** was similarly prepared from 2-methyl-1,3-benzenedicarboxylic acid (**11**). However, the condensation reaction did not proceed at room temperature. By refluxing the reaction mixture in benzene, **27** disappeared, giving a mixture of many unidentified products. This unusual reactivity of **27** toward pyrrole can be ascribed to the presence of two electron-withdrawing groups at the *ortho*-positions to the formyl group. We also found that 2, 6-dinitrobenzaldehyde did not react with pyrrole under the similar conditions.[13] This difficulty was avoided by using compound **15** where methylene groups were inserted between the methoxycarbonyl group and the benzene ring.

Cyclization to porphyrin ring was performed by a modified Adler-Longo procedure.[14] Pyrrylmethanol **8** and dipyrromethane **16** (both *ca.* 0.02 M) were condensed in propionic acid in the presence of $Zn(OAc)_2$ at 95℃, giving a mixture of trans- (**17**) and cis- (**18**) isomers without forming any other regioisomers (Scheme II). The yield was in the range of 9-17%. The cyclization completed within 10 min at 90 to 100℃. Reaction temperature higher than 105℃ gave many byproducts which exhibit close R_f values on TLC and consequently chromatographic separation was difficult.[15] The addition of $Zn(OAc)_2$ was needed to obtain reproducible results. Other cyclization conditions (trifluoroacetic acid/CH_2Cl_2,[16] or *p*-toluenesulfonic acid/MeOH,[17] followed by oxidation with 2, 3, 5, 6-tetrachlorobenzoquinone) were also employed but gave unsatisfactory results (no product obtained or only 2% yield, respectively).

The separation of the trans isomer **17** from cis isomers **18** can be performed at this stage (or after cleaving the methyl ether) by column chromatography on silica gel. Cleavage of the methyl ether by use of BBr_3 was carried out without affecting the ester groups, giving the free base of *trans*- (**1**), or *cis*- (**19**) host molecules. In the ether cleavage reaction, longer reaction time lowered the yield considerably. Because BBr_3 induced demetalation of the porphyrin complex, zinc was inserted

again. The ^{1}H NMR spectrum of the less polar fraction is characterized by a single signal assignable to the ester methyl protons appearing at 2.89 ppm, while that of the more polar fraction by two set of signals assignable to the ester methyl protons at 2.87 and 2.88 ppm. In the cis isomer, the hydroxyl groups on the phenyl ring bring about different magnetic environments for the ester methyl protons above and below the porphyrin ring. Therefore the more polar fraction was identified as cis **19** and less polar fraction as trans isomer **1**. Trans to cis (and cis to trans) isomerization (atropisomerization[6]) occurred in $CHCl_3$ solution for 1 to 2 days at 65℃, and for 1 month at room temperature. The first order rate constant[18] for the atropisomerization in $CHCl_3$ at 25℃ was 1.56×10^{-6} s^{-1} for the free base of **1** and 1.49×10^{-7} s^{-1} for zinc complex **1**. Attempts to prepare similar hosts which have more bulky substituents on *meso*-positions and thus are less likely to undergo atropisomerization were unsuccessful (*vide supra*). The separated sample can be stored at –20℃ as a dry powder for at least several months. Other evidence for the above assignment is that the less polar fraction can be separated into two peaks by HPLC with a chiral column, while the polar fraction cannot. This observation is consistent with the fact that the trans isomer is optically active and the cis isomer is not. The assignment above agreed with a trend observed for the similar systems[19] that the cis isomer is more polar than the trans isomer.

The ^{1}H NMR spectrum of the C_2 symmetric porphyrin **1** is characterized by two sets of signals corresponding to the ethyl protons on pyrrole β-positions. One set of the ethyl protons appears as a triplet and a quartet at almost the same chemical shifts as those observed for octaethylporphyrin. The other set of the ethyl protons appears at a higher magnetic field, as would be expected for ethyl protons in the deshielding region of the nearby phenyl group. The chemical shifts of the hydroxyl protons and the ester protons of host **1** are almost the same as those of the corresponding hydroxyl protons of host **2** and the ester protons of host **3**,

respectively. These observations together with the binding experiments in the following chapter indicate that intramolecular hydrogen bonding between the CH_2CO_2Me and the OH group does not occur in host **1**. Based on these observations, it is expected that the two groups (OH and CH_2CO_2Me) act as independent recognition sites for the guest binding.

The enantiomer separation of the free base of **1** was performed by HPLC with a chiral column,[20] and then zinc was incorporated. Both enantiomers exhibited very weak circular dichroism (CD) in the Soret region. Therefore, CD spectra were recorded after converting **1** to the benzyl ether, [*trans*-5, 15-bis(2-benzyloxyphenyl)-10-{2, 6-bis(methoxycarbonylmethyl)phenyl}-2, 3, 17, 18-tetraethylporphyrinato]zinc(II). The enantiomer separation of the benzyl ether was also carried out by HPLC.[21] It was confirmed that the benzyl ether of (+)-**1** was also the first eluted fraction on this column. The benzyl ether of (+)-**1** exhibited Cotton effects in the Soret region ($[\theta] = -1.6 \times 10^4$ at 420 nm, $[\theta] = +1.0 \times 10^4$ at 431 nm), whereas that of (-)-**1** mirror-image of the Cotton effects ($[\theta] = +1.6 \times 10^4$ at 420 nm, $[\theta] = -1.0 \times 10^4$ at 431 nm).

Reference hosts **2**-**4** used in the next chapter 4 were also prepared in a similar manner as shown in Scheme II.

Experimental Section

General Remarks. ^1H NMR spectra were obtained using either a JEOL A-500 or a JEOL GX-400 or a JEOL JNM FX 90Q FT NMR spectrometer and chemical shifts are reported relative to internal Me_4Si. IR spectra were recorded on a Bio-rad FTS-7 FT-IR spectrometer. UV-vis spectra were recorded on either a Hitachi U-3410 spectrometer or a Hewlett-Packard 8452 diode array spectrophotometer with a thermostatted cell compartment. Circular dichroism spectra were recorded on a JASCO J-600 spectropolarimeter with a thermostatted cell compartment. Mass spectra were obtained with a JEOL JMS DX-300 mass spectrometer. High resolution mass spectra were obtained with a JEOL JMS SX-102A instrument. Elemental analyses were performed at the Microanalysis Center of Department of Pharmacy of Kyoto University. High performance liquid chromatography (HPLC) was performed on a Waters Model 6000 instrument with a Waters 600E system controller and a Tosoh UV-8010 detector. Thin layer chromatography (TLC) was performed on either Merck Kieselgel 60 F_{254} or DC-Alufolien Aluminiumoxid 60 F_{254} neutral (Type E).

Materials. 3,4-Diethylpyrrole (**5**) was prepared by decarboxylation of 3,4-diethylpyrrole-2,5-dicarboxylic acid.[22] 2-Methyl-1, 3-benzenedicarboxylic acid (**11**) was prepared by methylation of 1,3-dicyanobenzene (**9**) with lithium diisopropylamide (LDA) and methyl iodide in THF,[10] followed by saponification in aqueous potassium hydroxide.[11] Ether and THF were distilled from sodium, and dichloromethane was distilled from CaH_2. Ag_2O(I) was purchased from Wako Pure Chemicals Industries.

3,4-Diethyl-2-(2-methoxybenzoyl)pyrrole (6). A solution of 3, 4-diethylpyrrole (**5**) (8.76 g, 71.2 mmol) in toluene (100 mL) was added dropwise to 1.8 M ethylmagnesium bromide in dry ether (45 mL) over a period of 1.5 h under

Ar in an ice bath in the dark and the mixture was stirred at room temperature for 2 h. The resulting Grignard reagent was added to a solution of *o*-methoxybenzoyl chloride (15.71g, 92.1 mmol) in toluene (100 mL) at –50℃ over 1.5 h. After the addition stirring was continued for 1 h, followed by the addition of saturated NH_4Cl (40 mL). The mixture was stirred for 1 h at room temperature. The organic layer was separated, washed with aqueous NaCl (40 mL), and dried over K_2CO_3. Evaporation of the solvent and separation by column chromatography on silica gel ($CHCl_3$) afforded 12.04g (46.8mmol, 66%) of a pale yellow powder **6**. Recrystallization from MeOH gave pale yellow crystals; mp 95.0-96.5℃; TLC R_f 0.35 (SiO_2, $CHCl_3$:ethyl acetate = 20:1); ^{1}H NMR ($CDCl_3$, 90MHz) δ 0.90 (t, J = 9Hz, 3H, CH_2CH_3), 1.18 (t, J = 9Hz, 3H, CH_2CH_3), 2.30 (q, J = 9Hz, 2H, CH_2CH_3), 2.47 (q, J = 9Hz, 2H, CH_2CH_3), 3.80 (s, 3H, OCH_3), 6.83 (d, J = 3Hz, 1H, α-H), 6.9-7.5 (m, 4H, phenyl-H), 9.03 (br s, 1H, NH); IR (KBr, cm^{-1}) 3282(NH, s), 2965 (w), 2932 (w), 2873 (w), 2835 (w), 1598 (C=O, s), 1494 (w), 1458 (w), 1403 (s), 1288 (w), 1242 (m), 1170 (w), 1111(w), 1023 (w); Anal. Calcd for $C_{16}H_{19}O_2N$•1/3(MeOH•H_2O): C, 71.59; H, 7.72; N, 5.11. Found: C, 71.64; H, 7.84; N, 5.01.; MS *m/e* 257 (M^+, 100), 242 (M^+-CH_3, 82), 135 (M^+-pyrrole), 122 (M^+-anisoyl, 29).

3, 3', 4, 4'-Tetraethyl-5, 5'-bis(2-methoxybenzoyl)-2, 2'-di pyrrylmethane (7). A solution of **6** (8.56g, 33.3 mmol) in ethanol (40 mL) and conc. hydrochloric acid (9 mL) was heated at 40℃ and dimethoxymethane (17 mL) was added. After heated at 40℃ for 3h, another portion of dimethoxymethane (8 mL) was added and the mixture was heated for 3 h. After evaporation of the solvent, the dark brown residue was redissolved in $CHCl_3$ (90 mL). The chloroform layer was washed with saturated aqueous $NaHCO_3$ (90 mL), saturated aqueous NaCl (60mL) and dried over Na_2SO_4. Evaporation of the solvent and separation by repeated column chromatography (SiO_2, hexane:ethyl acetate = 2:1)

afforded orange crystals **7** (5.64 g, 10.7 mmol, 64%). Recrystallization from MeOH afforded pale yellow crystals; mp 170.5-171.5℃; TLC R_f 0.18 (SiO_2, $CHCl_3$:ethyl acetate = 20:1); ^1H NMR ($CDCl_3$, 90 MHz) δ 0.87 (t, *J* = 9Hz, 6H, CH_2CH_3), 1.04 (t, *J* = 9Hz, 6H, CH_2CH_3), 2.24 (q, *J* = 9Hz, 4H, CH_2CH_3), 2.40 (q, *J* = 9Hz, 4H, CH_2CH_3), 3.78 (s, 6H, OCH_3), 3.92 (s, 2H, CH_2), 6.9-7.5 (m, 8H, phenyl-H), 9.00 (br s, 2H, NH); IR (KBr, cm^{-1}) 3300(NH, m), 3207(w), 2965 (w), 2928 (w), 2869 (w), 1607 (C=O, s), 1554 (s), 1489 (m), 1427 (s), 1370 (w), 1293 (m), 1250 (m), 1187(w), 1159 (w), 1114(w), 1055(w), 1023(w); Anal. Calcd for $C_{33}H_{38}O_4N_2$: C, 75.03; H, 7.39; N, 5.34. Found: C, 75.26; H, 7.27; N, 5.32.; MS *m/e* 526 (M^+, 15), 391 (3), 270 (12), 135 (100).

3, 3', 4, 4'-Tetraethyl-5, 5'-bis(α-hydroxy-2-methoxybenzyl)-2, 2'-dipyrrylmethane (8). To a stirred solution of **7** (1.04g, 1.98 mmol) in ethanol (35 mL) was added $NaBH_4$ (0.7 g, 18.5 mmol) and stirring was continued under Ar at room temperature in the dark for 28 h. Then another portion of $NaBH_4$ (0.5 g, 13.2 mmol) was added and stirring was continued under Ar for 19 h. The progress of the reaction was monitored by TLC (neutral alumina, $CHCl_3$:ethyl acetate = 20:1). After the reaction mixture was concentrated in a reduced pressure, water (50 mL) was added. The mixture was extracted with ether (50 mL × 3) and the ether layer was dried over K_2CO_3. Evaporation of the solvent afforded an orange foam 1.05 g, (1.98 mmol, 100%). The product was air sensitive and can be stored at –20℃ under Ar for 2-3 weeks. The product was used for the next reaction without purification. MS *m/e* 512 (M^+-H_2O, 89), 496 (M^+-2OH, 54).

Dimethyl 2-methyl-1, 3-benzenediacetate (13). A solution of of 2-methyl-1, 3-benzenedicarboxylic acid (**11**) (37.7 g, 0.21 mol) in pyridine (1.15 mL) and $SOCl_2$ (115 mL, 1.6 mol) was stirred at 45℃ for 1 hr, and then refluxed for 16 h. After excess $SOCl_2$ was distilled off, distillation at a reduced pressure (95-109℃/0.2mmHg) afforded 2-methyl-1, 3-benzenedicarbonyl dichloride (**12**) as

a pale yellow solid 43.3 g (200 mmol, 96%). mp 89-92℃; ^{1}H NMR ($CDCl_3$, 90 MHz) δ 2.67 (s, 3H, CH_3), 7.58 (t, J = 9Hz, 1H, phenyl-H), 8.28 (d, J = 9Hz, 2H, phenyl-H); IR (KBr, cm^{-1}) 3085(w), 1767 (C=O, s), 1570 (w), 1436 (w), 1386 (w), 1282 (w), 1237 (w), 1176 (w), 1076(m).

To 0.38M diazomethane in ether (410 mL) was added dropwise 2-methyl-1, 3-benzenedicarbonyl dichloride **12** (8.73 g, 40 mmol) in dry ether (200 mL). The nitrogen gas was evolved and pale yellow precipitates were formed soon. The reaction mixture was stirred at room temperature for 12.5 h. Evaporation of the ether gave the diazoketone as a pale yellow solid. The diazoketone was dissolved in MeOH (60 mL). The solution was heated at 50℃ and Ag_2O (I) (0.152 g, 0.66 mmol) was added. Three portions of Ag_2O (I) (0.076 g, 0.33 mmol) was added over 1.5 h. The reaction mixture was filtered through Cerite (545) while it is hot. Recrystallization from MeOH afforded 4.97 g (21 mmol, 53%) of **13** as colorless needles. mp 102-103℃; TLC R_f 0.25 (SiO_2, $CHCl_3$); ^{1}H NMR ($CDCl_3$, 90 MHz) δ 2.25 (s, 3H, CH_3), 3.70 (s, 10H, $CH_2CO_2CH_3$), 7.18 (s, 3H, phenyl-H); IR (KBr, cm^{-1}) 3002(w), 2953(w), 2848 (w), 1727 (C=O, s), 1456 (m), 1427 (m), 1353 (m), 1262 (w), 1208 (s), 1166(s); Anal. Calcd for $C_{13}H_{16}O_4$: C, 66.09; H, 6.83. Found: C, 65.79; H, 6.85.; MS *m/e* 236 (M^+, 47), 205 (M^+-OCH_3, 13), 177 (M^+-CO_2CH_3, 100), 18 (M^+-$2CO_2CH_3$, 30).

Dimethyl 2-(bromomethyl)-1, 3-benzenediacetate (14). A solution of **13** (8.24 g, 34.9 mmol) in CCl_4 (170 mL) was cooled in a constant temperature bath at 20℃ and irradiated with 500W light while Br_2 (7.32 g, 45.75 mmol) in CCl_4 (62 mL) was added dropwise over 4.6 h. The progress of the reaction was monitored by ^{1}H NMR. After the reaction was complete, the solution was washed with saturated aqueous $NaHCO_3$ (40mL), saturated aqueous NaCl (80mL), and dried over Na_2SO_4. Evaporation of the solvent and repeated separation on column chromatography (SiO_2, $CHCl_3$) yielded colorless crystals **14**, 5.85g (18.6mmol,

53%). Recrystallization from ether gave colorless needles. mp 56.0-57.0℃, TLC R_f 0.28 (SiO_2, $CHCl_3$), ^1H NMR ($CDCl_3$, 90 MHz) δ 3.72 (s, 6H, CO_2CH_3), 3.80 (s, 4H, $CH_2CO_2CH_3$), 4.68 (s, 2H, CH_2Br), 7.28 (s, 3H, phenyl-H); IR (KBr, cm^{-1}) 3011(w), 2960(w), 1714 (C=O, s), 1587 (w), 1434 (w), 1463 (m), 1008 (w); Anal. Calcd for $C_{13}H_{15}O_4Br$: C, 49.54; H, 4.80; Br, 25.35. Found: C, 49.82; H, 4.81; Br, 24.72.; MS *m/e* 316, 314 (M^+, 2), 257, 255 (M^+-CO_2CH_3), 235(M^+-Br, 100), 176 (M^+-Br, CO_2CH_3, 16), 117 (M^+-Br, $2CO_2CH_3$, 12).

Dimethyl 2-formyl-1,3-benzenediacetate (15). Dimethylsulfoxide (Me_2SO, 27 mL) was deaerated by bubbling with Ar for 1 h and the Me_2SO was added to **14** (1.35 g, 4.30 mmol) and $NaHCO_3$ (3.09 g, 36.8 mmol). The mixture was heated at 100℃ under Ar with vigorous stirring for 7 min. The reaction mixture was then immediately cooled in an ice bath, poured into saturated aqueous NaCl (100 mL) and extracted with ether (100 mL × 1, 50 mL × 2). The ether layer was combined and dried over Na_2SO_4. Evaporation of the solvent gave colorless crystals **15**, 957 mg (3.83 mmol, 89%). Recrystallization from ether afforded colorless crystals. mp 114.5-116.0℃; TLC R_f 0.32 (SiO_2, $CHCl_3$:ethyl acetate = 20:1); ^1H NMR ($CDCl_3$, 90 MHz) δ 3.75 (s, 6H, CO_2CH_3), 4.05 (s, 4H, $CH_2CO_2CH_3$), 7.25-7.6 (m, 3H, phenyl-H), 10.55 (s, 1H, CHO); IR (KBr, cm^{-1}) 3002(w), 2957(w), 2785(w), 1724 (C=O, s), 1590 (w), 1449 (w), 1352 (m), 1261 (w), 1211(m), 1170(m), 1033(w); Anal. Calcd for $C_{13}H_{14}O_5$: C, 62.39; H, 5.64. Found: C, 62.13; H, 5.75.; MS *m/e* 250 (M^+, 25), 219 (M^+-OCH_3, 67), 191(M^+-CO_2CH_3), 177 (M^+-$CH_2CO_2CH_3$, 60), 162 (M^+-CHO, CO_2CH_3, 57), 104(M^+-$2CH_2CO_2CH_3$, 23).

Dimethyl 2-bis(2-pyrryl)methyl-1, 3-benzenediacetate (16). A solution of aldehyde **15** (0.928 g, 3.71 mmol) in MeOH (50 mL) was added slowly to a solution of *p*-toluenesulfonic acid monohydrate (0.709g, 3.65 mmol) and a large excess of distilled pyrrole (12 mL, 147 mmol) in MeOH (28 mL) over 1 h at

room temperature in the dark. After the addition the reaction mixture was poured into saturated aqueous NaCl (100 mL). The mixture was extracted with ether (100 mL × 3) and the ether layer was dried over Na_2SO_4. Evaporation of the solvent and excess pyrrole and repeated column chromatographic separation (SiO_2, $CHCl_3$) afforded a pale yellow solid **16**, 0.924 g (2.52 mmol, 68%). Recrystallization from ether afforded a pale green powder. mp 120.0-120.5℃; TLC R_f 0.35 (SiO_2, $CHCl_3$:ethyl acetate = 20:1); ^{1}H NMR ($CDCl_3$, 90 MHz) δ 3.62 (s, 6H, CO_2CH_3), 3.70 (s, 4H, $CH_2CO_2CH_3$), 5.83 (s, 1H, CH), 5.97 (m, 2H, β-H), 6.13 (m, 2H, β-H), 6.73 (m, 2H, α-H), 7.10-7.30 (m, 3H, phenyl-H), 8.73 (br s. 2H, NH); IR (KBr, cm^{-1}) 3389(NH, s), 3004(w), 2948 (w), 1719 (C=O, s), 1554 (w), 1430 (m), 1341 (m), 1249 (m), 1208(m), 1159(m), 1107(w), 1033(w), 1005(w); Anal. Calcd for $C_{21}H_{22}O_4N_2$: C, 68.84; H, 6.05; N, 7.65. Found: C, 68.68; H, 6.01; N, 7.68.; MS *m/e* 366 (M^+, 100), 335 (M^+-OCH_3, 13), 307(M^+-CO_2CH_3, 11), 234 (M^+-2pyrrole,4).

[*trans*-5, 15-Bis(2-methoxyphenyl)-10-{2, 6-bis(methoxycarbonylmethyl)phenyl}-2, 3, 17, 18-tetraethylporphyrinato]zinc(II) (17), *cis*-atropisomer (18). A solution of $Zn(OAc)_2$ (0.204 g, 0.928mmol) in propionic acid (36 mL) was heated at 95℃. A heated solution of pyrrylmethanol **8** (0.476 g, 0.897 mmol) and dipyrrylmethane **16** (0.299g, 0.817 mmol) in 1, 2-dichloroethane (8.1 mL) was added quickly. The solution turned dark red immediately and was stirred for 1 h at 95℃ in the dark. The propionic acid was distilled off at room temperature. The repeated column chromatography (SiO_2, $CHCl_3$:ethyl acetate = 20:1) afforded *trans*- and *cis*-zinc complexes. The total yield was 82.5mg (0.09 mmol, 11%). Recrystallization from CH_2Cl_2 - MeOH afforded purple crystals.

17: mp >300℃; TLC R_f 0.57 (SiO_2, $CHCl_3$:ethyl acetate = 20:1); ^{1}H NMR ($CDCl_3$, 400 MHz) δ 1.27 (t, J = 7.6 Hz, 6H, CH_2CH_3), 1.89 (t, J = 7.6 Hz, 6H,

CH_2CH_3), 2.80 (s, 6H, CO_2CH_3), 2.98-3.21 (m, 4H, CH_2CH_3), 3.16 (s, 4H, $CH_2CO_2CH_3$), 3.62 (s, 6H, OCH_3), 4.03 (q, J = 7.6 Hz, 4H, CH_2CH_3), 7.27-7.90 (m, 11H, phenyl H), 8.49 (AB q, J = 4.66 Hz, 2H, β-H), 8.54 (AB q, 2H, J = 4.66 Hz, 2H, β-H), 10.13 (s, 1H, *meso*-H); FAB MS (*m*-nitrobenzylalcohol matrix) *m/e* 917 (M^+); UV-vis ($CHCl_3$) λ_{max} (log ε) 421 (5.56), 549 (4.30), 570 (sh, 3.67).

18: mp >300℃; TLC R_f 0.42 (SiO_2, $CHCl_3$:ethyl acetate = 20:1); ^1H NMR ($CDCl_3$, 400 MHz) δ 1.27 (t, J = 7.6 Hz, 6H, CH_2CH_3), 1.89 (t, J = 7.6 Hz, 6H, CH_2CH_3), 2.69 (s, 3H, CO_2CH_3), 2.86 (s, 3H, CO_2CH_3), 3.03-3.17 (m, 4H, CH_2CH_3), 3.14 (s, 2H,$CH_2CO_2CH_3$), 3.18(s, 2H, $CH_2CO_2CH_3$), 3.62 (s, 6H,OCH_3), 3.99-4.09 (m, 4H, CH_2CH_3), 7.26-7.88 (m, 11H, phenyl H), 8.48 (AB q, J = 4.66 Hz, 2H, β-H), 8.54 (AB q, J = 4.66 Hz, 2H, β-H), 10.13 (s, 1H, meso-H); FAB MS (*m*-nitrobenzylalcohol matrix) *m/e* 917 (M^+); UV-vis ($CHCl_3$) λ_{max} (log ε) 420 (5.52), 548 (4.26), 572 (sh, 3.38).

The free bases of **17** and **18** were obtained by treating **17** and **18** with 10% HCl, recrystallized from CH_2Cl_2-MeOH: mp 272 - 273 ℃; TLC R_f 0.68 (SiO_2, $CHCl_3$:ethyl acetate = 20:1); UV-vis ($CHCl_3$) λ_{max} (log ε) 415.5 (5.43), 510.9 (4.27), 535.5 (sh, 3.50), 582.9 (3.80).; Anal. Calcd for $C_{54}H_{54}O_6N_4 \cdot CH_3OH$: C, 74.47; H, 6.59; N, 6.32. Found: C, 74.57; H, 6.51; N, 6.17.

[*trans*-5, 15-Bis(2-hydroxyphenyl)-10-{2, 6-bis(methoxycarbonylmethyl)phenyl}-2, 3, 17, 18-tetraethylporphyrinato]zinc(II) (1), *cis*-atropisomer (19). The methoxy derivative **17** (43.5 mg, 0.047 mmol) was dissolved in dry CH_2Cl_2 (2.2 mL) under Ar. The solution was cooled to –40℃ and 1M BBr_3 in CH_2Cl_2 (0.75 mL) was added. The reaction mixture was allowed to warm up slowly over 3 h to room temperature and stirred for 3 h. The solution was cooled to –20℃ and MeOH (0.68 mL) was added. Saturated aqueous $NaHCO_3$ was added and the mixture was extracted with CH_2Cl_2. The organic layer was

washed with water and dried over Na_2SO_4 and the solvent was evaporated. Purification by column chromatography (SiO_2, $CHCl_3$:ethyl acetate = 10:1) afforded 27 mg (0.033 mmol, 69.5%) of the free base porphyrin. The free base porphyrin was dissolved in $CHCl_3$ and refluxed with $Zn(OAc)_2$-saturated MeOH. Evaporation of the solvent, extraction with CH_2Cl_2, followed by chromatographic separation on silica gel ($CHCl_3$:ethyl acetate = 10:1) gave the zinc complex **1**.

1: TLC R_f 0.61 (SiO_2, $CHCl_3$:ethyl acetate = 5:1); ^1H NMR ($CDCl_3$, 400 MHz) δ 1.32 (t, J = 7.6 Hz, 6H, CH_2CH_3), 1.90 (t, J = 7.6 Hz, 6H, CH_2CH_3), 2.89 (s, 6H, $CH_2CO_2CH_3$), 3.09-3.20 (m, 8H, CH_2CH_3, $CH_2CO_2CH_3$), 4.04 (q, J = 7.6 Hz, 4H, CH_2CH_3), 4.90 (br s. 2H, OH), 7.27-7.94 (m, 11H, phenyl H), 8.54 (AB q, J = 4.58 Hz, 2H, β-H), 8.62 (AB q, J = 4.58 Hz, 2H, β-H), 10.18 (s, 1H, meso-H); FAB MS (*m*-nitrobenzylalcohol matrix) *m/e* 889 (M^+); UV-vis ($CHCl_3$) λ_{max} (log ε) 422 (5.43), 551 (4.15), 579 (sh, 3.39); High resolution mass spectrum (HRFAB MS) of the free base of **1** (*m*-nitrobenzylalcohol matrix) *m/e* calcd for $C_{52}H_{51}O_6N_4$ 827.3809, found 827.3823 (+1.7 ppm).

Compound **19** was also prepared in a similar manner from **18**. Compounds **18** and **19** can also be prepared by cleaving the methyl ether of a mixture of **17** and **18**, followed by the column chromatographic separation.

19: TLC R_f 0.24 (SiO_2, $CHCl_3$:ethyl acetate = 5:1); ^1H NMR ($CDCl_3$, 400 MHz) δ 1.31 (t, J = 7.6 Hz, 6H, CH_2CH_3), 1.90 (t, J = 7.6 Hz, 6H, CH_2CH_3), 2.87 (s, 3H, $CH_2CO_2CH_3$), 2.88 (s, 3H, $CH_2CO_2CH_3$), 3.07 (s, 2H, $CH_2CO_2CH_3$), 3.12-3.16 (m, 4H, CH_2CH_3), 3.19 (s, 2H, $CH_2CO_2CH_3$), 4.03 (q, J = 7.6 Hz, 4H, CH_2CH_3), 4.94 (br s, 2H, OH), 7.26-7.95 (m, 11H, phenyl H), 8.60 (AB q, J = 2.5 Hz, 2H, β-H), 8.61 (AB q, 2H, J = 2.5 Hz, 2H, β-H), 10.17 (s, 1H, meso-H); FAB MS (*m*-nitrobenzylalcohol matrix) *m/e* 889 (M^+, 100).

Bis(2-pyrryl)methylbenzene (20). Compound **20** was prepared by a procedure similar to that described for **16**. The product was purified by repeated

column chromatography (SiO_2, $CHCl_3$). Recrystallization from ether gave a white solid 0.706 g (3.18 mmol, 36.5%). mp 102-103℃; TLC R_f 0.33 (SiO_2, $CHCl_3$); ^1H NMR ($CDCl_3$, 90 MHz) δ 5.50 (s, 1H, CH), 5.93 (m, 2H, β-H), 6.17 (m, 2H, β-H), 6.72 (m, 2H, α-H), 7.20-7.33 (m, 5H, phenyl-H), 7.98 (br s. 2H, NH); IR (KBr, cm^{-1}) 3345(NH, s), 3134(w), 3092 (w), 3058 (w), 2860 (w),1554 (w), 1490 (w), 1456 (w), 1411 (w), 1315 (w), 1260(w), 1181(w), 1107(w); Anal. Calcd for $C_{15}H_{14}N_2$: C, 81.05; H, 6.35; N, 12.60. Found: C, 81.31; H, 6.21; N, 12.76.; MS *m/e* 222 (M^+, 100), 156 (M^+-pyrrole, 32), 145(M^+-benzene, 54).

2-Benzoyl-3, 4-diethylpyrrole (21). This compound was prepared in a similar manner to that for **6** in 71% yield. Recrystallization from hexane afforded pale yellow prisms: mp 54.0-55.5℃; TLC R_f 0.30 (SiO_2, hexane:ether = 5:1); ^1H NMR ($CDCl_3$, 90 MHz) δ 1.0 (t, 3H, CH_2CH_3), 1.2 (t, 3H, CH_2CH_3), 2.5 (dq, 4H, CH_2CH_3), 6.8 (d, 1H, α-H), 7.3-7.8 (m, 5H, phenyl-H), 8.8 (br s. 1H, NH); IR (KBr, cm^{-1}) 3268(NH, s), 3181(sh), 1608 (C=O), 1562 (w); Anal. Calcd for $C_{15}H_{17}ON$: C, 79.26; H, 7.54; N, 6.16. Found: C, 79.25; H, 7.61; N, 6.19.; MS *m/e* 227 (M^+).

3, 3', 4, 4'-Tetraethyl-5, 5'-bisbenzoyl-2, 2'-dipyrrylmethane (22). This compound was prepared from **21** in 76 % yield in a similar manner to that for **7**. mp 66.0-73.0℃; TLC R_f 0.20 (SiO_2, $CHCl_3$:ethyl acetate = 20:1); ^1H NMR ($CDCl_3$, 90 MHz) δ 0.93 (t, 6H, CH_2CH_3), 1.07 (t, 6H, CH_2CH_3), 2.50 (dq, 8H, CH_2CH_3), 3.97 (s, 2H, CH_2), 7.3-7.6 (m, 10H, phenyl-H), 9.30 (br s, 2H, NH); IR (KBr, cm^{-1}) 3281(NH), 1595 (C=O, s), 1560 (m); Anal. Calcd for $C_{31}H_{34}O_2N_2$: C, 79.79; H, 7.34; N, 6.00. Found: C, 79.51; H, 7.35; N, 5.84.; MS *m/e* 466 (M^+).

3, 3'-4, 4'-Tetraethyl-5, 5'-bis(α-hydroxybenzyl)-2, 2'-dipyrryl methane (23). This compound was prepared in a similar manner to that for **8**

from **22**. The reduction with $NaBH_4$ was finished in 12 h. MS *m/e* 434 (M^+ - $2H_2O$).

[*trans*-5, 15-Bis(2-methoxyphenyl)-2, 3, 17, 18-tetraethyl-10-phenylporphyrinato]zinc(II) (24), *cis*-atropisomer (25) This complex was prepared in a similar manner as that for **17** and **18**.

24: Yield 4%; TLC R_f 0.50 (SiO_2, $CHCl_3$); ^1H NMR ($CDCl_3$, 400 MHz) δ 1.25 (t, *J* = 9 Hz, 6H, CH_2CH_3), 1.90 (t, *J* = 9 Hz, 6H, CH_2CH_3), 3.15 (q, *J* = 9 Hz, 4H, CH_2CH_3), 3.65 (s, 6H, OCH_3), 4.05 (q, *J* = 9 Hz, 4H, CH_2CH_3), 7.65-8.25 (m, 13H, phenyl-H), 8.66 (AB q, *J* = 4.5Hz, 2H, β-H), 8.82 (AB q, *J* = 4.5Hz, 2H, β-H), 10.18 (s, 1H, meso-H); FAB MS (*m*-nitrobenzylalcohol matrix) *m/e* 773 (M^+).

25: Yield 4%; TLC R_f 0.15 (SiO_2, $CHCl_3$); FAB MS (*m*-nitrobenzylalcohol matrix) *m/e* 773 (M^+).

[*trans*-5, 15-Bis(2-hydroxyphenyl)-2, 3, 17, 18-tetraethyl-10-phenylporphyrinato]zinc(II) (2), *cis*-atropisomer (26). This complex was prepared in a similar manner to that for **1**.

2: TLC R_f 0.40 (SiO_2, $CHCl_3$:ethyl acetate = 20:1); ^1H NMR ($CDCl_3$, 90 MHz) δ 1.33 (t, *J* = 9 Hz, 6H, CH_2CH_3), 1.93 (t, *J* = 9 Hz, 6H, CH_2CH_3), 3.20 (q, *J* = 9 Hz, 4H, CH_2CH_3), 4.10 (q, *J* = 9 Hz, 4H, CH_2CH_3), 4.90 (br s, 2H, OH), 7.65-8.25 (m, 13H, phenyl-H), 8.78 (AB q, *J* = 4.5Hz, 2H, β-H), 8.90 (AB q, *J* = 4.5Hz, 2H, β-H), 10.25 (s, 1H, meso-H); FAB MS (*m*-nitrobenzylalcohol matrix) *m/e* 745 (M^+); UV-vis ($CHCl_3$) λ_{max} (log ε) 419 (5.58), 546 (4.29), 573 (sh, 3.62); HRFAB MS of the free base of **2** (*m*-nitrobenzylalcohol matrix) *m/e* calcd for $C_{46}H_{43}O_2N_4$ 683.3386, found 683.3368 (-2.6 ppm).

26: TLC R_f 0.16 (SiO_2, $CHCl_3$:ethyl acetate = 20:1); FAB MS (*m*-nitrobenzyl-alcohol matrix) *m/e* 745 (M^+); UV-vis ($CHCl_3$) λ_{max} (log ε) 418 (5.33), 545 (4.07), 570 (sh, 3.48).

[2, 3, 17, 18-Tetraethyl-10-{2, 6-bis(methoxycarbonylmethyl) phenyl}-5, 15-diphenylporphyrinato]zinc(II) (3). This complex was prepared in a similar manner to that for **17** and **18**. Column chromatographic separation (SiO_2, $CHCl_3$), and recrystallization from CH_2Cl_2-hexane afforded **3**. Yield 17.5%; mp 258-262℃; TLC R_f 0.30 (SiO_2, CH_2Cl_2); ^{1}H NMR ($CDCl_3$, 90 MHz) δ 1.25 (t, J = 9 Hz, 6H, CH_2CH_3), 1.90 (t, J = 9 Hz, 6H, CH_2CH_3), 2.90 (s, 6H, CO_2CH_3), 3.00 (q, J = 9 Hz, 4H, CH_2CH_3), 3.20 (s, 4H, $CH_2CO_2CH_3$), 4.08 (q, J = 9 Hz, 4H, CH_2CH_3), 7.58-8.23 (m, 13H, phenyl-H), 8.55 (AB q, 4H, β-H), 10.25 (s, 1H, meso-H); FAB MS (*m*-nitrobenzylalcohol matrix) *m/e* 857 (M^+); UV-vis ($CHCl_3$) λ_{max} (log ε) 423 (5.57), 551 (4.28), 582 (sh, 3.45); HRFAB MS of the free base of **3** (*m*-nitrobenzylalcohol matrix) *m/e* calcd for $C_{52}H_{51}O_4N_4$ 795.3910, found 795.3942 (+4.0 ppm).

(2, 3, 17, 18-Tetraethyl-5, 10, 15-triphenylporphyrinato) zinc (II) (4). This complex was prepared in a similar manner to that for **17** and **18**. Column chromatographic separation (SiO_2, hexane:$CHCl_3$ = 1:3) and recrystallization from CH_2Cl_2-hexane afforded **4**. Yield 8.6%; mp > 300℃; TLC R_f 0.28 (SiO_2, $CHCl_3$:hexane = 1:1); ^{1}H NMR ($CDCl_3$, 90 MHz) δ 1.30 (t, J = 9 Hz, 6H, CH_2CH_3), 1.95 (t, J = 9 Hz, 6H, CH_2CH_3), 3.05 (q, J = 9Hz, 4H, CH_2CH_3), 4.10 (q, J = 9 Hz, 4H, CH_2CH_3), 7.75-8.30 (m, 15H, phenyl-H), 8.70 (AB q, J = 4.5 Hz, 2H, β-H), 8.90 (AB q, J = 4.5 Hz, 2H, β-H), 10.30 (s, 1H, meso-H); FAB MS (*m*-nitrobenzylalcohol matrix) *m/e* 713 (M^+); UV-vis ($CHCl_3$) λ_{max} (log ε) 416 (5.54), 544 (4.23), 576 (sh, 3.40);55 HRFAB MS of the free base of **4** (*m*-nitrobenzylalcohol matrix) *m/e* calcd for $C_{46}H_{43}N_4$ 651.3488, found 651.3480 (-1.2 ppm).

References

(1) (a) Paine, J. B. In *The Porphyrins*; Dolphin, D., Ed.; Academic Press: New York, 1978; Vol. 1, pp101-234. (b) Johnson, A. W. In *The Porphyrins*; Dolphin, D., Ed.; Academic Press: New York, 1978; Vol. 1, pp101-234.

(2) (a) Little, R. G.; Anton, J. A.; Loach, P. A.; Ibers, J. A. *J. Heterocyclic Chem.* **1975**, *12*, 343. (b) Walker, F. A.; Balke, V. L.; McDermott, G. A. *Inorg. Chem.* **1982**, *21*, 3342. (c) Milgrom, L. R. *J. Chem. Soc., Perkin Trans.* 1, **1984**, 1483.

(3) Wallace, D. M.; Smith, K. M. *Tetrahedron Lett.* **1990**, *31*, 7265.

(4) Ema, T.; Kuroda, Y.; Ogoshi, H. *Tetrahedron Lett.* **1991**, *32*, 4529.

(5) (a) Miller, J. R.; Dorough, G. D. *J. Am. Chem. Soc.* **1952**, *74*, 3977. (b) Kirksey, C. H.; Hambright, P.; Storm, C. B. *Inorg. Chem.* **1969**, *8*, 2141.

(6) (a) Gottwald, L. K.; Ullman, E. F. *Tetrahedron Lett.* **1969**, 3071. (b) Eaton, S. S.; Eaton, G. R. *J. Am. Chem. Soc.* **1975**, *97*, 3660. (c) Freitag, R. A.; Mercer-Smith, J. A.; Whitten, D. G. *J. Am. Chem. Soc.* **1981**, *103*, 1226. (d) Young, R.; Chang, C. K. *J. Am. Chem. Soc.* **1985**, *107*, 898.

(7) Cram, D. J. *Angew. Chem. Int. Ed. Engl.* **1988**, *27*, 1009.

(8) Aoyama, Y.; Uzawa, T.; Saita, K.; Tanaka, Y.; Toi, H.; Ogoshi, H. *Tetrahedron Lett.* **1988**, *29*, 5271.

(9) No reaction occurred in the case of $NaBH_4$ and decomposition of the substrate was observed in the case of $LiAlH_4$.

(10) Krizan, T. D.; Martin, J. C. *J. Org. Chem.* **1982**, *47*, 2681.

(11) Lindsay, W. S.; Stokes, P.; Humber, L. G.; Boekelheide, V. *J. Am. Chem. Soc.* **1961**, *83*, 943.

(12) Kornblum, N.; Jones, W. J.; Anderson, G. J. *J. Am. Chem. Soc.* **1957**, *79*, 4113.

(13) (a) Lecas-Nawrocka, A.; Levisalles, J.; Mariacher, C.; Renko, Z.; Rose, E. *Can. J. Chem.* **1984**, *62*, 2054, 2059. (b) Lindsey, J. S.; Wagner, R. W. *J. Org. Chem.* **1989**, *54*, 828.

(14) Adler, A. D.; Longo, F. R.; Finarelli, J. D.; Goldmacher, J.; Assour, J.; Korsakoff, L. *J. Org. Chem.* **1967**, *32*, 476.

(15) ^{1}H NMR and UV-vis spectra of the byproduct indicated that the phenyl groups on *meso*-positions disappeared. See also ref. 17.

(16) Lindsey, J. S.; Schreiman, I. C.; Hsu, H. C.; Kearney, P. C.; Marguerettaz, A. M. *J. Org. Chem.* **1987**, *52*, 827.

(17) Ogoshi, H. ; Sugimoto, H. ; Nishiguchi, T. ; Watanabe, T. ; Matsuda, Y. ; Yoshida, Z. *Chem. Lett.* **1978**, 29.

(18) The rate of trans to cis isomerization was measured. The molar ratio of trans to cis at equilibrium was 1:1 for both **1** and the free base of **1**.

(19) (a) Ogoshi, H.; Saita, K.; Sakurai, K.; Watanabe, T.; Toi, H.; Aoyama, Y. *Tetrahedron Lett.* **1986**, *27*, 6365. (b) Aoyama, Y.; Saita, K.; Toi, H.; Ogoshi, H.; Okamoto, Y. *Tetrahedron Lett.* **1987**, *28*, 4853.

(20) HPLC was performed by use of YMC A-K03, Yamamura Chemical Labs. Co., Ltd. using hexane:$CHCl_3$:ethanol = 19:80:1 as eluent. Because the peak separation was not complete, column chromatographic separation was repeated until the optically pure free base of (+)-**1** was obtained. Attempts to resolve the zinc complex **1** were unsuccessful.

(21) A chiral column, Daicel Chiralcel OD, was used with hexane:isopropanol=4:1 as eluent.

(22) Eisner, U.; Lichtarowicz, A.; Linstead, R. P. *J. Chem. Soc.* **1957**, 733.

Chapter 4

Chiral Recognition of Asymmetric Amino Acid Esters by Trifunctional Chiral Porphyrin and its Mechanism.

Abstract

The chiral host (+)-**1**, whose preparation is described in chapter 3, was found to show an enantioselectivity of 2.0 to 2.8 in respect to L- and D-enantiomers of Ile-OMe, Leu-OMe, Leu-OBzl, Val-OMe, Pro-OMe, and Phe-OMe. The binding constants of isoleucine methyl ester to chiral (+)-**1** determined by UV-vis titration were 6780 M^{-1} for L-Ile-OMe and 2420 M^{-1} for D-Ile-OMe. The binding constants of serine benzyl ester to (+)-**1** were 1340 M^{-1} for L-Ser-OBzl and 2840 M^{-1} for D-Ser-OBzl, indicating that the enantioselectivity was reversed. Reference porphyrins **2** - **4**, which lack some of the recognition groups, were used to clarify the roles of the recognition groups of (+)-**1** in thermodynamics of the binding processes. Total free energy change upon binding of L- and D-Ile-OMe to host (+)-**1** ($\Delta G°_{total}$, L: –5.05; D: –4.46 kcal/mol) was separated into three terms; metal coordination energy ($\Delta G°_{Zn}$) –4.15 kcal/mol, hydrogen bond energy ($\Delta\Delta G°_{OH}$) –1.30 kcal/mol, and steric repulsion energy for L-isomer ($\Delta\Delta G°^{L}_{COOMe}$) +0.40 kcal/mol, and that for D-isomer ($\Delta\Delta G°^{D}_{COOMe}$) +0.99 kcal/mol , respectively. The third recognition group (CH_2CO_2Me) of (+)-**1** was found to destabilize the complexes owing to steric repulsions. In contrast, the CH_2CO_2Me group was found to stabilize the complex between D-Ser-OBzl and (+)-**1**, suggesting that hydrogen bonding between the OH group of serine and the C=O group of (+)-**1** takes place. Based on these thermodynamic studies, chiral recognition was found to be achieved by cooperative functions of these three recognition groups.

Introduction

In order to achieve chiral recognition, recognition groups should be fixed in a convergent fashion to constitute a chiral recognition pocket. Approaches to the design and preparation of a chiral recognition host have been extensively reported.[1, 2, 3, 4, 5]

Chiral recognition of a flexible molecule like amino acid is an interesting problem, because it is considered that for highly enantioselective recognition the internal rotational freedom of amino acid derivatives should be effectively frozen at least by three-point interactions. The physicochemical aspect, such as thermodynamic properties, of such multi-point chiral recognition process has not yet been clarified. The assignment of the free energy changes of each recognition pair used in the chiral recognition will be helpful in understanding fundamental processes for a range of biological and chemical phenomena[6, 7] and in developing a new method of, for example, asymmetric synthesis and chromatographic enantiomer separation. For that purpose, it is important to design a host-guest system so that the nature of the elementary interactions can be clarified unambiguously. In the previous chapter, the syntheses of the trifunctional chiral porphyrin, together with other reference porphyrins, whose structure and interaction sites are well-defined, are described.

In the present chapter, the binding features of chiral α-amino acid esters by trifunctional chiral host, and the roles of the three recognition sites, the zinc ion, the OH group, and the CH_2CO_2Me group, in binding processes of amino acid esters are investigated from the thermodynamic viewpoints.

Results and Discussion

Chart I.

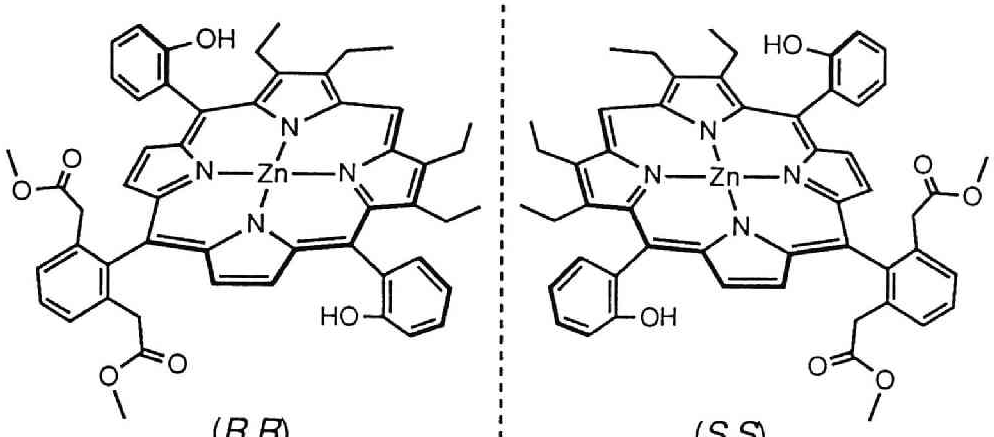

1

Thermodynamic Studies. Association constants between hosts **1**-**4** and a series of optically active amino acid esters (methyl esters of alanine, valine, leucine, isoleucine, phenylalanine and proline, benzyl esters of serine and leucine) or related amines were determined by UV-vis spectrophotometric titration, and are summarized in Table I. For chiral host **1**, the first eluted enantiomer (+)-**1** resolved by means of HPLC on an optically active column was used. The benzyl ester of serine was used instead because the methyl ester of serine showed poor solubility in $CHCl_3$. Host (+)-**1** showed enantioselectivities except for Ala-OMe and 1-phenylethylamine. The ratios of association constants of (+)-**1** for L-amino acid ester to those of (+)-**1** for D-isomer were in the range of 2.0 to 2.8 for Ile-OMe, Leu-OMe, Leu-OBzl, Val-OMe, Pro-OMe, and Phe-OMe, and 0.5 for Ser-OBzl. It was confirmed that the enantiomer host (-)-**1** showed the reversed enantioselectivity for Leu-OMe. It is interesting to note that the enantioselectivity was reversed for Ser-OBzl.

Table I. Binding Constants (K) between Zinc Porphyrins (**1**-**4**) and Chiral Amino Acid Esters or Related Amines.[a]

	$K(M^{-1})$			
	(+)-**1** [b]	**2**	**3**	**4**
L-Ile-OMe	6780 ± 40	13700 ± 90	780 ± 30	1420 ± 20
D-Ile-OMe	2420 ± 20			
L-Leu-OMe	6160 ± 40	13300 ± 70	680 ± 20	1130 ± 20
D-Leu-OMe	2460 ± 20			
L-Val-OMe	6130 ± 40	12600 ± 100	650 ± 30	1240 ± 20
D-Val-OMe	2440 ± 30			
L-Pro-OMe	48100 ± 400	113000 ± 900	6700 ± 300	13200 ± 200
D-Pro-OMe	21100 ± 200			
L-Phe-OMe	4130 ± 30	9650 ± 50	1000 ± 40	1770 ± 30
D-Phe-OMe	2060 ± 20			
L-Ala-OMe	1590 ± 20	3460 ± 20	720 ± 30	740 ± 10
D-Ala-OMe	1420 ± 20			
L-Leu-OBzl	3450 ± 30	10100 ± 60	560 ± 30	1060 ± 20
D-Leu-OBzl	1540 ± 10			
L-Ser-OBzl	1340 ± 10	2400 ± 50	920 ± 20	480 ± 10
D-Ser-OBzl	2840 ± 10			
EA[c]	5040 ± 30	4500 ± 50	5250 ± 110	2410 ± 20
(*R*)-PEA[d]	700 ± 20	1460 ± 20	1250 ± 20	1570 ± 50
(*S*)-PEA[d]	680 ± 10			

[a] In $CHCl_3$ at 15°C. [b] The optical resolution of **1** was performed by means of HPLC, and the first eluted enantiomer (+)-**1** was used.

[c] Abbreviation: EA, ethanolamine. [d] Abbreviation: PEA, 1-phenylethylamine.

The roles of three recognition sites; Zn ion (a metal coordination site), the OH groups (a hydrogen bond donor site), and the CH_2CO_2Me groups (a hydrogen bond acceptor and/or steric repulsion site) of host (+)-**1**, can be clarified by comparing the association constants between hosts (+)-**1**, **2** - **4** and a series of amino acid esters. The basic assumptions are as follows.

By considering (n-1) hypothetical intermediate states between the initial (an uncomplexed state) and the final states (a complexed state), the total free energy change can be separated into n terms.

$$\Delta G^\circ_{total} = \Delta G^\circ_1 + \Delta G^\circ_2 + \cdots + \Delta G^\circ_n$$

where ΔG°_1 is the free energy difference between the initial state (an ideal solution containing a standard concentration (1M) of host and a standard concentration of guest with no association complex formation), and the one-point adduct state (an ideal solution containing a standard concentration of a host-guest complex, in which only recognition group 1 of host and recognition group 1 of guest interact each other and other recognition groups have no specific interaction). ΔG°_2 is similarly defined as the free energy change between the one-point adduct state and the two-point adduct state. We assume that the **4**-amino acid ester complex is the one-point adduct state and the **2**-amino acid ester complex is the two-point adduct state. Then, the free energy changes associated with each interaction can be evaluated according to equations (1)~(5) in Chart II. This assumption is valid if the introduction of the functional groups into the *ortho*-position of the *meso*-phenyl moieties has negligibly small inductive effect on the metal coordination site and has little effect on the translational and rotational entropy of the whole molecules. To determine each association constant in equations (1)~(5) experimentally, the following requiement shoul be met. The free energy changes at three kinds of the interaction site are different enough, for example, to meet the following relationship.

Chart II.

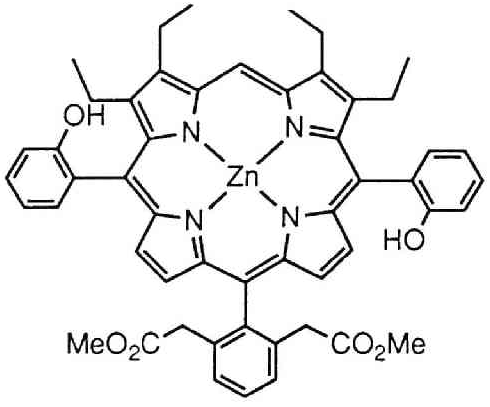

1

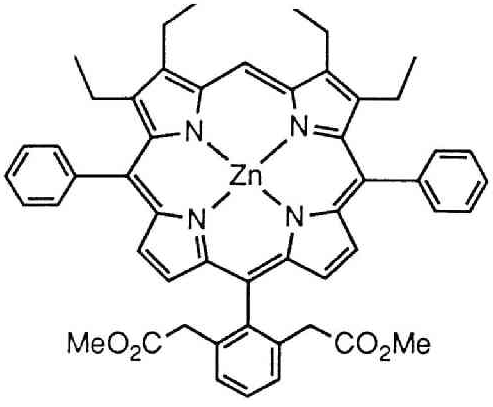

3

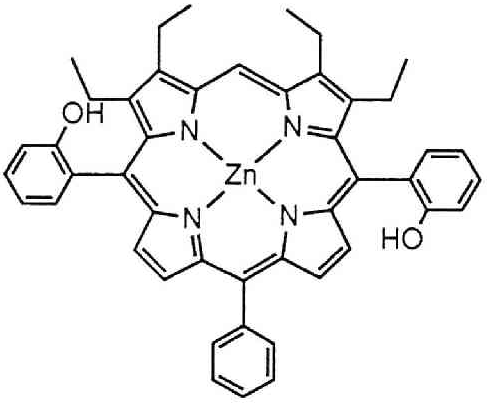

2

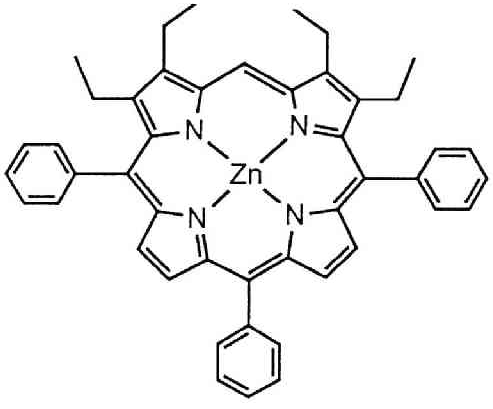

4

$$\Delta G^{\circ}_{Zn} = -RT\ln K(\mathbf{4}) \quad (1)$$

$$\Delta\Delta G^{\circ}_{OH} = -RT\ln(K(\mathbf{2}) / K(\mathbf{4})) \quad (2)$$

$$\Delta\Delta G^{\circ}_{COOMe} = -RT\ln(K(\mathbf{3}) / K(\mathbf{4})) \quad (3)$$

$$\Delta\Delta G^{\circ L}_{COOMe} = -RT\ln(K((+)\text{-}\mathbf{1}, L) / K(\mathbf{2})) \quad (4)$$

$$\Delta\Delta G^{\circ D}_{COOMe} = -RT\ln(K((+)\text{-}\mathbf{1}, D) / K(\mathbf{2})) \quad (5)$$

Table II. Contribution from Various Recognition Interactions to Total Free Energy Changes upon Complexation (kcal/mol).[a]

	$\Delta G°_{Zn}$	$\Delta\Delta G°_{OH}$	$\Delta\Delta G°_{COOMe}$	$\Delta\Delta G°^{L}_{COOMe}$	$\Delta\Delta G°^{D}_{COOMe}$
Ile-OMe	−4.15	−1.30	+0.35	+0.40	+0.99
Leu-OMe	−4.02	−1.41	+0.29	+0.44	+0.97
Val-OMe	−4.08	−1.33	+0.37	+0.41	+0.94
Pro-OMe	−5.43	−1.23	+0.39	+0.49	+0.96
Phe-OMe	−4.28	−0.97	+0.33	+0.49	+0.89
Ala-OMe	−3.78	−0.89	+0.02	+0.45	+0.51
Leu-OBzl	−3.99	−1.29	+0.37	+0.61	+1.08
Ser-OBzl	−3.53	−0.92	−0.37	+0.33	−0.10
ethanolamine	−4.46	−0.36	−0.45	---[b]	---[b]

[a] In $CHCl_3$ at 15°C. [b] $-RT\ln(K((+)\text{-}\mathbf{1}) / K(\mathbf{2})) = -0.06$ kcal/mol.

$|\Delta G°_{Zn}| >> |\Delta\Delta G°_{OH}| > |\Delta\Delta G°^{L}_{COOMe}|$.

Especially, the stabilization of the strongest interaction, coordination, should be large enough to compensate well for the loss of the translational as well as the rotational entropy associated with the bimolecular association.[8]

It is considered that the porphyrins **1**~**4** meet well the above conditions. Another method to use reference amines instead of the reference porphyrins was avoided because slight difference in the structure of small and flexible amines had drastic effect on the affinity (Compare, for example, the association constants between **4** and a series of amino acid esters or related amines in Table I. See also Table I in chapter 1).

Free energy changes associated with metal coordination interaction between the zinc ion and the amino group of guest were estimated from the association constants for host **4**. The metal coordination energies ($\Delta G°_{Zn}$) were calculated by $\Delta G°_{Zn} = -RT \ln K(\mathbf{4})$,[9] and were almost the same for Ile-OMe, Leu-OMe, and Val-OMe (Table II). Much stronger binding was observed for Pro-OMe, which can be ascribed to a strong basicity of the secondary amino group of proline. Slightly stronger binding for Phe-OMe may be ascribed to the additional attractive energy owing to the π-stacking interaction as suggested in chapter 1.

The OH groups of host (+)-**1** and **2** were also found to stabilize the host-guest complexes as evident from comparisons between $K(\mathbf{2})$ and $K(\mathbf{4})$ (or between K((+)-**1**) and $K(\mathbf{3})$). The stabilization energies owing to the OH group were evaluated from $\Delta\Delta G°_{OH} = -RT \ln (K(\mathbf{2}) / K(\mathbf{4}))$ and listed in Table II. The stabilization energies amount to −1.2 to −1.4 kcal/mol for Ile-OMe, Leu-OMe, Leu-OBzl, Val-OMe and Pro-OMe, whereas the stabilization energies for Phe-OMe, Ala-OMe and Ser-OBzl were smaller. These energies and trends are similar to the binding of amino acid esters to [*trans*-5, 15-bis(2-hydroxylnaphthyl)-2, 3, 7, 8, 12, 13, 17, 18-octaethylporphyrinato]zinc(II) studied in chapter 1 both by

thermodynamic and spectroscopic (^{1}H NMR and CD) analyses. A comparison between K((+)-**1**) and K(**3**) indicates that the OH group in (+)-**1** can also stabilize the complexes even in the presence of the CH_2CO_2Me groups. These observations indicate that hydrogen bonding between the OH group of host (+)-**1** and the C=O group of guest takes place. Spectroscopic evidence for the hydrogen bonding was obtained from ^{1}H NMR titration (*vide infra*). The differential stabilization energies calculated from $-RT \ln (K((+)\text{-}\mathbf{1})/K(\mathbf{3}))$ range from –1.1 to –1.3 kcal/mol for L-Ile-OMe, Leu-OMe, Val-OMe and Pro-OMe and –0.6 to –0.8 kcal/mol for the D-enantiomers.

The third recognition group, the CH_2CO_2Me group, was found to serve three different functions depending on the side chain of the guest. It acted as (1) a minor repulsive site for L-amino acid esters, (2) a major repulsive site for D-amino acid esters except Ser-OBzl and (3) an attractive interaction site for D-Ser-OBzl. The repulsive function of the CH_2CO_2Me group can be clearly indicated by comparing between K((+)-**1**) and K(**2**), or between K(**3**) and K(**4**). Comparisons between K(**3**) and K(**4**) indicate the steric repulsion in the absence of the hydrogen bonding (the amino acid esters can freely rotate), whereas comparisons between K((+)-**1**) and K(**2**) indicate the steric repulsion in the presence of the hydrogen bonding (the orientation of the amino acid esters is fixed). Table I shows that the ratios of K((+)-**1**) to K(**2**) ranged between 0.42 and 0.56 for all the L-isomers. This result implies that the CH_2CO_2Me groups of host (+)-**1** restrict the size of the recognition pocket, resulting in a weak destabilization effect on the binding of L-isomers. These effects are not sensitive to the variations of the side chain of the guests. In the case of D-isomers, the ratios of K((+)-**1**) to K(**2**) ranged between 0.18 and 0.21 except for Ser-OBzl and Ala-OMe, indicating the larger inhibitory effects of the CH_2CO_2Me group for the D-enantiomers. The repulsive energies between the CH_2CO_2Me groups of host (+)-**1** and the L-, and D-amino acid esters were calculated by

$\Delta\Delta G^{\circ L}_{COOMe} = -RT \ln (K((+)\text{-}\mathbf{1}, L) / K(\mathbf{2}))$, and $\Delta\Delta G^{\circ D}_{COOMe} = -RT \ln (K((+)\text{-}\mathbf{1}, D) / K(\mathbf{2}))$, respectively. The repulsive energies between the CH_2CO_2Me groups of host **3** and the amino acid esters were similarly calculated by $\Delta\Delta G^{\circ}_{COOMe} = -RT \ln (\mathbf{3}) / K(\mathbf{4}))$. It should be noted that the values of $\Delta\Delta G^{\circ L}_{COOMe}$ are only slightly larger than $\Delta\Delta G^{\circ}_{COOMe}$ except for Ala-OMe and are almost constant, and that the values of $\Delta\Delta G^{\circ D}_{COOMe}$ are much larger than $\Delta\Delta G^{\circ}_{COOMe}$. This trend indicates that the steric repulsion between (+)-**1** host and L-isomers is small even if the orientation of the amino acid esters is fixed by the hydrogen bonding interaction, but that the steric repulsion energies between (+)-**1** host and D-isomers are enhanced by the two-point fixation of D-isomer. The stabilization energies associated with the hydrogen bonding, $\Delta\Delta G^{\circ}_{OH}$, are nearly cancelled by the destabilization energy associated with the steric repulsion, $\Delta\Delta G^{\circ D}_{COOMe}$.[10]

The enantioselectivity of host (+)-**1** was reversed for Ser-OBzl. Because host (+)-**1** binds L-Leu-OBzl more strongly than D-isomer, the reversal of enantioselectivity cannot be ascribed to the benzyl ester but can be ascribed to the serine side chain. The differential stabilization energies ($\Delta\Delta G^{\circ D}_{COOMe}$) estimated from the ratios $K((+)\text{-}\mathbf{1})$ to $K(\mathbf{2})$ were –0.10 kcal / mol for the D-Ser-OBzl (+)-**1** complex and the differential stabilization energies ($\Delta\Delta G^{\circ}_{COOMe}$) estimated from the ratios $K(\mathbf{3})$ to $K(\mathbf{4})$ were –0.45 kcal / mol for the ethanolamine - **3** complex (Table II). Although these stabilization energies seem to be small, it should be noted that repulsive energies ranging between +0.5 and +1.0 kcal / mol are observed for all the D-amino acid esters (Table II). If the steric repulsion energy between (+)-**1** and D-Ser-OBzl can be assumed to be comparable to those observed for D-Ala-OMe and D-Val-OMe, the additional attractive interaction between the CH_2CO_2Me group and Ser-OBzl would amount to –0.6 to –1.1 kcal / mol. This attractive interaction may be attributable to hydrogen bonding between the OH group of serine side chain and

the CH_2CO_2Me group of (+)-**1**. The binding behavior of Ser-OBzl and ethanolamine to the reference hosts is also consistent with the above discussions that attractive interaction between the CH_2CO_2Me group of host and the OH group of the guest exists. The attractive energies between the CH_2CO_2Me group of host and the OH group of the guests can be calculated from $-RT \ln (K(3) / K(4))$, and those between the OH group of host and the C=O group of the guests from $-RT \ln (K(2) / K(4))$. The free energies thus estimated were: (**2**) OH•••O=C(Ser), –0.92kcal/mol; (**3**) C=O•••HO(Ser), –0.37 kcal/mol; (**2**) OH•••OH(ethanolamine), –0.36 kcal/mol; (**3**) C=O•••HO(ethanolamine), –0.45 kcal/mol. These attractive interactions may be attributable to hydrogen bonding interaction. The fact that (**2**) OH•••O=C (Ser) interaction is stronger than (**3**) C=O•••HO(Ser) interaction may indicate that the geometry for the latter hydrogen bond is not optimum. Contributions from entropy changes associated with changes in the internal rotation of the guest may also be important because the formation of the latter hydrogen bond would freeze more C-C bond rotations.

^{1}H NMR Studies. The chemical shift change of the signals of the enantiomer (+)-**1** was monitored by addition of L- (or D-) Ala-OMe and Leu-OMe. Typical saturation behavior of the chemical shift values was observed. Complexation-induced shift (CIS) values of **1** were obtained by adding excess amino acid estes or computer-assisted extrapolation, and listed in Figure 1(a), (b). The displacements were largest for the OH proton, and the downfield shift of the OH protons indicates the hydrogen bonding to the guest carbonyl group. Other protons whose chemical shifts are affected are *meso*-protons, CH_2 and CH_3 of the carbomethoxymethyl groups, and 2- (or 18-)ethyl protons further from the phenyl group. In Figure 1(c), (d) are shown the differences between $\Delta\delta$ of L-enantiomer and that of D-enantiomer ($\Delta\Delta\delta = \Delta\delta(D) - \Delta\delta(L)$). This value ($\Delta\Delta\delta$) can be taken as a measure of diastereomeric intereaction. The $\Delta\Delta\delta$ values for Leu-OMe are larger

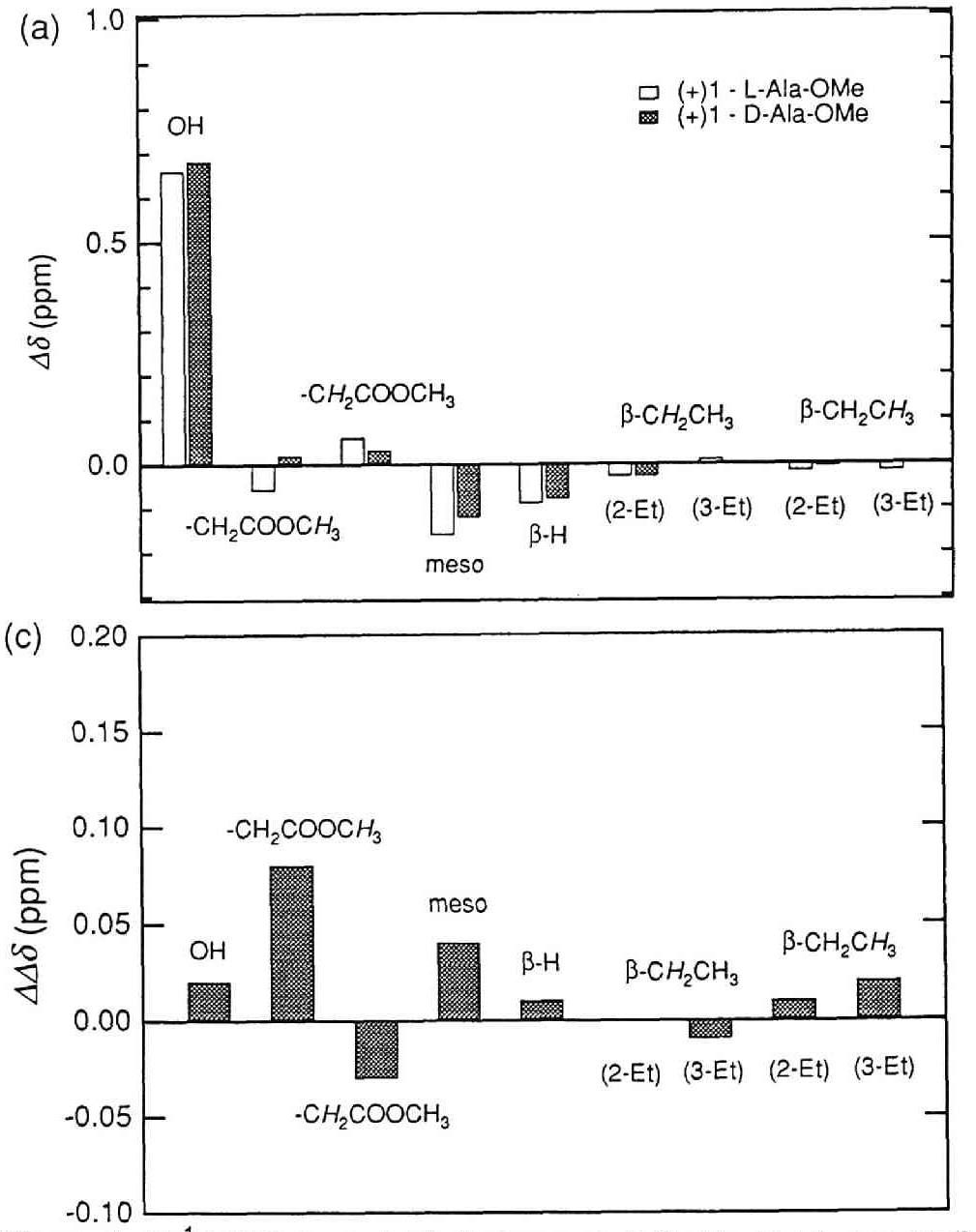

Figure 1. (a) ^{1}H NMR chemical shift displacements ($\Delta\delta$) of host (+)-**1** upon binding of (L)-, and (D)-Ala-OMe. (c) The difference in ^{1}H NMR chemical shift displacements ($\Delta\delta$) of host (+)-**1** upon binding of Ala-OMe between D-guest and L-guest ($\Delta\Delta\delta$).

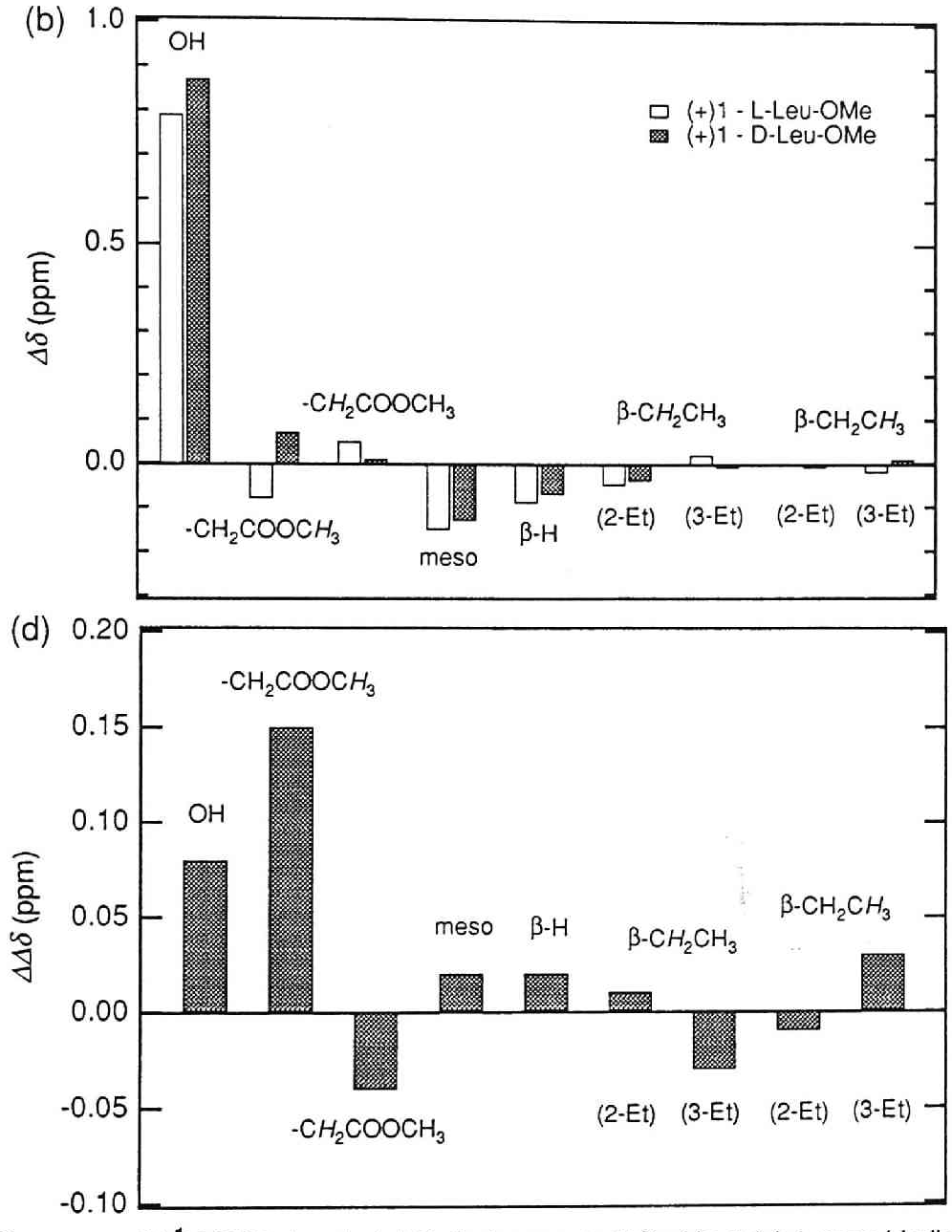

Figure 1. (b) ^{1}H NMR chemical shift displacements ($\Delta\delta$) of host (+)-**1** upon binding of (L)-, and (D)-Leu-OMe. (d) The difference in ^{1}H NMR chemical shift displacements ($\Delta\delta$) of host (+)-**1** upon binding of Leu-OMe between D-guest and L-guest ($\Delta\Delta\delta$).

than those for Ala-OMe, in accord with the higher enantioselectivity of **1** for Leu-OMe than Ala-OMe. The largest difference in $\Delta\Delta\delta$ was observed for the methyl group of the CH_2CO_2Me group for both Ala-OMe and Leu-OMe. The methylene group of the CH_2CO_2Me group was also affected much. The signal for the methyl group of the CH_2CO_2Me group was shifted to lower magnetic field and in the opposite direction to that for methylene group of the CH_2CO_2Me group. These observation suggest that the methyl groups of CH_2CO_2Me were directed outside by the steric repulsion of the side chain of the D-amino acid esters (*vide infra*). The values of $\Delta\Delta\delta$ of 3- (or 17-) ethyl groups is larger than those of 2- (or 18-) ethyl groups. This may reflect the chiral interaction for the second recognition group (the OH of the phenyl group), since the closer ethyl groups to the OH are more affected.

Mechanism of Chiral Recognition. The observed selectivities of host **1**-**4** allow us to discuss the mechanism of chiral recognition and conformation of the host-guest complexes. We observed that the CH_2CO_2Me group of host (+)-**1** served a repulsive function for L-Ser-OBzl and an attractive function for D-Ser-OBzl. This dual function of the third recognition group may be made possible by the simultaneous two-point fixation of the guest through the metal coordination and the hydrogen bonding interaction between the OH groups of host (+)-**1** and the C=O group of the amino acid esters. These selectivities of host (+)-**1** strongly suggest that the side chain of the D-amino acid is in close proximity to the CH_2CO_2Me group of (+)-**1** host by the two-point fixation, wheras that of L-amino acid is directed away from the CH_2CO_2Me group. Thus steric repulsion will be smaller for L-guest, leading to the preference for L-guest as observed for host (+)-**1**. In the case of the (+)-**1** D-Ser-OBzl complex, the two-point fixation will direct the side chain of serine to the CH_2CO_2Me group, resulting in the further stabilization. (The stabilization by the CH_2CO_2Me can be ascribed to the hydrogen bonding interaction between the OH group of Ser-OBzl and the C=O group of the host.)

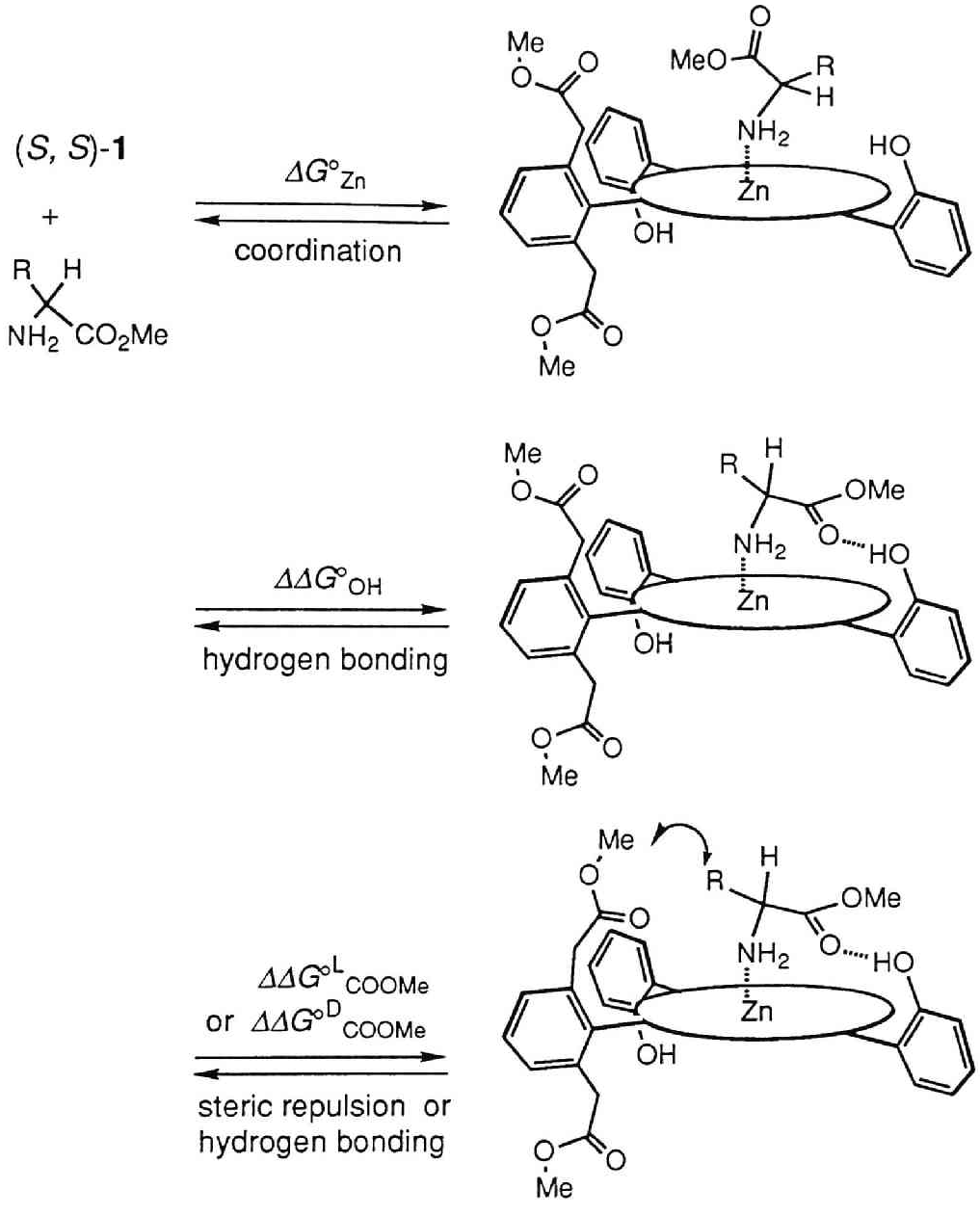

Figure 2. Proposed mechanism of chiral recognition. The binding of amino acid ester to (*S*, *S*)-host **1** is assumed to occur in three steps.

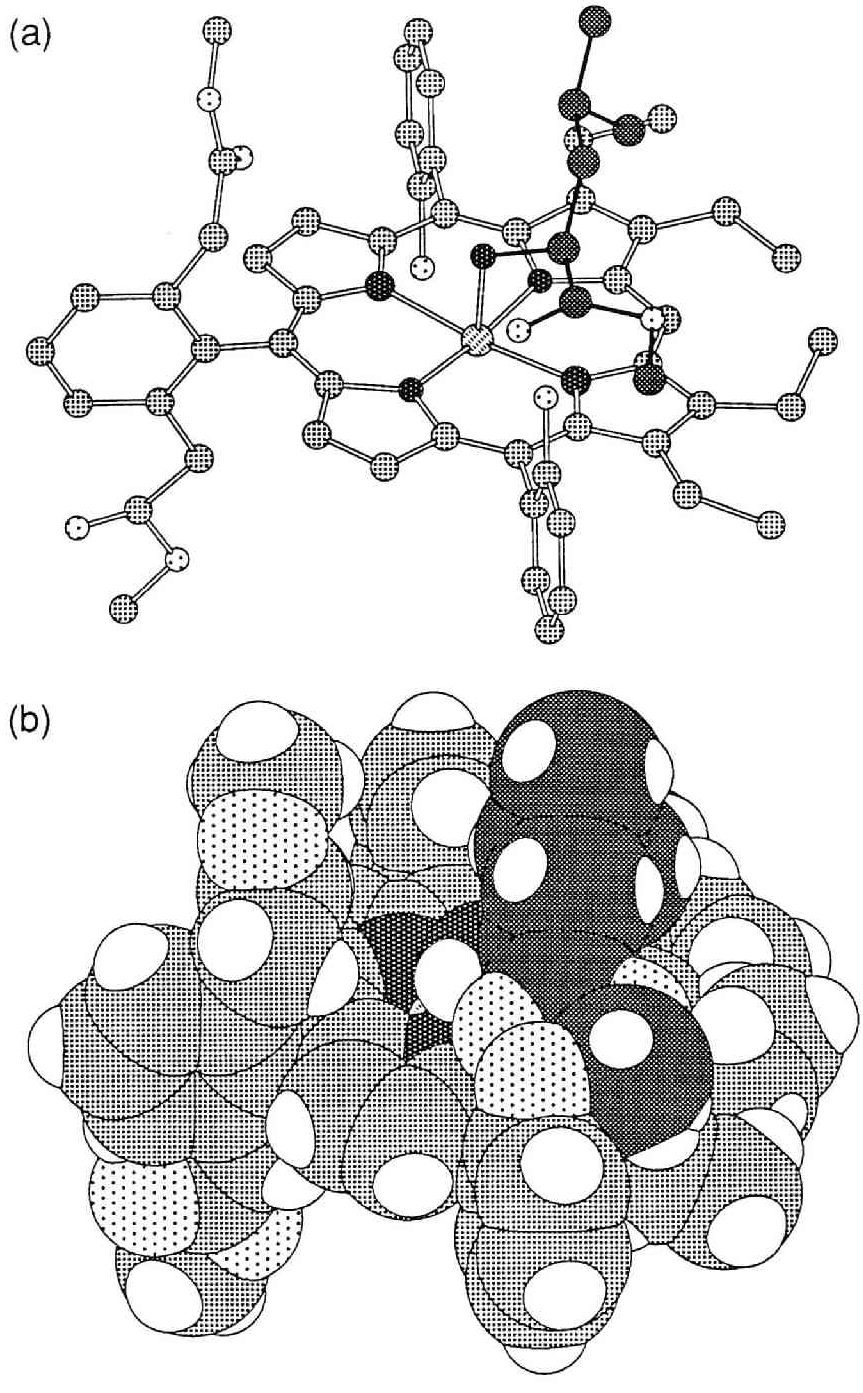

Figure 3. Proposed conformation of the (*S*, *S*)-**1** – L-Leu-OMe complex.
(a) Ball and stick model. The hydrogen atoms are omitted for clarity.
(b) Space filling model.

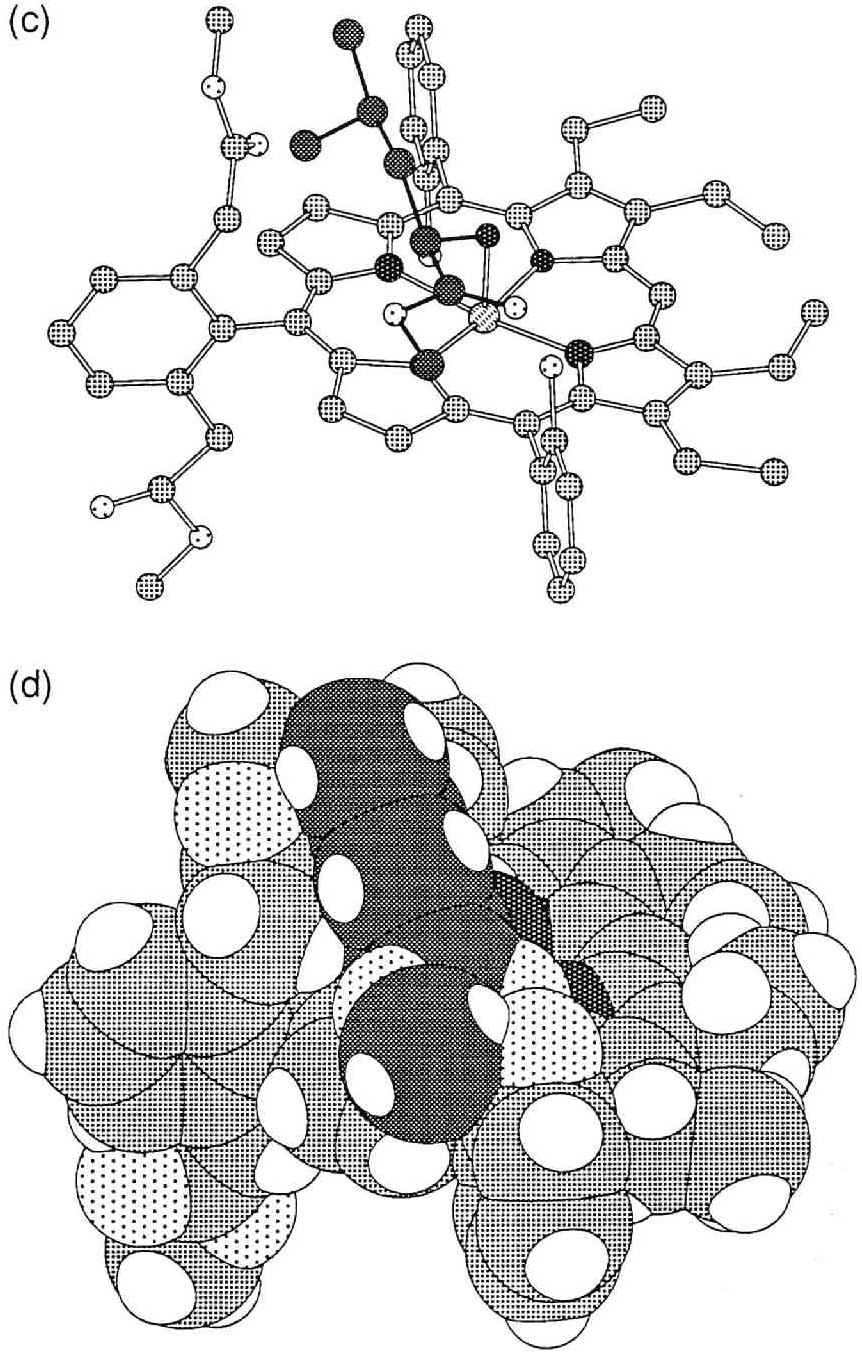

Figure 3. Proposed conformation of the (*S*, *S*)-**1** – D-Leu-OMe complex.
(c) Ball and stick model. The hydrogen atoms are omitted for clarity.
(d) Space filling model.

By assuming these conformations, enantioselectivity of host (+)-**1** can be consistently explained for all the amino acid esters examined. Furthermore, the poor enantioselectivity for (*S*)-or(*R*)-1-phenylethylamine, which has no hydrogen bonding site (Table I), demonstrates the importance of the two-point fixation in the chiral recognition process. Based on these observations we suggest (+)-**1** has (*S S*) and (-)-**1** (*R R*) configuration (Chart I). The proposed chiral recognition process are shown in Figure 2. The proposed conformations of the diastereomeric complexes, which were supported by molecular orbital calculations (MOPAC/PM3),[11] are shown in Figure 3.

Other evidence supporting the above proposed mechanism of chiral recognition is that there is a correlation between chiral recognition energy and hydrogen bonding energy. Figure 4 shows that the chiral recognition energies (| $\Delta G°$((+)-**1**, L) $-\Delta G°$((+)-**1**, D) |) were correlated to the hydrogen bonding energy ($-\Delta\Delta G°_{OH}$) between the OH group of host and the C=O group of guest. The chiral recognition energies were increased with increasing hydrogen bonding energy ($-\Delta\Delta G°_{OH}$). The correlation coefficient ρ between the two energies was 0.76. On the other hand, poor correlation (ρ = 0.25) was found between the chiral recognition energy and the coordination energy ($-\Delta G°_{Zn}$). These observations indicate that hydrogen bonding is a driving force for the present chiral recognition. The above correlation implies that the magnitude of the first recognition ($-\Delta G°_{Zn}$, metal coordination) is relatively unimportant and the magnitude of the second recognition ($-\Delta\Delta G°_{OH}$, hydrogen bonding) is important for chiral recognition. This may be the direct consequence that the rotation of guest along the Zn N axis should be restricted for the chiral recognition to occur.

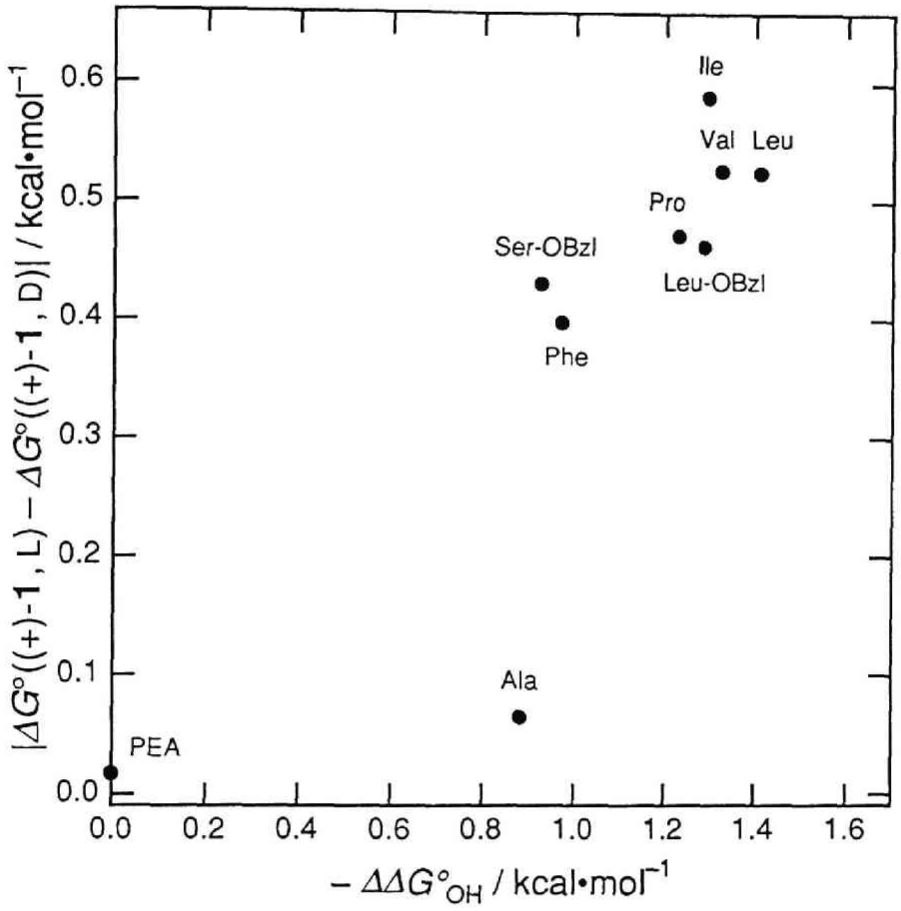

Figure 4. Correlation between hydrogen bonding interaction($-\Delta\Delta G°_{OH}$) and chiral recognition energy ($|\Delta G°((+)\text{-}\mathbf{1}, L) - \Delta G°((+)\text{-}\mathbf{1}, D)|$)

Experimental Section

General Remarks. ^{1}H NMR spectra were obtained using a JEOL A-500 spectrometer. UV-vis spectra were recorded on either a Hitachi U-3410 spectrometer or a Hewlett-Packard 8452 diode array spectrophotometer with a thermostatted cell compartment. Association constants between host **1-4** and amino acid esters were determined by UV-vis spectrophotometric titration at 15℃ in $CHCl_3$, and the procedure of the UV-vis titration are described in chapter 1. The $CHCl_3$ was Spectrosol purchased from Dojindo Laboratories, which contains *ca.* 1% ethanol as a stabilizer. The porphyrins **1~4** were synthesized as described in chapter 3. Amino acid esters were purchased or prepared as described in chapter 1, and were distilled just before titration experiments. Molecular orbital calculations were carried out on a Silicon Graphics IRIS Indigo XS 24 workstation.

References

(1) For chiral binaphthyl hosts, see: (a) Lehn, J. M.; Simon, J.; Moradpour, A. *Helv. Chim. Acta.* **1978**, *61*, 2407. (b) Peacock, S. C.; Domeier, L. A.; Gaeta, F. C. A.; Helgeson, R. C.; Timko, J. M.; Cram, D. J. *J. Am. Chem. Soc.* **1978**, *100*, 8190. (c) Newcomb, M.; Toner, J. L.; Helgeson, R. C.; Cram, D. J. *J. Am. Chem. Soc.* **1979**, *101*, 4941. (d) Castro, P. P.; Georgiadis, T. M.; Diederich, F. *J. Org. Chem.* **1989**, *54*, 5835. (e) Castro, P. P.; Diederich, F. *Tetrahedron Lett.* **1991**, *32*, 6277. (f) Garcia-Tellado, F.; Albert, J.; Hamilton, A. D. *J. Chem. Soc., Chem. Commun.* **1991**, 1761.

(2) For chiral cyclophane hosts, see: (a) Petti, M. A.; Shepodd, T. J.; R. E. Barrans, J.; Dougherty, D. A. *J. Am. Chem. Soc.* **1988**, *110*, 6825.(b) Sanderson, P. E. J.; Kilburn, J. D.; Still, W. C. *J. Am. Chem. Soc.* **1989**, *111*, 8314. (c) Webb, T. H.; Suh, H.; Wilcox, C. S. *J. Am. Chem. Soc.* **1991**, *113*, 8554. (d) Hong, J.-I.; Namgoong, S. K.; Bernardi, A.; Still, W. C. *J. Am. Chem. Soc.* **1991**, *113*, 5111. (e) Bhattarai, K. M.; Bonar-Law, R. P.; Davis, A. P.; Murray, B. A. *J. Chem. Soc., Chem. Commun.* **1992**, 752. (v) Yoon, S. S.; Still, W. C. *J. Am. Chem. Soc.* **1993**, *115*, 823.

(3) For chiral molecular clefts, see: (a) Jeong, K.-S.; Muehldorf, A. V.; Rebek, J., Jr. *J. Am. Chem. Soc.* **1990**, *112*, 6144. (b) Famulok, M.; Jeong, K.-S.; Deslongchamps, G.; Rebek, J., Jr. *Angew. Chem. Int. Ed. Engl.* **1991**, *30*, 858.

(4) For cyclodextrin hosts, see: (a) Tabushi, I.; Kuroda, Y.; Mizutani, T. *J. Am. Chem. Soc.* **1986**, *108*, 4514.(b) Impellizzeri, G.; Maccarrone, G.; Rizzarelli, E.; Vecchio, G.; Corradini, R.; Marchelli, R. *Angew. Chem. Int. Ed. Engl.* **1991**, *30*, 1348. (c) Lipkowitz, K. B.; Raghothama, S.; Yang, J. *J. Am. Chem. Soc.* **1992**, *114*, 1554.

(5) For other chiral hosts, see: (a) Echavarren, A.; Galán, A.; Lehn, J.-M.; de Mendoza, J. *J. Am. Chem. Soc.* **1989**, *111*, 4994. (b) Dobashi, Y.; Dobashi, A.; Ochiai, H.; Hara, S. *J. Am. Chem. Soc.* **1990**, *112*, 6121. (c) Galan, A.; Andreu, D.; Echavarren, A. M.; Prados, P.; Mendoza, J. d. *J. Am. Chem. Soc.* **1992**, *114*, 1511. (d) Wang, X.; Erickson, S. D.; Iimori, T.; Still, W. C. *J. Am. Chem. Soc.* **1992**, *114*, 4128.

(6) (a) Conn, E. E.; Stumpf, P. K. *Outlines of Biochemistry*; John Wiley & Sons, Inc.: 1963. (b) Alberts, B.; Bray, D.; Lewis, J.; Raff, M.; Roberts, K.; Watson, J. D. *Molecular Biology of the Cell*; Garland Publishing, Inc.: New York, 1989; chapter 5. (c) Attias, J.; Schlesinger, M. J.; Schlesinger, S. *J. Biol. Chem.* **1969**, *244*, 3810. (d) Kohno, T.; Kohda, D.; Haruki, M.; Yokoyama, S.; Miyazawa, T. *J. Biol. Chem.* **1990**, *265*, 6931.

(7) Poulos, T. L. In *Cytochrome P-450*; Montellano, P. R. O. Ed.; Plenum Press: New York, 1986.

(8) The total enthalpy change and the total entropy change can be separated into contributions from each recognition pair:

$$\Delta H^\circ_{\text{total}} = \Delta H^\circ_1 + \Delta H^\circ_2 + \cdots + \Delta H^\circ_n \qquad (1)$$

$$\Delta S^\circ_{\text{total}} = \Delta S^\circ_1 + \Delta S^\circ_2 + \cdots + \Delta S^\circ_n \qquad (2)$$

where ΔH°_i and ΔS°_i are defined in a similar manner to ΔG°_i. The one-point adduct state and two-point adduct state can be realized by using reference hosts and/or reference guests which lack some of the recognition groups. The entropy change can also be separated according to the motional changes:

$$\Delta S_{total} = \sum_{complex} S_{trans}+S_{rot}+S_{int.rot}+S_{vib}+S_{electronic}+S_{solvation}$$
$$- \sum_{host} S_{trans}+S_{rot}+S_{int.rot}+S_{vib}+S_{electronic}+S_{solvation}$$
$$- \sum_{guest} S_{trans}+S_{rot}+S_{int.rot}+S_{vib}+S_{electronic}+S_{solvation}$$
$$= \Delta S_{trans}+\Delta S_{rot}+\Delta S_{int.rot}+\Delta S_{vib}+\Delta S_{electronic}+\Delta S_{solvation} \quad (3)$$

where ΔS_{trans} is the translational entropy change of host and guest, ΔS_{rot} is the rotational entropy change of host and guest, $\Delta S_{int.rot}$ is the internal rotational entropy change of host and guest, ΔS_{vib} is the vibrational entropy change of host and guest, $\Delta S_{electronic}$ is the electronic entropy change of host and guest and $\Delta S_{solvation}$ is the entropy changes due to changes in solvation. By considering the motional changes caused by the interaction between recognition groups, we can assign each term in eq. (3) to the term in eq. (2). For example, the ΔS°_{1} term corresponds to the difference between the initial state and the one-point adduct state, which involves the translational entropy change and most of the rotational entropy change: $\Delta S^{\circ}_{1} \sim -T(\Delta S_{trans} + \Delta S_{rot})$. The translational and rotational entropy change is the largest term in eq. (3). The term $(-T(\Delta S_{trans} + \Delta S_{rot}))$ amounts to approximately 10 ~ 15 kcal/mol for porphyrin - amino acid complexation around 300K, which was determined by the van't Hoff plot. Therefore the recognition enthalpy $-\Delta H^{\circ}_{1}$ should be large enough to overcome $-T(\Delta S_{trans} + \Delta S_{rot})$, so that we can determine experimentally the free energy change associated with the first recognition pair using the following approximation.

$$\Delta G^{\circ}_{1} = \Delta H^{\circ}_{1} - T\Delta S^{\circ}_{1} \sim \Delta H^{\circ}_{1} - T(\Delta S_{trans} + \Delta S_{rot}).$$

Other entropy terms ($\Delta S_{int.rot}$, ΔS_{vib}, $\Delta S_{electronic}$), which are much smaller in magnitude, can be ascribed to ΔS°_{2}, ΔS°_{3}, and so on.

If the condition above does not hold, the enthalpy change $-\Delta H^\circ_1$ would be largely compensated by a large negative entropy change ($\Delta S_{trans} + \Delta S_{rot}$). That results in a very small free energy change of ΔG°_1 and experimental determination of ΔG°_1 would be difficult.

(9) We should examine correlation between the chiral recognition energy and $\Delta\Delta G^\circ_{Zn}$ instead of ΔG°_{Zn}. To evaluate $\Delta\Delta G^\circ_{Zn}$, the reference host for host **4** is needed, which is difficult to find. Even if we use the free base of **4** as a reference host, the binding constant between the free base of **4** and L-Leu-OMe in $CHCl_3$ is too weak to determine. We assume that $\Delta\Delta G^\circ_{Zn}$ is approximately equal to ΔG°_{Zn}. It should be noted that ΔG°_{Zn} involves the large entropy term $-T(\Delta S^\circ_{trans} + \Delta S^\circ_{rot})$.

(10) The relative magnitudes of these terms are $| \Delta G^\circ_{Zn} | > | \Delta\Delta G^\circ_{OH} | > | \Delta\Delta G^{\circ L}_{COOMe} |$ for L-amino acid esters and $| \Delta G^\circ_{Zn} | > | \Delta\Delta G^\circ_{OH} | \approx | \Delta\Delta G^{\circ D}_{COOMe} |$ for D-amino acid esters. Therefore, in the case of D-amino acid esters, the magnitude of hydrogen bonding energy is comparable to that of steric repulsion energy and the assumption that hydrogen bonding interaction observed for host **2** was the same as that observed for host (+)-**1** does not hold. In this case explicit separation between hydrogen bonding energy and steric repulsion energy is difficult.

(11) MOPAC Ver. 5 and Ver. 6, Stewart, J. J. P. *QCPE Bull.* **1989**, *9*, 10.

Chapter 5

Molecular Recognition and Complexation-Induced Metalation of Water-Soluble Cationic Porphyrin in Aqueous Media.

Abstract

Water-soluble cationic porphyrin, *trans*-5,15-bis(2-hydroxy-1-naphthyl)-2, 8, 12, 18-tetra[3-(*N*, *N*, *N*-trimethylamino)propyl]-3,7,13,17-tetramethylporphyrin tetrachloride salt (**1**), which does not self-aggregate, was designed and synthesized. Molecular recognition of the porphyrin host **1** for several guest molecules in aqueous media was studied. The complex formations between **1** and guests in 50 mM Tris buffer (pH 7.0) at 25 ℃ were monitored by UV-vis spectrophotometric titration, and the binding constants were successfully determined by use of a computer-assisted nonlinear least-squares method assuming that **1** bound two guests on both sides of the porphyrin plane; e.g. $K_1 = 5800 \pm 1200\ M^{-1}$, $K_2 = 40 \pm 10\ M^{-1}$ for **1** – terephthalate (**G 1**) complex. UV-vis spectral change and ^1H NMR titration suggested that the π-stacking interaction (or hydrophobic interaction) as well as the electrostatic interaction operate in the host guest complexes.

Reaction rates of metal insertion reaction into porphyrin cavity both in the presence of and in the absence of the guest molecules were also measured. Anionic guests **G 1** and 1, 8-dihydroxy-3, 6-naphthalanedisulfonate (**G 3**) accelerated the metalation, while 2, 2'-bipyridine-4, 4'-dicarboxylate (**G 5**) decelerated.

Introduction

Many biological molecules have highly polar recognition site exposed to bulk water phase,[1] and so model study in aqueous media is required regardless of its difficulty and complexity. Several model studies have been reported.[2] Solvation energies are one of the important terms in the energetics of association for these systems, and the hydrophobic interaction is the dominant driving force for association between host and guest in water.

Porphyrin chromophore is the useful spectroscopic probe to study molecular recognition as demonstrated in the preceding chapters. Fundamental studies of molecular recognition using a water-soluble porphyrin is also important because some porphyrin derivatives such as hematoporphyrin derivatives are reported to accumulate in the tumor cell,[3] and because some porphyrins are reported to interact with DNA.[4] However, many water-soluble porphyrins so far reported have tendencies to self-aggregate in aqueous media, because the large porphyrin surface is hydrophobic.[5] In order to study molecular recognition in water, water soluble porphyrin, which does not self-aggregate, is necessary. In this respect, cationic porphyrin is superior to anionic porphyrins, because almost all the anionic porphyrins reported so far self-aggregate so easily, whilst some cationic porphyrins do not at a wide range of pH.[5]

In this chapter, the synthesis of new water-soluble cationic porphyrin host **1** and molecular recognition of **1** for several guests are described. The host-guest complexation-induced metal insertion into porphyrin cavity are also investigated and presented briefly.[6] The present metalation rate accerelation is interesting in connection with ferrochelatase, the membrane-bound enzyme which catalyzes the insertion of ferrous ion into the protoporphyrin.[7] It has been suggested that ferrochelatase has the hydrophobic pocket to accommodate the porphyrin

macrocycle as well as the metal binding site which consists of serine or cystein residues.

Results and Discussion

The water-soluble cationic porphyrin **1** designed is shown in Scheme I. Four propylammonium substituents, which have been reported from our group to be effective both as recognition groups and as solubilizing groups in water,[8] are introduced into the β-positions. The naphthyl moieties are attached at the *meso*-positions in order to prevent self-aggregation.[9] The hydroxyl groups are necessary to facilitate the separation of *trans*- and *cis*-atropisomers by chromatography, and might also act as additional recognition sites.

Preparation of Water-Soluble Cationic Porphyrin. The synthetic route for the desired water-soluble porphyrin **1** is shown in Scheme I. The dipyrrylmathane **8** was prepared as described in the literature.[10] 5,15-Diaryl-substituted coproporphyrin tetramethyl ester derivative **9** was prepared by condensation of dipyrrylmethane **8** with 2-hydroxy-1-naphthylaldehyde in the presence of *p*-toluenesulfonic acid in MeOH. The atropisomers (trans and cis) were separated by chromatography on a silica gel column. Reduction of the tetraester derivative **9** with $LiAlH_4$ in dry THF afforded the corresponding tetraol derivative **10**. Treatment of **10** with methanesulfonyl chloride in dry pyridine afforded hexamesylated porphyrin **11**. Aminolysis of **11** with dimethylamine in THF, followed by hydrolysis with KOH, afforded tetrakis(dimethylaminopropyl) porphyrin derivative **12**. Alkylation of amino groups of **12** with CH_3I in MeOH gave tetrammonium porphyrin **13** which is still insoluble in water. Subsequent counter ion-exchange by ion-exchange column afforded water-soluble porphyrin **1**. UV-vis absorption spectra of various concentrations ($9.8 \times 10^{-7} \sim 6.3 \times 10^{-5}$ M) of **1** in 50 mM Tris buffer (pH 7.0) at 25 ℃ showed linear concentration-dependence

Scheme I. Synthesis of Water-Soluble Porphyrin.[a]

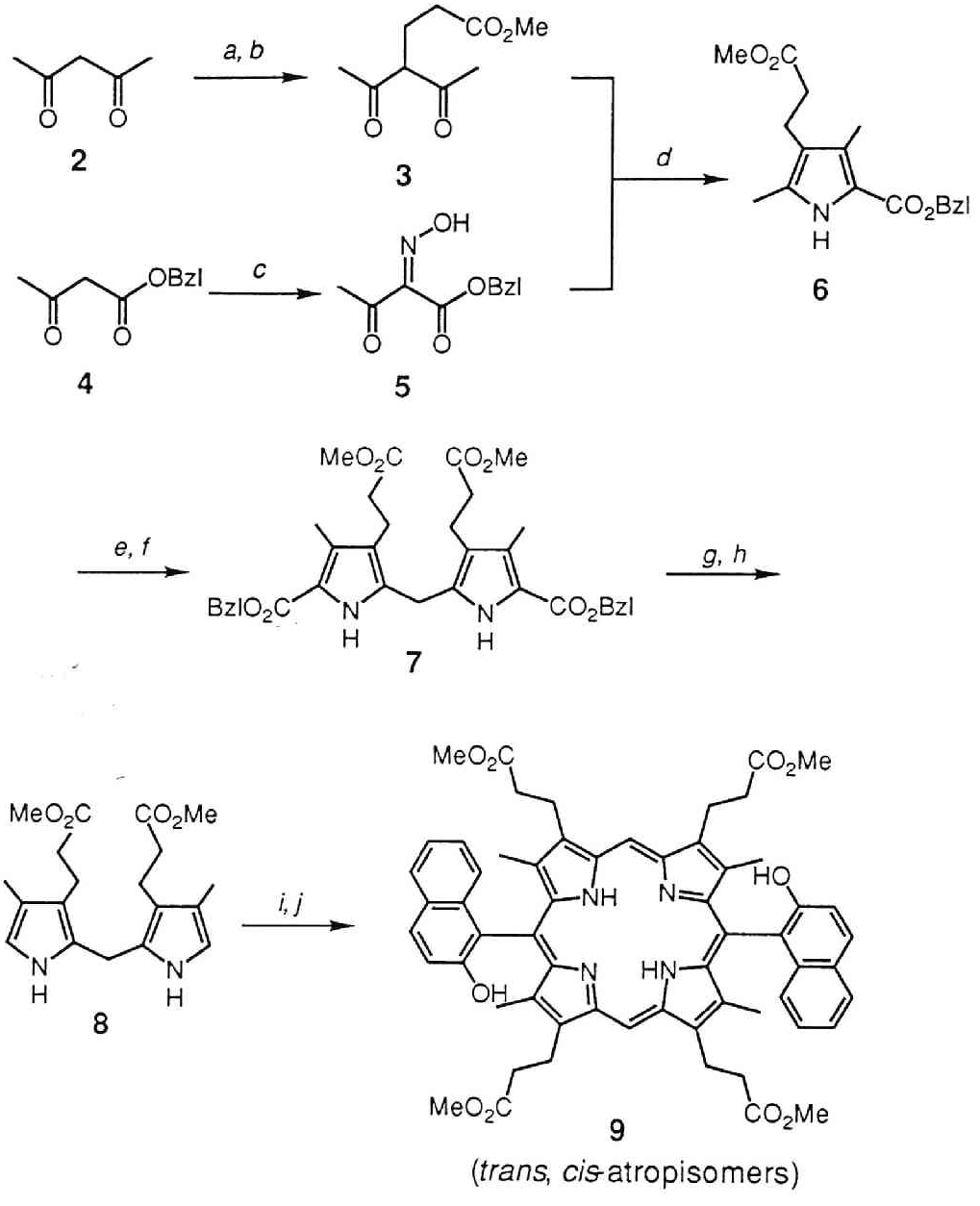

(Scheme I. continued.)

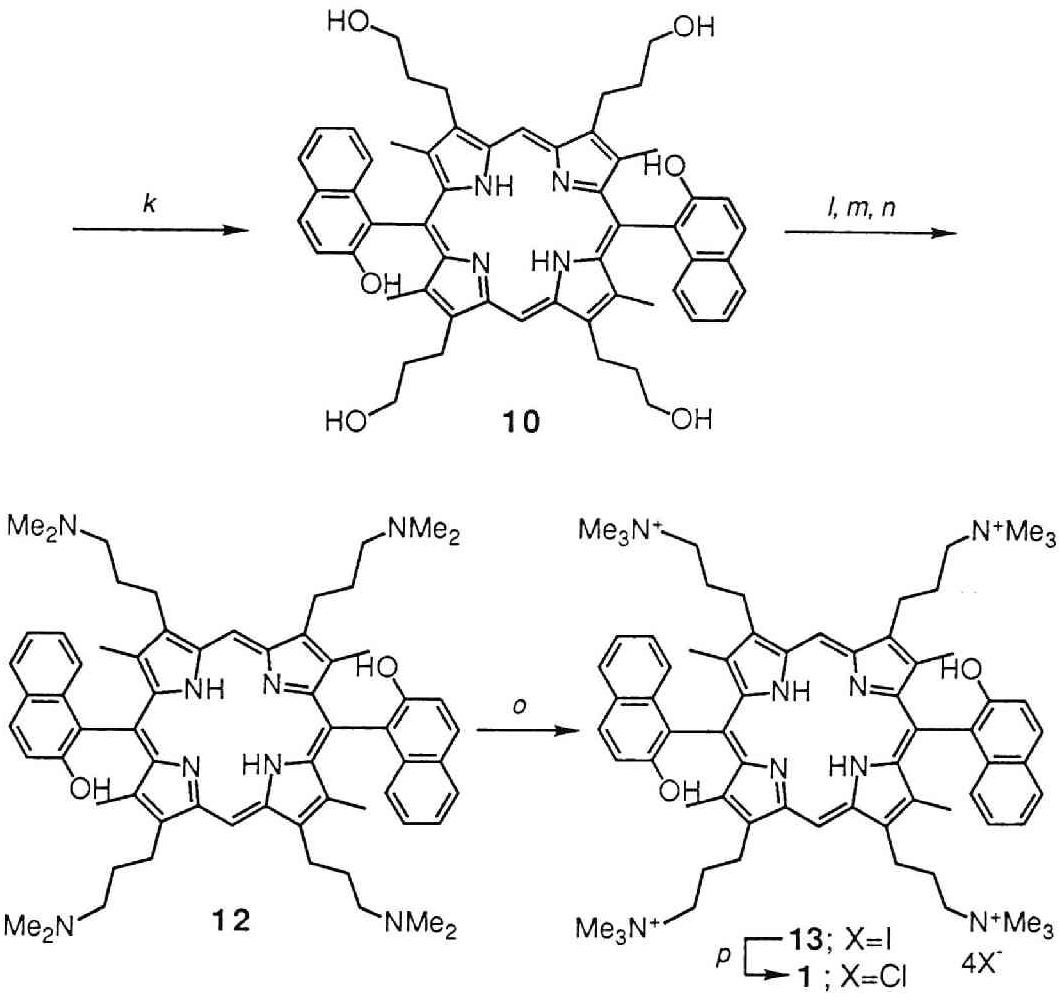

[a] Reagents: (a) NaOMe/MeOH. (b) Methylacrylate. (c) $NaNO_2/H_2O/AcOH$.
(d) Zn/AcOH/NaOAc. (e) $Pb(OAc)_4$/AcOH (f) $AcOH/H_2O$. (g) H_2/10%Pd/C/MeOH.
(h) DMF/Δ. (i) 2-Hydroxyl-1-naphthylaldehyde/*p*-TsOH/MeOH. (j) Chloranil/THF.
(k) $LiAlH_4$ / THF. (l) MsCl/pyridine. (m) Me_2NH/THF. (n) $NaOH/H_2O$/THF.
(o) MeI/MeOH. (p) Ion-exchange column.

obeying the Lambert-Beer's law, which indicates that no self-aggregation occurred. ^{1}H NMR specra of **1** (up to 5.0×10^{-3} M) also indicated no aggregation in D_2O at 25 ℃. Thus **1** can be used to study molecular recognition in aqueous media.[9]

Associations between Porphyrin Host 1 and Guests. Associations between porphyrin host **1** and guests (**G1** ~ **G6**) shown in Chart I were investigated in 50 mM Tris buffer (pH 7.0) at 25 ℃, and the association constants were determined by means of UV-vis spectrophotometric titration. Typical examples of the UV-vis spectral change are shown in Figure 1(a) (c), together with the difference spectra around the Soret region (Figure 1(b) (d)). The guests do not absorb light in this wavelength region. In all cases examined, the absorbance of the Soret band of the pophyrin **1** was decreased and slightly red-shifted upon addition of the guests, which indicates that complexation did occur.

The decrease of absorbance of the Soret band strongly suggests the face-to-face π-stacking interaction mode between the porphyrin surface and aromatic moiety of the aromatic guests, because the hypochromic shift is often characteristic of π-stacking mode.[4b] Interestingly, the spectra have no isosbestic point around the Soret region (Figure 1(b) (d)), which indicates that a binding mode different from simple 1 : 1 complexation occurred. If the π-stacking binding mode did occur, it is reasonable to assume that the porphyrin **1** bound two guests on both sides of the porphyrin plane. Assuming the 1 : 2 complex, the association constants (K_1, K_2)

$$\text{Host} + \text{Guest} \overset{K_1}{\rightleftharpoons} \text{Host} \cdot \text{Guest}$$

$$\text{Host} \cdot \text{Guest} + \text{Guest} \overset{K_2}{\rightleftharpoons} \text{Host} \cdot (\text{Guest})_2 \qquad (1)$$

between the porphyrin **1** and the guests were successfully determined from the absorbance change by use of a nonlinear least-squares curve fitting method as listed in Table I.[11] The association constant of the first step (K_1) is much larger than that

of the second step (K_2). This may be ascribed to the electrostatic interaction between the positively charged ammonium groups of **1** and the negatively charged carboxylate or sulfonate groups of the guests (the positively charged ammonium group in the case of L-Trp-OMe·HCl (**G 6**)). In the first step, strong positive electrostatic potential generated by four ammonium groups exists around the porphyrin, and part of the positive electrostatic potential around the porphyrin will be cancelled upon complexation with a negatively charged guest molecule, which will lead to weaker binding in the second step. Another reason might be the difference in the desolvation energies at four trimethylammonium groups. The desolvation energies might become higher as the number of ammonium groups solvated by water are decreased.

Addition of 1, 8-dihydroxy-3, 6-naphthalenedisulfonate (**G 3**) or 2, 6-naphthalenedisulfonate (**G 4**) to a solution of **1** caused very large hypochromic shift of the Soret band of **1** compared with that of terephthalate (**G 1**), which suggests the effective π-stacking interaction. Because the association constants between **1** and **G 3** and between **1** and **G 4** are comparable with that between **1** and **G 1**, the stabilization due to the π-stacking interaction may be cancelled by other destabillization costs such as puckering of the porphyrin plane. Smaller UV-vis spectral change of **1** was observed upon addition of *trans*-cyclohexanedicarboxylate (**G 2**) to a solution of **1**. The association constant was determined in the same fashion, and was found to be comparable with that between **1** and **G 1**. The CPK model examinations suggested that the similar binding mode to that of **1**-**G 1** complex is possible for **1**-**G 2** complex. The smaller UV-vis spectral change can be ascribed to the weaker perturbation ability of the aliphatic moiety (cyclohexyl) compared with the aromatic chromophore. The relatively small association constant between **1** and **G 6** can be ascribed to the electrostatic repulsion.

Several attempts to investigate the binding mode by means of ^{1}H NMR

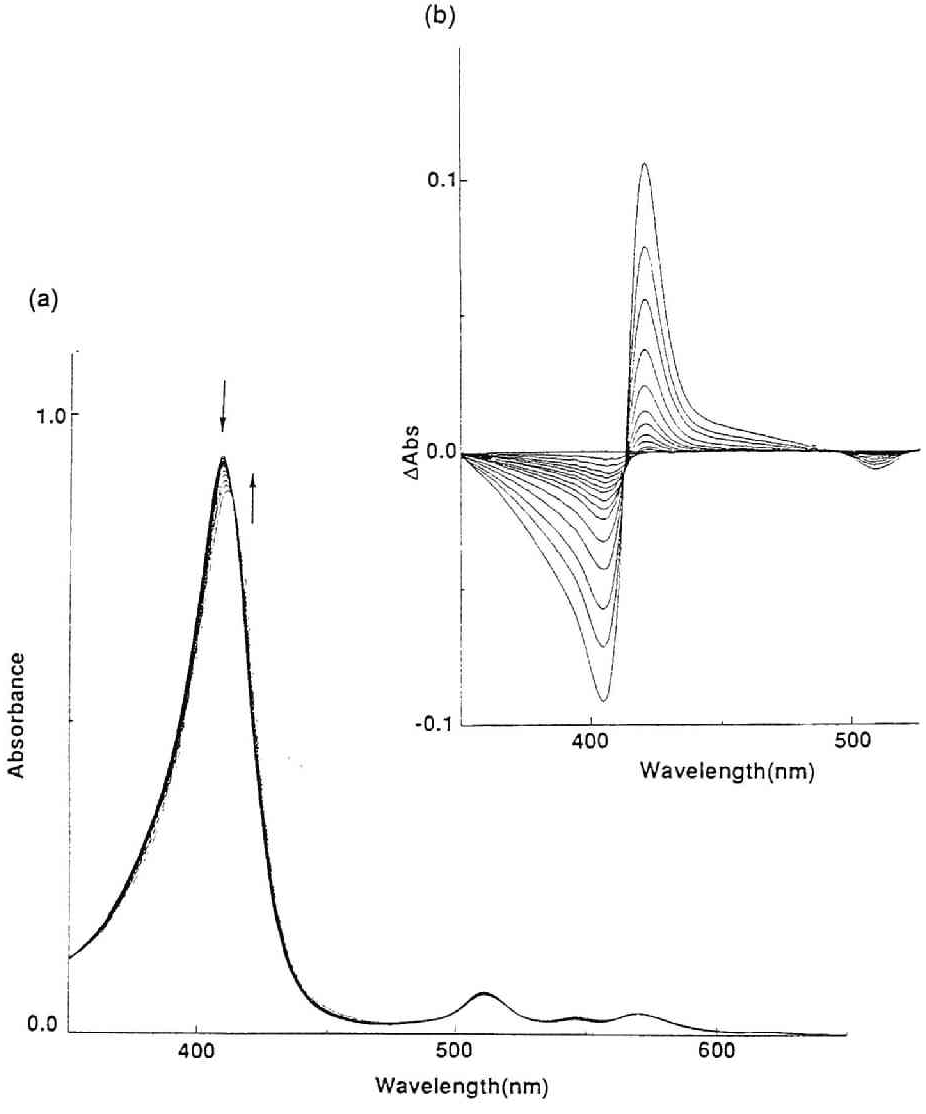

Figure 1. (a) Spectral change of **1** upon addition of terephthalate (**G1**) in 50 mM Tris buffer (pH 7.0) at 25 ℃. (b) Difference spectra around the Soret region.

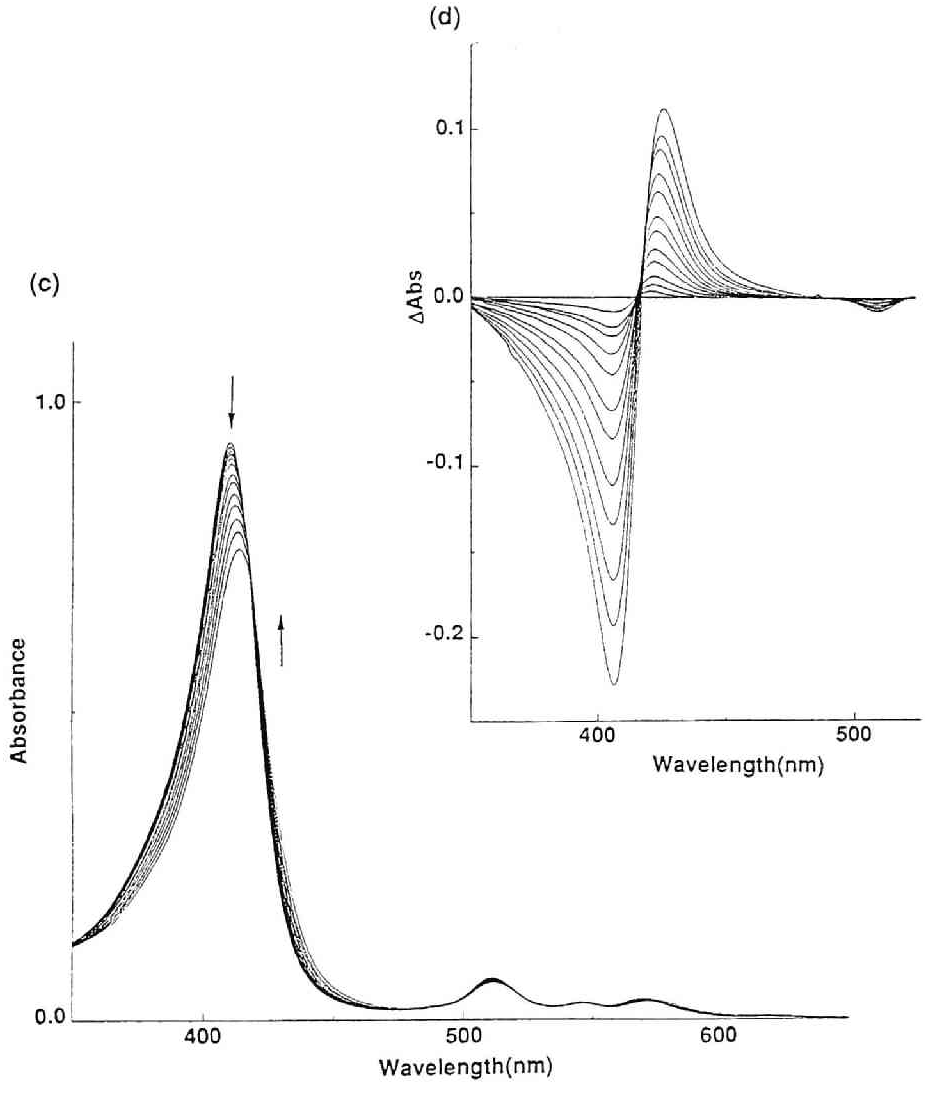

Figure 1. (c) Spectral change of **1** upon addition of 2, 6-naphthalenedisulfonate (**G4**) in 50 mM Tris buffer (pH 7.0) at 25 ℃. (d) Difference spectra around the Soret region.

Chart I.

G1

G2

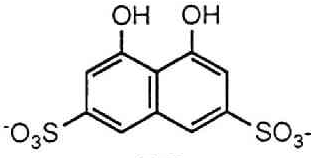

G3

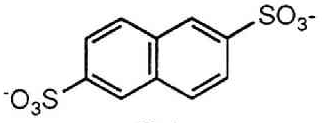

G4

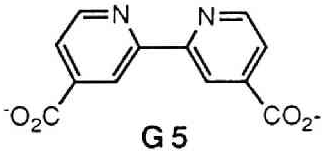

G5

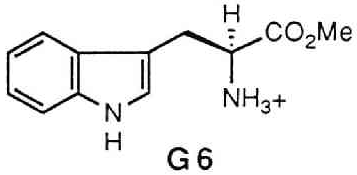

G6

Table I. Association Constants between Porphyrin Host **1** and Guests in 50 mM Tris buffer (pH 7.0) at 25°C.

guest	K_1, M^{-1}	K_2, M^{-1}
G1	5800 ± 1200	40 ±10
G2	6500 ± 900	110 ± 40
G3	7800 ± 2100	———[a]
G4	2500 ± 900	210 ± 50
G5	8100 ± 2800	710 ± 70
G6	1900 ± 850	30 ± 10

[a] Only the first association was analyzed at low concentration of **G3**

titration in D_2O were unsuccessful because at a higher concentration the complex of **1** with terephthalate was easily precipitated owing to the low solubility of the complex, in contrast to the good solubility of **1**. D_2O/DMF(20/1) mixed solvent was found to be useful, and upfield shift (0.46 ppm) of the signal of terephthalate (3.0 mM) was observed upon addition of porphyrin **1** (2.0 mM) in D_2O/DMF (20/1) in accord with the proposed π-stacking binding mode. The signal of the -NMe_3 groups of **1** was upfield-shifted (0.11 ppm) upon complexation. It was impossible to distinguish between the 1 : 1 complex and the 1 : 2 complex by this method.

The proposed structure of the complex of **1** with **G1** is shown in Figure 2. The adjacent two ammonium groups of **1** are directed in the opposite directions due to the electrostatic repulsion, and interestingly the shallow clefts are formed on both sides of the porphyrin plane. The benzene ring of the guest is stacked nicely in this hydrophobic cleft, and the carboxylate groups of the guest are interacting with the ammonium groups of **1**. Thus, the complex is considered to be stabilized by simultaneous π-stacking interaction and the electrostatic interaction. This good fitting geometry of the host and the guest can explain the comparable binding ability to those observed for the various inclusion complexes.[2a] (For example, compare the assocation constants in Table I with K_a = 1950 M^{-1} between β-cyclodextrin and **G4** in 0.1 M phosphate buffer (pH 7.2) at 25 ℃.[12])

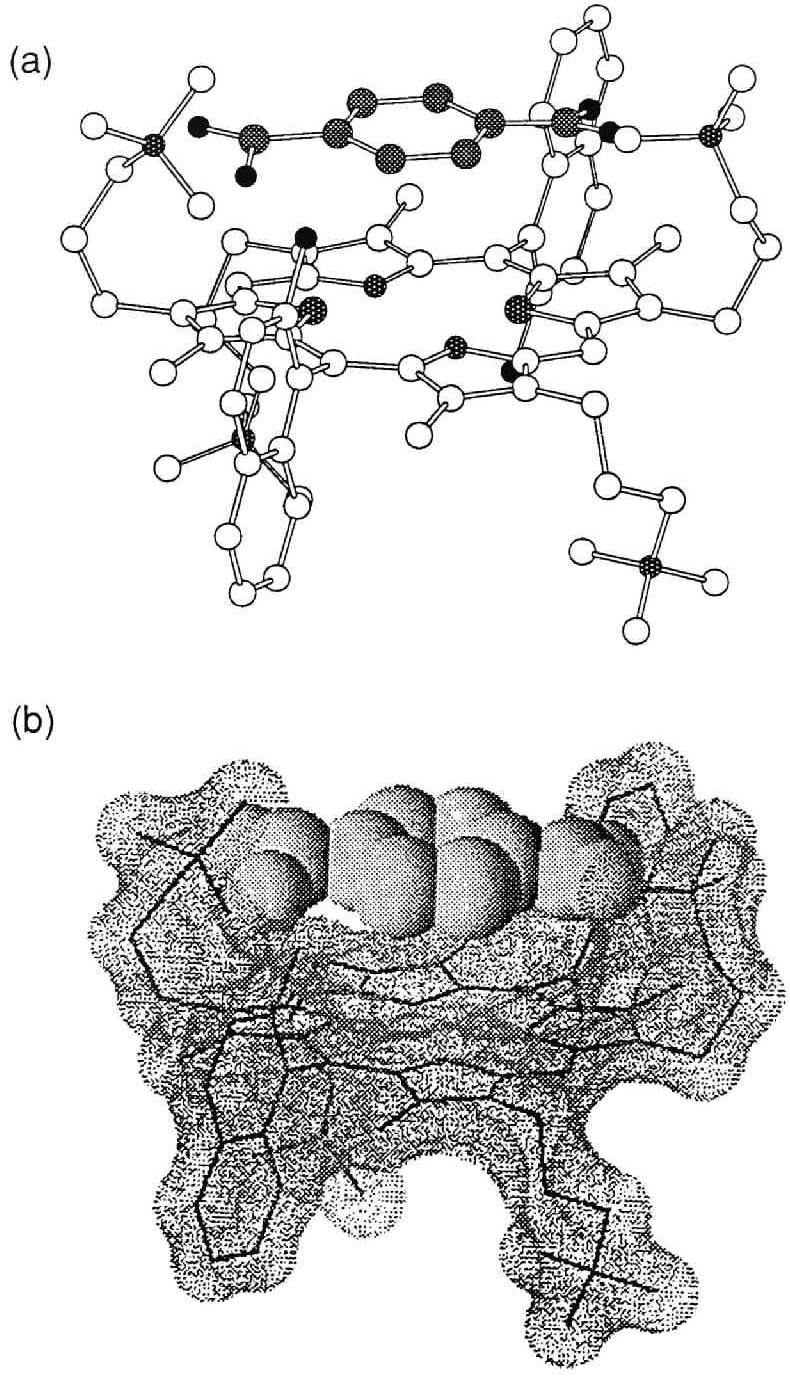

Figure 2. Proposed structure of the complex of **1** with terephthalate. (a) Ball and stick model. The hydrogen atoms are omitted for clarity. (b) Surface model for **1**, and space filling model for terephthalate.

Metal Insertion Reaction Promoted by Host-Guest Complexation. The zinc insertion reactions into the porphyrin cavity both in the presence of and in the absence of the guests (**G1**, **G3**, **G5**) in 50 mM Tris buffer (pH 7.0) at 25 ℃ were monitored by UV-vis spectroscopy. Zinc was selected because the product (zinc complex of **1**) existed as a monomer in water and because the reaction rate was appropriately fast at room temperature. The pseudo-first-order rate constants at various concentrations of anionic aromatic guests were determined according to the following equation (2), and are plotted against the guest concentrations in Figure 3.

$$\ln\left(\frac{\Delta Abs^{\infty}}{\Delta Abs^{\infty}-\Delta Abs}\right) = k_{obsd} \cdot t \qquad (2)$$

where t, ΔAbs, and ΔAbs^{∞}, k_{obsd} represent time (in second), the absorbance change at t second, the absorbance change at final state, and the rate constant, respectively. The metalation reaction rate was accelerated in the presence of **G1** and **G3** compared with that in the absence of the guest, on the other hand, the metalation was decelerated in the presence of **G5**.

The observed rate accerelation can be explained as follows. The local concentration of (cationic) zinc ion around the porphyrin **1** can be increased if anionic guests weaken the positive electrostatic potential produced by the ammonium groups by complexation, or if they function as a metal carrier. The fact that addition of large excess of KCl (20 mM) did not affect the metalation rate indicates that the contribution of the former is relatively minor. Because the binding between the porphyrin **1** and anionic guests **G1** and **G3** are sufficiently strong as described above, it will be possible that anionic guests carry the zinc ion in the bulk water phase into the porphyrin cavity if the anionic guests bind zinc ion effectively.

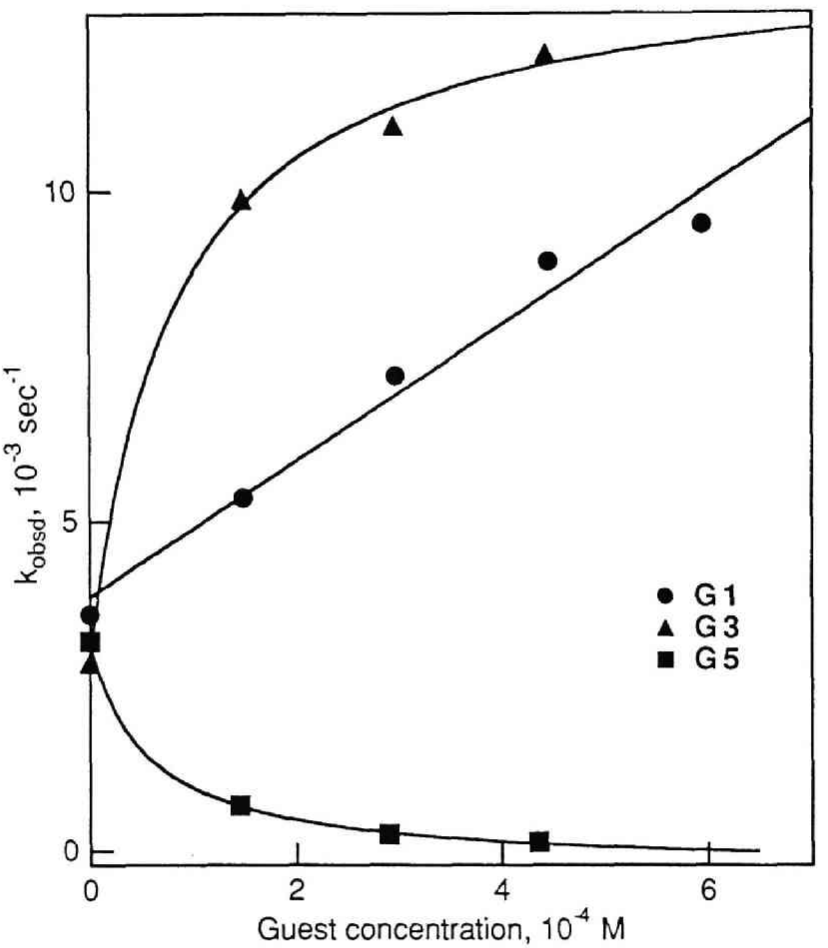

Figure 3. Plot of the apparent first-order rate constant (k_{obsd}) against the guest concentrations.

UV-vis titration indicated that complexation of **G 3** with zinc ion occurred. Upon addition of $ZnCl_2$ to a solution of **G 3**, a new band increased in the visible region (425 nm).[13] Although π-stacking binding mode, which may inhibit the access of zinc ion to the porphyrin cavity, are proposed on the basis of the UV-vis and ^1H NMR titration (*vide supra*), the present binding process is reversible and the geometries of the complexes are considered to be dynamically fluctuating, and so even the transient complexes which are not stable thermodynamically can contribute dominantly in the kinetics. It should be noted that bipyridyl guest **G 5** decelerated the metalation. The bidentate nitrogen ligand **G 5** is considered to bind zinc ion so strongly that the demetalation from **G 5** is retarded, which will lead to the poor function as a metal carrier. Interestingly, the naturally-occurring enzyme ferrochelatase, which catalyze the metalation of ferrous ion, has a metal binding site consisting of serine or cystein residues (neither histidine nor lysine).[7]

Other mechanisms are also possible. Anionic guests may function as a metal carrier to desolvate water molecules from the metal, which facilitates the metal incorporation into the porphyrin cavity, because it has been reported that the rate of metalation into the porphyrin cavity is strongly dependent on the ionic species in water [14] Otherwise, complexation might induce the puckering of the porphyrin plane to promote the metalation reaction. It has been suggested that, in the transition state of the metalation reaction, the porphyrin plane is distorted in a saddle shape and metal is coordinated by the nitrogen atoms of the pyrroles on the opposite sides (A and C rings).[14] Furthermore, it has been believed that ferrochelatase makes use of this mechanism for the catalytic reaction.[7]

Experimental Section

General Remarks. ^{1}H NMR spectra were obtained using either a JEOL A-500 spectrometer or a JEOL JNM FX 90Q FT NMR spectrometer. IR spectra were recorded on a Bio-rad FTS-7 FT-IR spectrometer. UV-vis spectra were recorded on either a Hitachi U-3410 spectrometer or a Hewlett-Packard 8452 diode array spectrophotometer with a thermostatted cell compartment. Mass spectra were obtained with a JEOL JMS DX-300 mass spectrometer. The pH's were measured on a Horiba pH meter F-14. Thin layer chromatography (TLC) was performed on either Merck Kieselgel 60 F254 or DC-Alufolien Aluminiumoxid 60 F254 neutral (Typ E).

UV-vis spectrophotometric titrations. Association constants between the porphyrin host **1** and the guest molecules (**G 1** ~ **G 6**) were determined by UV-vis spectrophotometric titration in 50 mM Tris buffer (pH 7.0) at 25 ℃ in a similar manner to that described in chapter 1, and it was checked that the buffer solution of **1** showed negligibly small pH change upon addition of the guests. Tris buffer was selected because zinc can be solubilized. Tris buffer solution (pH 7.0) was prepared by diluting the mixture of 0.1 M tris(hydroxymethyl)aminomethane (50 mL) and 0.1 M HCl (46.6 mL) to 100 ml with H_2O. The guests (**G 1**~**G 4**) used in the titration experiments were their sodium salts, which were either purchased or prepared by neutralization of the acid form with NaOH and subsequent crystallization.

Measurement of metalation kinetics. The zinc insertion reactions into the porphyrin in the presence of or in the absence of the anionic guest molecules were investigated in 50 mM Tris buffer (pH 7.0) at 25 ℃ by means of UV-vis spectroscopy using a Hewlett-Packard 8452 diode array spectrophotometer with a thermostatted cell compartment, and the spectral changes in the Soret region were

monitored by the kinetic analysis mode of the above instrument. A typical procedure is as follows. Porphyrin free base (6 μM) was dissolved in the buffer solution (2 mL) and then a solution of guest (0 ~ 0.5 mM) was added to this solution. As soon as 10 μL of 28 mM aqueous $ZnCl_2$ (ca. 20 equiv.) was added to the above solution, the reaction was followed at ten seconds intervals. The rate constants were determined according to equation (2) by use of a computer-assisted least-squares method.

Materials. Dry tetrahydrofuran (THF) was distilled from sodium. Dry pyridine was distilled from KOH. 5,15-Bis(2-hydroxy-1-naphthyl)-2,8,12,18-tetra(2-methoxycarbonylethyl)-3,7,13,17-tetramethylporphyrin (**3**) was prepared according to the reported method.[10]

***trans*-5,15-Bis(2-hydroxy-1-naphthyl)-2,8,12,18-tetra(3-hydroxypropyl)-3,7,13,17-tetramethylporphyrin (4).** To a suspension of $LiAlH_4$ (191 mg, 5.03 mmol) in dry THF (30 mL) was added dropwise tetraester porphyrin (**3**) (87 mg, 88 μmol) in dry THF (48 mL) under Ar, and the slurry was stirred at room temperature for twenty minutes. The reaction mixture was poured into ice-water carefully, extracted with ethylacetate, and dried over Na_2SO_4. Evaporation of the solvent gave deep purple solid (65 mg, 84 %), which was used in the following reaction without purification.

***trans*-5,15-Bis(2-methanesulfonyloxy-1-naphthyl)-2,8,12,18-tetra(3-methanesulfonyloxypropyl)-3,7,13,17-tetramethylporphyrin (5).** To a solution of tetraol derivative **3** (65 mg, 74 μmol) in dry pyridine (8.2 mL) was added methanesulfonyl chloride (0. 3mL, 74 μmol) under Ar cooled in an ice bath. After the reaction mixture was stirred for 75 minutes, the mixture was poured into ice-water (100 mL), extracted with dichloromethane (100 mL), washed with water (100 mL), and dried over Na_2SO_4. After evaporation, the residue was purified with column chromatography (SiO_2, ϕ1.5 × 33 cm) eluted with

$CHCl_3$/ethylacetate (5:1) to affod reddish purple solid (57 mg, 57 %). This compound is relatively unstable and used in the next reaction as soon as separated. FABMS (3-nitrobenzyl alcohol matrix) m/e 1351(M+1)

***trans*-5,15-Bis(2-hydroxy-1-naphthyl)-2,8,12,18-tetra[3-(*N*, *N*-dimethylamino)propyl]-3,7,13,17-tetramethylporphyrin (6).** A solution of hexamesylated porphyrin **5** (51 mg, 38 μmol) in dimethylamine (large excess)-THF (5 mL) was heated to 70 ℃ in autoclave for 15 hours. The reaction mixture was cooled, poured into water, extracted with $CHCl_3$, and dried with Na_2SO_4. The solvent was removed by evaporation, and the column chromatography (basic alumina, ϕ1.5 × 25cm, dichloromethane/MeOH (40:1) afforded purple solid (42 mg, 97 %). ^{1}H NMR ($CDCl_3$, 90MHz) δ -2.2 (br. s, 2H, NH), 0.96 (s, 6H, OSO_2CH_3), 2.23 (s, 12H, CH_3), 2.27 (s, 32H, $CH_2CH_2CH_2N(CH_3)_2$), 2.58 (t, *J* = 7.0 Hz, 8H, CH_2CH_2N), 4.02 (t, *J* = 7.0 Hz, 8H, $CH_2CH_2CH_2N$), 7.2-8.4 (m, 12H, naphthyl-H), 10.41 (s, 2H, meso-H)

To a refluxing solution of dimesylated porphyrin (42 mg, 37 μmol) in MeOH (15 mL)-THF (15 mL) was added 10 N NaOH (2.8 mL). After refluxing for 15 hours, the reaction mixture was poured into saturated aqueous NaCl (200 mL), extracted with dichloromethane (200 mL), washed with water (200 mL), and dried over K_2CO_3. Evaporation of the solvent and column chromatography (basic alumina, ϕ1.5 × 35 cm) eluted with dichloromethane/MeOH (25:1) afforded purple solid (26 mg, 70 %). Recrystallization from $CHCl_3$-hexane afforded purple crystals. ^{1}H NMR($CDCl_3$, 90MHz) δ-2.25 (br. s, 2H, NH), 2.18 (s, 24H, $N(CH_3)_2$), 2.22 (br. s, 8H, $CH_2CH_2CH_2N$), 2.28 (s, 12H, CH_3), 2.50 (br. s, 8H, $CH_2CH_2CH_2N$), 3.91 (br. s, 8H, $CH_2CH_2CH_2N$), 6.7-8.3 (m, 12H, naphthyl-H), 10.31 (s, 2H, meso-H).; FAB MS (*m*-nitrobenzylalcohol matrix) *m/e* 991(M^++1); Anal. Calcd for $C_{64}H_{78}O_2N_8$: C, 77.54; H, 7.93; N, 11.30. Found: C, 77.10; H, 7.89; N, 11.37.

***trans*-5,15-Bis(2-hydroxy-1-naphthyl)-2,8,12,18-tetra[3-(*N*, *N*, *N*-trimethylamino)propyl]-3,7,13,17-tetramethylporphyrin tetrachloride salt (1).** To a refluxing solution of **6** (21 mg, 21 μmol) in MeOH (66 mL) was added CH_3I (2.8 mL, 45 mmol), and the reaction mixture was refluxed for 50 minutes with stirring. Evaporation of the solvent gave deep green residue, which was dissolved in a small amount of MeOH, and passed through ion-exchange column (Dowex, 1-X2, 50-100 mesh, Cl^- form; ϕ1.5 × 20 cm) eluted with H_2O. Evaporation of solvent afforded purple solid (25 mg, 98 %). ^1H NMR (D_2O, 500 MHz) δ 2.16 (s, 12H, CH_3), 2.40 (s, 8H, $CH_2CH_2CH_2N$), 2.75 (s, 36H, $N(CH_3)_3$), 3.33 (s, 8H, $CH_2CH_2CH_2N$), 3.94 (s, 8H, $CH_2CH_2CH_2N$), 6.3-8.4 (m, 12H, naphthyl-H), 10.15 (s, 2H, meso-H).; UV-vis (H_2O) λ_{max} 410, 511, 547, 570.

References

(1) (a) Stryer, L. *Biochemistry*; Freeman: New York, 1988. (b) Alberts, B.; Bray, D.; Lewis, J.; Raff, M.; Roberts, K.; Watson, J. D. *Molecular Biology of the Cell*; Garland Publishing, Inc.: New York, 1989. (c) Branden, C.; Tooze, J. *Introduction to Protein Structure*; Garland Publishing, Inc.: New York, 1991.

(2) (a) Bender, M. L.; Komiyama, M. *Cyclodextrin Chemistry*; Springer-Verlag: 1978. (b) Breslow, R. *Acc. Chem. Res.* **1980**, *13*, 170. (c) Tabushi, I. *Acc. Chem. Res.* **1982**, *15*, 66. (d) Hosseini, M. W.; Blacker, A. J.; Lehn, J.-M. *J. Am. Chem. Soc.* **1990**, *112*, 3896. (e) Ferguson, S. B.; Sanford, E. M.; Seward, E. M.; Diederich, F. *J. Am. Chem. Soc.* **1991**, *113*, 5410. (f) Schneider, H.-J.; Shiestel, T.; Zimmermann, P. *J. Am. Chem. Soc.* **1992**, *114*, 7698. (g) Rotello, V. M.; Viani, E. A.; Deslongchamps, G.; Murray, B. A.; Rebek, J., Jr. *J. Am. Chem. Soc.* **1993**, *115*, 797.

(3) (a) Kessel, D.; Cheng, M.-L. *Photochemistry and Photobiology*, **1985**, *41*, 277. (b) Kessel, D.; Thompson, P.; Musselman, B.; Chang, C. K. *Cancer Research*, **1987**, *47*, 4642.

(4) (a) Fiel, R. J.; Howard, J. C.; Mark, E. H.; Gupta, N. D. *Nucleic Acids Res.* **1979**, *6*, 3093. (b) Pasternack, R. F.; Antebi, A.; Ehrlich, B.; Sidney, D. J. *J. Mol. Cat.* **1984**, *23*, 235. (c) Pasternack, R. F.; Giannetto, A.; Pagano, P.; Gibbs, E. J. *J. Am. Chem. Soc.* **1991**, *113*, 7799.

(5) (a) Pasternack, R. F.; Huber, P. R.; Boyd, P.; Engasser, G.; Francesconi, L.; Gibbs, E.; Fasella, P.; Venturo, G. C.; Hinds, L. C. *J. Am. Chem. Soc.* **1972**, *94*, 4511. (b) Turay, J.; Hambright, P.; Datta-Gupta, N. *J. Inorg. Nucl. Chem.* **1978**, *40*, 1687.

(6) (a) Fleischer, E. B.; Choi, E. I.; Hambright, P.; Stone. A. *Inorg. Chem.* **1964**, *3*, 1284. (b) Stein, T. P.; Plane, R. A. *J. Am. Chem. Soc.* **1969**, *91*,

607. (c) Hambright, P.; Chock, P. B. *J. Am. Chem. Soc.* **1974**, *96*, 3123. (d) Schneider, W. In *Structure and Bonding*, **1975**, *23*, 123. (e) Tabata, M.; Tanaka, M. *Inorg. Chem.* **1988**, *27*, 203.

(7) (a) Mazanowska, A. M.; Neuberger, A.; Tait, G. H. *Biochem. J.* **1966**, *98*, 117. (b) Daily, H. A. *Biochemistry*, **1985**, *24*, 1287. (c) Daily, H. A.; Jones, C. S.; Karr, S. W. *Biochim. Biophys. Acta*, **1989**, *999*, 7. (d) Abbas, A.; Labbe-Bois, R. *J. Biological Chem.* **1993**, *268*, 8541.

(8) Hatakeyama, H. *Doctor Thesis*. Kyoto Univ. **1992**.

(9) Preliminary syntheses of other water-soluble cationic porphyrins and investigation by UV-vis and ^{1}H NMR spectra indicated that the replacement of the *meso*-naphthyl moieties of **1** with hydrogen atoms or phenyl groups led to the self-aggregation of the porphyrins.

(10) Aoyama, Y.; Uzawa, T.; Saita, K.; Tanaka, Y.; Toi, H.; Ogoshi, H. *Tetrahedron Lett.* **1988**, *29*, 5271.

(11) The association constants between porphyrin **1** and terephthalate were also determined in other solvents: $K_1 = 3700 \pm 700$, $K_2 = 14 \pm 4\ M^{-1}$ (50mM phosphate buffer (pH 7.0) at 25 ℃); $K_1 = 3600 \pm 1200$, $K_2 = 360 \pm 40\ M^{-1}$ (H_2O/DMF (20/1) at 25 ℃). The addition of the large amount of KCl (up to 40 mM) caused very small spectral change (< 0.01 Abs), which indicates that the spectral change observed upon addition of terephthalate was not due to the change of the ionic strength of the solution.

(12) Inoue, Y.; Hakushi, T.; Liu, Y.; Tong, L.-H.; Shen, B.-J.; Jin, D.-S. *J. Am. Chem. Soc.* **1993**, *115*, 475.

(13) 1, 8-Dihydroxy-3, 6-naphthalenedisulfonic acid disodium salt (**G3**) has been used as colorimetric metal indicator, and is commercially available.

(14) Hambright, P. In *Porphyrins and Metalloporphyrins*; Smith, K. M. Ed., Elsevier: Amsterdam. 1975; pp 233-278.

List of Publications

Chapter 1. Recognition of α–Amino Acid Esters by Zinc Porphyrin Derivatives via Coordination and Hydrogen Bonding Interactions. Evidence for Two-point Fixation from Thermodynamic and Induced Circular Dichroism Spectroscopic Studies.
Mizutani, T.; Ema, T.; Yoshida, T.; Kuroda, Y.; Ogoshi, H. *Inorg. Chem.* **1993**, *32*, 2072-2077.

Chapter 2. Mechanism of Induced Circular Dichroism of Amino Acid Ester-Porphyrin Supramolecular System. Implication to the Origin of the Circular Dichroism of Hemoprotein.
Mizutani, T.; Ema, T.; Yoshida, T.; Renné, T.; Ogoshi, H.
to be submitted.

Chapter 3. Selective Syntheses of Unsymmetrical *Meso*-Arylporphyrins.
Ema, T.; Kuroda, Y.; Ogoshi, H. *Tetrahedron Lett.* **1991**, *32(35)*, 4529-4532.

Chapter 4. Recognition of Chirality and Residual Groups of Amino Acid Esters using New Trifunctional Chiral Porphyrins with C_2 Symmetry.
Mizutani, T.; Ema, T.; Tomita, T.; Kuroda, Y.; Ogoshi, H. *J. Chem. Soc., Chem. Commun.*, **1993**, *6*, 520-522.

Design and Synthesis of Trifunctional Chiral Porphyrin with C_2 Symmetry as a Chiral Recognition Host for Amino Acid Esters.
Mizutani, T.; Ema, T.; Tomita, T.; Kuroda, Y.; Ogoshi, H. *J. Am. Chem. Soc.*, submitted for publication.

Chapter 5. Molecular Recognition and Complexation-Induced Metalation of Water-Soluble Cationic Porphyrin in Aqueous Media.
Mizutani, T.; Ema, T.; Nomura, A.; Yoshida, T.; Ogoshi H.
to be submitted.

List of Other Publications

Synthesis and Photoreaction of 1,2,3,4-Tetra-t-butylnaphthalene: A Highly Crowded Naphthalene Derivative and its Valenceisomers.
Miki, S.; Ema, T.; Shimizu, R.; Nakatsuji, H.; Yoshida, Z.
Tetrahedron Lett. **1992**, *33(12)*, 1619-1620.

List of Oral Presentations

1. New Type of Chiral Porphyrins with C_2 Symmetry.
   Ogoshi, H.; Ema, T.; Hamashima, J.; Kuroda, Y. The 1989 International Chemical Congress of Pacific Basin Societies, Hawaii, December, 1989.(poster presentation)

2. Interaction of Metalloporphyrin with Amino Acids Detected by CD Spectroscopy.
   Ema, T.; Naka, A.; Kuroda, Y.; Ogoshi, H. The 5th Symposium on Biofunctional Chemistry, Hiroshima, June, 1990.

3. Selective Syntheses of *Meso*-Aryl Unsymmetrical Porphyrins.
   Ema, T.; Kuroda, Y.; Ogoshi, H. The 61st Annual Meeting of Chemical Society of Japan, Kanagawa, April, 1991.

4. Trifunctional Metalloporphyrin Receptor (1) Design and Synthesis.
   Ema, T.; Tomita, T.; Kuroda, Y.; Ogoshi, H. The 63rd Annual Meeting of Chemical Society of Japan, Osaka, April, 1992.

5. Trifunctional Metalloporphyrin Receptor (2) Interaction with Amino Acid Derivatives.
   Ema, T.; Tomita, T.; Kuroda, Y.; Ogoshi, H. The 63rd Annual Meeting of Chemical Society of Japan, Osaka, April, 1992.

6. Chiral Recognition of Amino Acid Esters with Trifunctional Chiral Porphyrin Host.

Ogoshi, H.; Ema, T.; Tomita, T.; Mizutani, T.; Kuroda, Y.; The 7th International Symposium of Molecular Recognition and Inclusion, Kyoto, July, 1992.(poster presentation)

7. Chiral Recognition of Amino Acid Esters by Trifunctional Chiral Porphyrin.
Ema, T.; Tomita, T.; Mizutani, T.; Kuroda, Y.; Ogoshi, H. The 42nd Symposium on Coordination Chemistry of Japan, Nara, October, 1992.

8. Detection of Molecular Recognition Mode by means of CD Spectroscopy (1)
Mizutani, T.; Ema, T.; Yoshida, T.; Renné, T.; Ogoshi, H. The 65th Annual Meeting of Chemical Society of Japan, Tokyo, March, 1993.

9. Detection of Molecular Recognition Mode by means of CD Spectroscopy (2) Theoretical Calculations.
Mizutani, T.; Ema, T.; Yoshida, T.; Renné, T.; Ogoshi, H. The 65th Annual Meeting of Chemical Society of Japan, Tokyo, March, 1993.

10. CD Induced in the Soret Region as Probe for Molecular Recognition: Mechanistic Study and Implication to Hemoprotein CD.
Mizutani, T.; Ema, T.; Yoshida, T.; Renné, T.; Ogoshi, H. The 2nd International Symposium on Bioorganic Chemistry, Fukuoka, June, 1993.(poster presentation)

11. Synthesis of Water-Soluble Porphyrins and Molecular Recognition.
Mizutani, T.; Ema, T.; Nomura, A.; Yoshida, T.; Ogoshi, H. The 26th Symposium on Synthetic Organic Chemistry at Niigata, Niigata, December, 1993.